Supplementary information

Highly Selective Low-Temperature Acetylene Semihydrogenation Guided by Multi-scale Machine Learning

Lin Chen[†§], Xiao-Tian Li[†§], Sicong Ma[‡], Yi-Fan Hu[†], Cheng Shang[†], Zhi-Pan Liu*[,†]

[†] Collaborative Innovation Center of Chemistry for Energy Materials (iChEM), Shanghai Key Laboratory of Molecular Catalysis and Innovative Materials, Key Laboratory of Computational Physical Science, Department of Chemistry, Fudan University, Shanghai 200433, China

[‡] Key Laboratory of Synthetic and Self-Assembly Chemistry for Organic Functional Molecules, Shanghai Institute of Organic Chemistry, Chinese Academy of Sciences, Shanghai 200032, China

Corresponding Author: *zpliu@fudan.edu.cn

Contents

1. Experimental details

1.1. Materials used: Palladium nitrate hydrate ($Pd(NO_3)_2·2H_2O$, 40% Pd basis), anatase titanium dioxide(a-TiO_2, 99.7%), Hydrotalcite (HT, $Mg_6Al_2(CO_3)(OH)_{16}·4H_2O$,), Borane dimethylamine complex (DMAB, 97%), Pd/C(5%), Lindlar catalyst(Pd/$CaCO_3$, poisoned with Pb, 5%) were obtained from Sigma-Aldrich. Silver nitrate ($AgNO_3$, 63.5%), green silicon carbide (SiC, 99.0%, an average particle size of 80 mesh), quartz wool, Titanium tetrachloride (98%), nitric acid (HNO_3, 68%), lithium aluminum hydride ($LiAlH_4$, 97, titanium dioxide(P25), silicon dioxide (SiO_2, 99.99%), cerium oxide (CeO_2, 99.95%), α-aluminum oxide (α-Al_2O_3, 99.9%), γ-aluminum oxide (γ-Al_2O_3, 99.9%), Yttrium oxide (Y_2O_3, 99.99%), calcium carbonate ($CaCO_3$, 99.0%) , zirconium dioxide(ZrO_2, 99.5%), stannic oxide(SnO_2, 99.5%), Vulcan XC-72R carbon (C) were purchased from Sinopharm Chemical Reagent Co., Ltd. Graphene oxide(GO), SM-5 (SiO_2/Al_2O_3 ratio is between 40 to 50), MCM-41, Al-MCM-41 (SiO_2/Al_2O_3 ratio is 25), SAPO-34, Ti-MOR and Ti-MWW were bought from Nanjing XFNANO Tech Co., Ltd. Nitrogen (N_2, 99.99%), hydrogen (H_2, 99.99%), carbon monoxide (CO, 99.99%), helium (He, 99.99%), and the mixed gas hydrogen (5% H_2 and 95% Ar), (0.5% C_2H_2, 50.0% C_2H_4, 5.0% H_2, 4.0% He and 40.5% N_2) were supplied by Shanghai Air Liquide Co., Ltd. All the chemicals were used directly without further purification.

1.2. Synthesis of rutile-TiO_x: The r-TiO_x (r-TiO_2 with oxygen vacancy) was synthesized using the procedure reported in literatures[1], Briefly, the r-TiO_2 by reducing it in pure H_2 for 24 hours at 750 ^oC at the ambient pressure.

1.3. Loading metals onto support: A range of supporting materials (r-TiO_2, r-TiO_x, a-TiO_2, P25, ZSM-5, γ-Al_2O_3, α-Al_2O_3, CeO_2, ZrO_2, SiO_2, SnO_2, Y_2O_3, HT, $CaCO_3$, GO, C, MCM-41, Al-MCM-41, Ti-MWW, Ti-MOR, SAPO-34) were considered in this work and the PdAg/support mixture were prepared using the similar approach, the co-impregnation method. Taking r-TiO_2 as an example, we first added an equal volume of distilled water to the support (960 mg r-TiO_2 with 2.0 mL H_2O) and sonicated the mixture for 10 min followed by vigorously stirring for 30 min to permeate the support. Then, we prepared 50 mg mL^{-1} of $Pd(NO_3)_2·2H_2O$ and 94.4 mg mL^{-1} $AgNO_3$ of aqueous solutions. Next, the Ag salt solution was quickly added to the vigorously stirred support, followed by the addition of Pd salt aqueous solutions. It might be mentioned that the loading of metal alloy can be tuned at this step. For example, to synthesize a 1% loading amount of Pd_1Ag_3/TiO_2, 0.5 mL $AgNO_3$ solution and 0.5 mL $Pd(NO_3)_2·2H_2O$ aqueous solution were added to the 960 mg of r-TiO_2. The suspension was stirred for 12 h and aged for 12 h at ambient temperature. Finally, the samples were freeze-dried for 24 hours.

1.4. Reduction of catalyst: After the loading of the PdAg precursor onto the supports, there are two choices in the next step, samples either being pre-oxidized before reduction or being directly reduced in a quartz tube. This information can be found in Table S1 and S4. Specifically, for the reduction of the pre-oxidized sample, the procedure is described as follows. A 200 mg sample was placed in a ceramic ark in the air at atmospheric pressure, and then the ceramic ark was heated at 450 ^oC for 5 hours in a muffle furnace to complete the pre-oxidation. And then the samples were transferred to a quartz tube furnace, in which reduction was performed by gas (5% H_2/Ar, 100% H_2, N_2, Air or keep vacuum), and the gas flow was controlled to maintain 50 mL min^{-1}. The temperature was increased to the specified temperature (150, 300, 450, 600, 750, and 900 °C) at a rate of 10 °C min^{-1}, and kept for 4 hours to obtain the reduced catalyst.

1.5. Characterization: Power X-ray diffraction (XRD) patterns were obtained on a Bruker D8 in which Cu (Kα=0.15406 nm) was used as an X-ray source. In-situ XRD patterns were obtained on a Rigaku SmartLab X-ray diffractometer using Cu Kα (λ = 0.15406 nm) at 50 kV and 150 mA. Sample powders were slowly heated up to 950°C with XRD profiles collected at 30, 50, 100, 150, 200, 250, 300, 350, 400, 450, 470, 490, 510, 530, 550, 570, 590, 610, 630, 650, 670, 690, 710, 730, 750, 770, 790, 810, 830, 850, 870, 890, 900, 910, 930 and 950 °C as well as 30 °C after cooling down. High-resolution transmission electron microscopy (HR-TEM) data were obtained on an FEI Tecnai G2 F20 S-TWIN transmission electron microscopy instrument operating at 200 kV. Scanning transmission electron microscopy (STEM), elemental mapping, and line analysis were performed using a JEOL-ARM 200F instrument equipped with a Kevex EDX detector (JED 2300T) operated at 200 kV. The experiments of temperature-programmed desorption (TPD) were also performed on a VDSorb-91i chemisorption analyzer. The Brunauer-Emmett-Teller (BET) surface area of the products was measured by N2 adsorption-desorption (TriStar II 3020). The actual Pd and Ag loading amounts were determined by inductively coupled plasma−optical emission spectroscopy (ICP-OES). The sample was digested with concentrated nitric acid before analysis in an Aglient720ESinstrument.

In characterizing the solid phase structure, X-ray absorption fine structure (XAFS) for the Ag-K edge (25514 eV) and Pd-K edge (24350 eV) were performed at the BL11B beamlines at the Shanghai Synchrotron Radiation Facility (SSRF) (Shanghai, China). Before the analysis at the beamline, samples were pressed into thin sheets 1 cm in diameter and sealed using Kapton tape film. The XAFS spectra were recorded at room temperature using a 4-channel Silicon Drift Detector (SDD) Bruker 5040. Pd and Ag *K*-edge extended X-ray absorption fine structure (EXAFS) spectra were recorded in fluorescence mode. Negligible changes in the line-shape and peak position of Pd and Ag *K*-edge XANES spectra were observed between two scans taken for a specific sample. The XAFS spectra of these standard samples (Pd foil, PdO, Ag foil, and Ag_2O) were recorded in transmission mode.

The obtained XAFS data was processed in Athena (version 0.9.26) for background, pre-edge line, and post-edge line calibrations[2-3]. Data fitting was carried out using the Artemis package over an R range of 1.0−3.8 Å and a k-range of 3.0−11.0 $Å^{-1}$ at the Pd edge, an R range of 1.1−3.0 Å and a k-range of 3.0−13.0 Å−1 at the Ag edge. The model of Ag foil, Ag_2O, Pd foil, PdO_2, and $PdAg_3$ were used to calculate the simulated scattering paths. The four parameters, coordination number, bond length, Debye-Waller factor, and E0 shift (CN, R, σ2, ΔE0) were fitted and partially fixed. For Wavelet Transform analysis, the χ(k) exported from Athena was imported into the Hama Fortran code[4]. The parameters were listed as follows: R range, 0 - 3 Å, k range, 3 – 13.9 Å−1; k weight, 3; and Morlet function with κ=5, σ=1 was used as the mother wavelet to provide the overall distribution.

2. SSW-NN method and the generation of Pd-Ag-Ti-C-H G-NN potential

2.1 Architecture of neural network potential

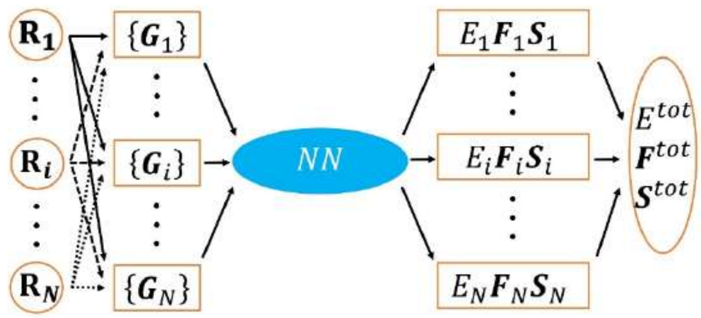

Scheme S1. Scheme of the HDNN architecture. The subscripts (1, *i*,…, *N*) are atom indices and represent the total atoms in a structure. The inputs of NN are a set of structural descriptors, which are constructed from the Cartesian coordinates of the structure, while the outputs of NN are the atomic properties, i.e., energies, forces, and stresses. The overall properties, E^{tot}, $\boldsymbol{F}^{tot}$, and $\boldsymbol{S}^{tot}$, can be calculated from the individual atomic contributions.

In this work, we utilized the high dimensional neural network (HDNN) scheme to construct the global NN (G-NN) potential, as shown in Scheme S1. The input nodes to NN are a set of structural descriptors of a structure, as detailedly discussed in our previous works[5-7]. The total energy E^{tot} of the structure can be composed as a linear combination of its atomic energy E^i from the output of NN

$$E^{tot} = \sum_i E_i \qquad (1)$$

Consistently, the atomic force can be analytically derived from the total energy, i.e., the force component $F_{k,\alpha}$ (α = *x*, *y*, or *z*) acting on atom *k* is the derivative of the total energy E^{tot} with respect to coordinate $R_{k,\alpha}$. In combination with Eq. 1, the force component $F_{k,\alpha}$ then is related to the derivatives of the atomic energy E^i with respect to the j^{th} structural descriptors of atom *i*, $G_{j,i}$

$$F_{k,\alpha} = -\frac{\partial E^{tot}}{\partial \mathrm{R}_{k,\alpha}} = -\sum_{i,j} \frac{\partial E_i}{\partial G_{j,i}} \frac{\partial G_{j,i}}{\partial \mathrm{R}_{k,\alpha}} \qquad (2)$$

Similarly, the element $\sigma_{\alpha\beta}$ of the static stress tensor matrix can be analytically derived as

$$\sigma_{\alpha\beta} = -\frac{1}{V} \sum_{i,j,d} \frac{(\boldsymbol{r}_d)_\alpha (\boldsymbol{r}_d)_\beta}{r_d} \frac{\partial E_i}{\partial G_{j,i}} \frac{\partial G_{j,i}}{\partial r_d} \qquad (3)$$

where $\boldsymbol{r}_d$ and r_d are the distance vector, constituted by $G_{j,i}$ and its module, respectively, and *V* is the volume of the structure.

2.2 Generation of global dataset using SSW-NN

Undoubtedly, the quality of the potential energy surface (PES) of G-NN is largely determined by its training dataset. Here we utilized the stochastic surface walking (SSW) global[8-10] optimization to generate a global dataset, which is fully automated and does not need a priori knowledge of the system, such as the structural motif, e.g. bonding patterns and symmetry. The final obtained Pd-Ag-Ti-C-H global dataset contains a variety of structural patterns on the global PES, as summarized in Table S2.

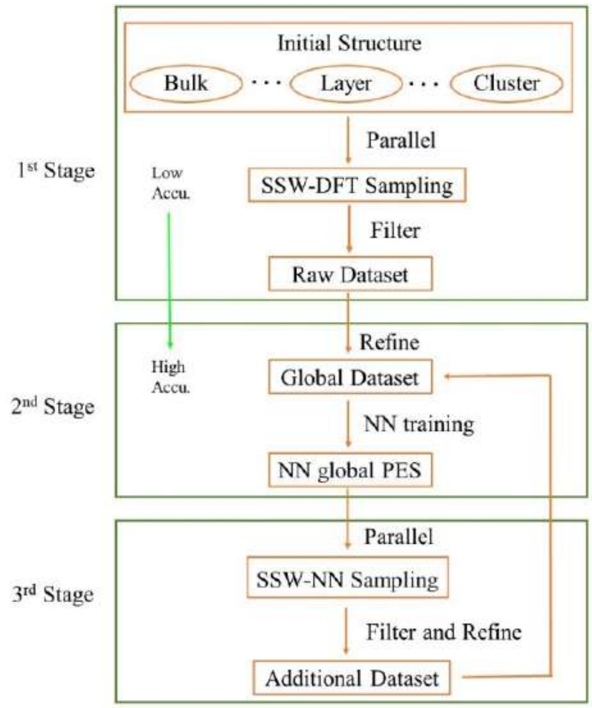

Scheme S2. Procedure for the generation of the global training dataset by SSW global optimization. In the first stage, the SSW sampling is typically performed by low accuracy DFT calculations. In the second stage, the global dataset is first refined with high accuracy DFT setups, and then NN training is performed based on the accurate global dataset. In the third stage, an additional dataset is generated by SSW sampling utilizing the previously obtained NN PES and is fed into the global dataset. A new cycle of NN training then starts based on the new global dataset (back to stage 2).

In brief, the SSW-NN method involves three stages to generate the global dataset (see Scheme S2), as described below.

(i) **The first stage** generates a raw dataset, which contains the most common atomic environment and serves to build an initial NN PES. This is done by performing density functional theory (DFT) SSW global optimization in a massively parallel way. In this stage, the DFT calculations have low accuracy setups and small unit cells to speed up the SSW search. By collecting and screening the structures from SSW trajectories, a raw dataset is obtained.

(ii) **The second stage** trains a NN global PES. This is done by refining the dataset using DFT calculations with high accuracy setups, followed by NN training on the accurate global dataset (see our previous work[11] for details). The NN architecture applied in this stage utilizes a small set of structural descriptors and a small network size.

(iii) **The third stage** iteratively expands the global dataset. It targets to increase the predictive power of NN PES by incorporating more structural patterns into the dataset. This is done by performing SSW PES search using the NN PES obtained in the second stage, starting from a variety of initial structures. These initial structures are randomly constructed and include large systems with many atoms per unit cell. The structures from all the SSW trajectories are collected and filtered to generate an additional dataset. The new dataset is then fed to the global dataset to start a new cycle of NN training (back to stage 2).

3. Random forest ML

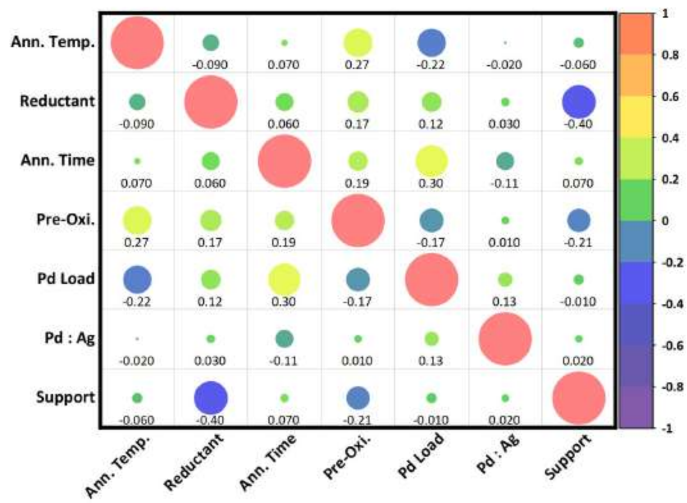

Figure S1. Pearson's correlation analysis of descriptors.

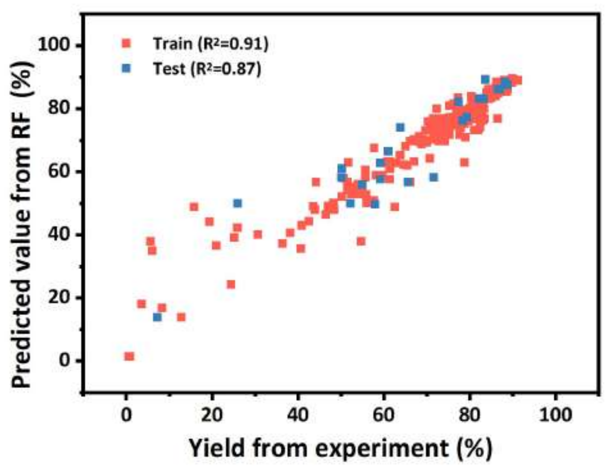

Figure S2. Correlation between the experimental yield of acetylene semi-hydrogenation and the predicted yield from RF.

4. ML atomic simulations for Pd-Ag nanoparticles on TiO_2

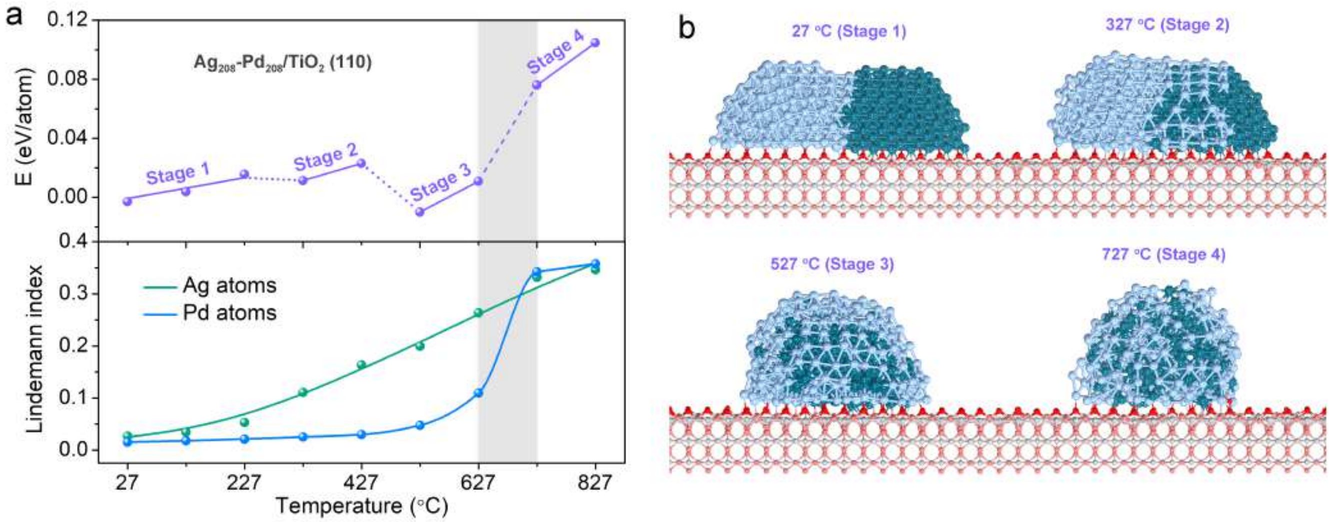

Figure S3. Isothermal Nose-Hoover molecular dynamics (MD) simulations for a Pd_{208} and an Ag_{208} nanoparticle at a series of temperatures (from 27 to 827 °C at the interval 100 °C). (a) Potential energy and Lindemann index against the simulated temperature from the last 1.2 ns simulations. The local Lindemann index of atom *i* is calculated by $q_i = \frac{1}{N-1}\sum_{j\neq i}\frac{\sqrt{\langle r_{ij}^2\rangle_T - \langle r_{ij}\rangle_T^2}}{\langle r_{ij}\rangle_T}$, while the Lindemann index of the system is averaged by $q = \frac{1}{N}\sum_i q_i$. (b) Structures for the Pd-Ag nanoparticle after 2.2 ns simulations at different temperatures.

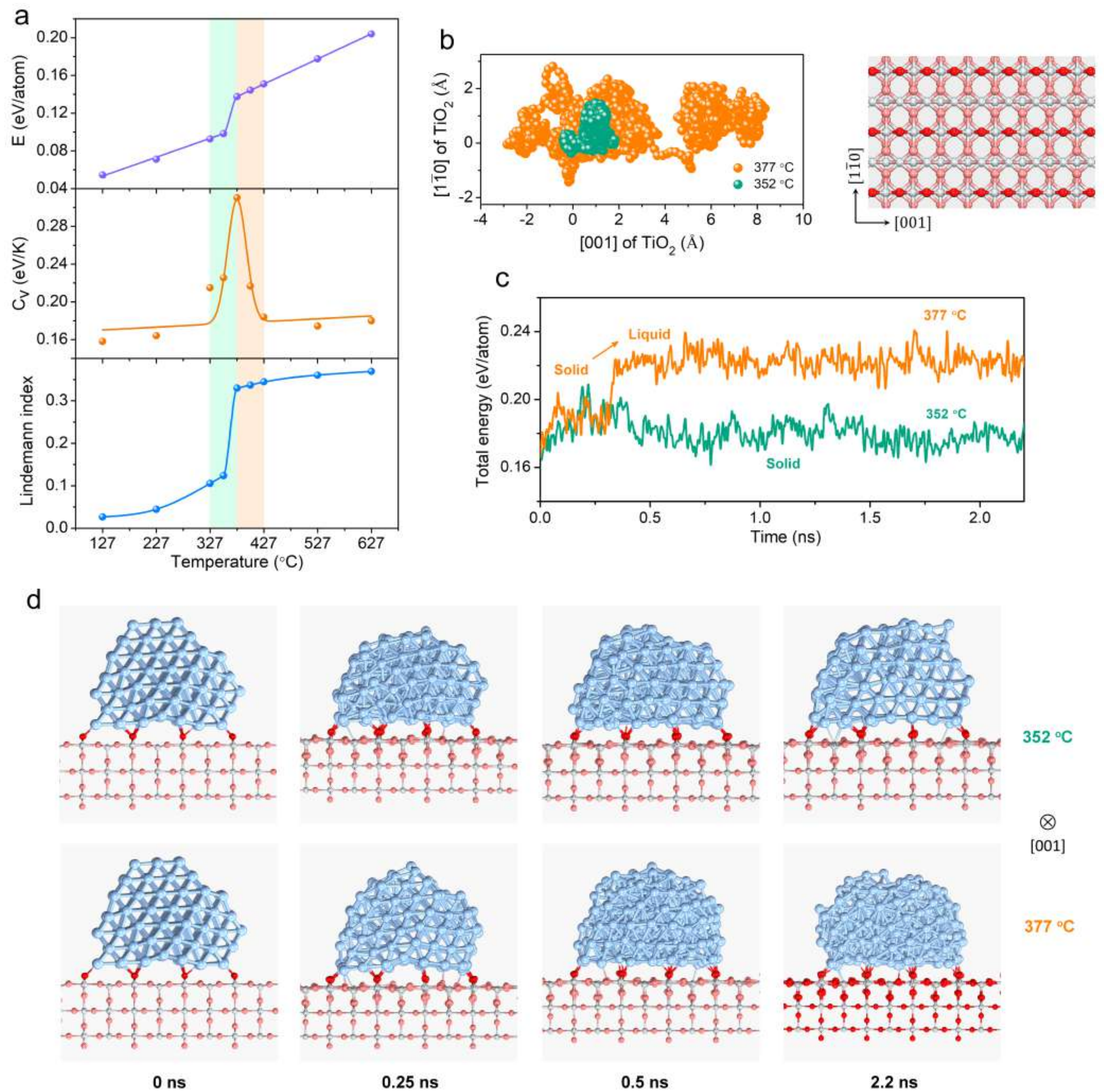

Figure S4. Isothermal Nose-Hoover molecular dynamics (MD) simulations for an Ag_{208} nanoparticle at a series of temperatures. (a) Potential energy, heat capacity, and Lindemann index against the simulated temperature showing the melting point of Ag_{208} at ~377 °C. (b) The trajectory of the geometric center of Ag_{208} at 352 and 377 °C (just below and above the melting point), respectively. (c) Total energy variation of Ag_{208} nanoparticle at 352 and 377 °C during the 2.2 ns simulations. (d) Snapshots showing the structural change of Ag_{208} after 2.2 ns simulations at 352 and 377 °C, respectively.

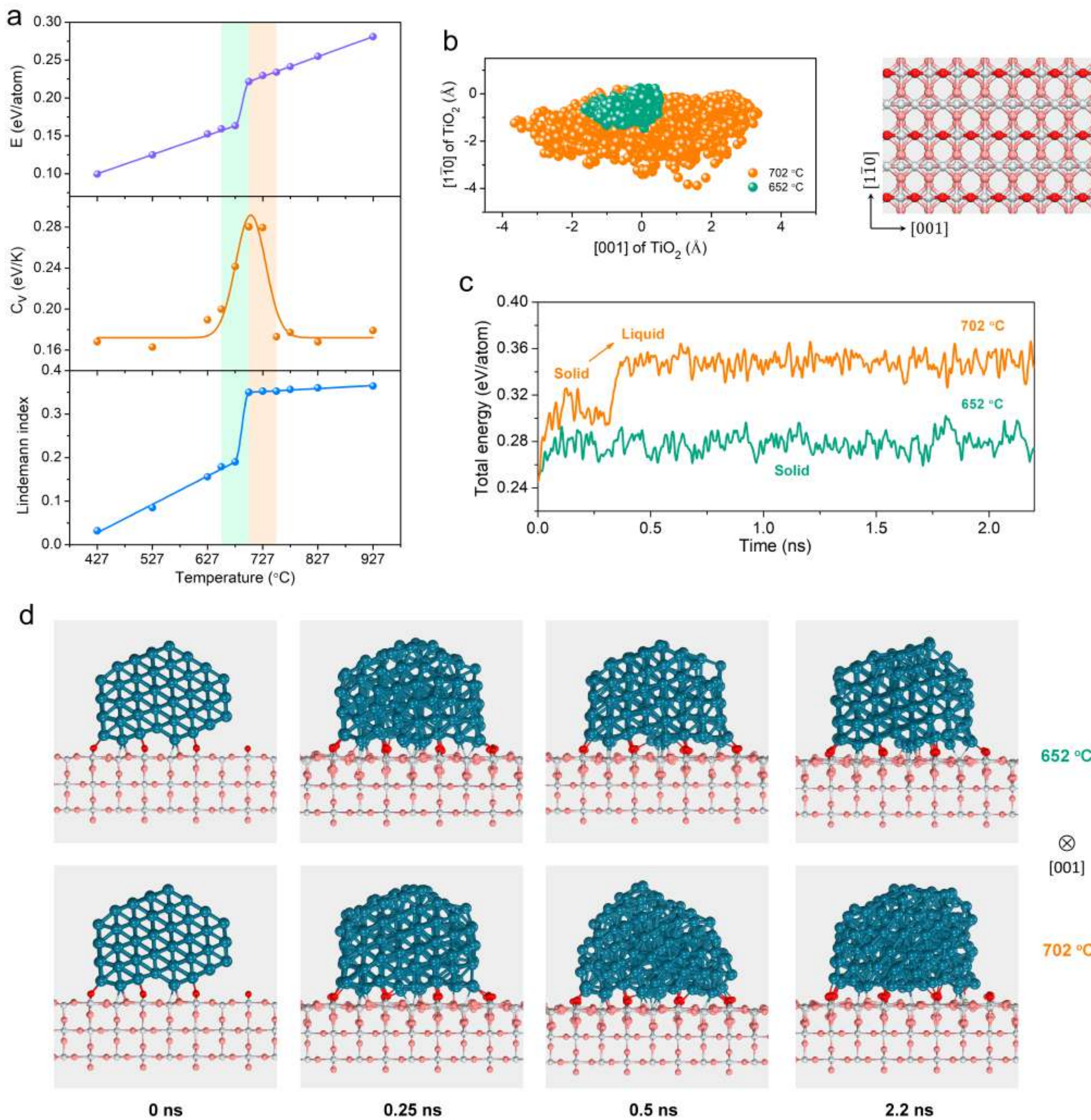

Figure S5. Isothermal Nose-Hoover molecular dynamics (MD) simulations for a Pd_{208} nanoparticle at a series of temperatures. (a) Potential energy, heat capacity, and Lindemann index against the simulated temperature showing the melting point of Pd_{208} at ~702 °C. (b) The trajectory of the geometric center of Pd_{208} at 652 and 702 °C (just below and above the melting point), respectively. (c) Total energy variation of Pd_{208} nanoparticle at 652 and 702 °C during the 2.2 ns simulations. (d) Snapshots showing the structural change of Pd_{208} after 2.2 ns simulations at 652 and 702 °C, respectively.

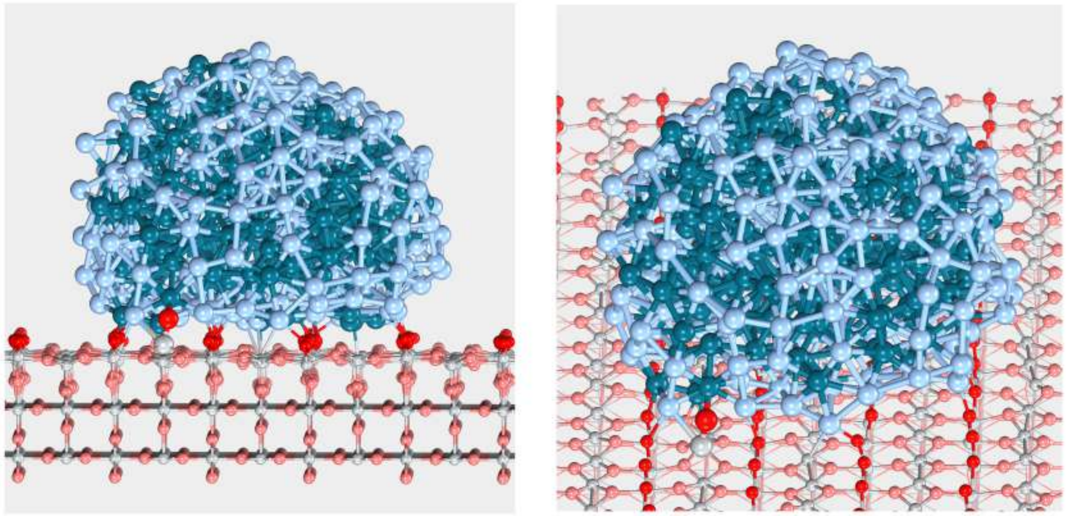

Figure S6. The detailed structure of the $Pd_{208}Ag_{208}$ nanoparticle after 2.2 ns simulation at 727 ^{o}C, where an O_{br} atom diffused out from the original (110) bridging row to the five-coordinated Ti site for stabilizing the PdAg nanoparticle by forming Pd-O bond.

5. The characterization of Pd_1Ag_3 alloy on different supports

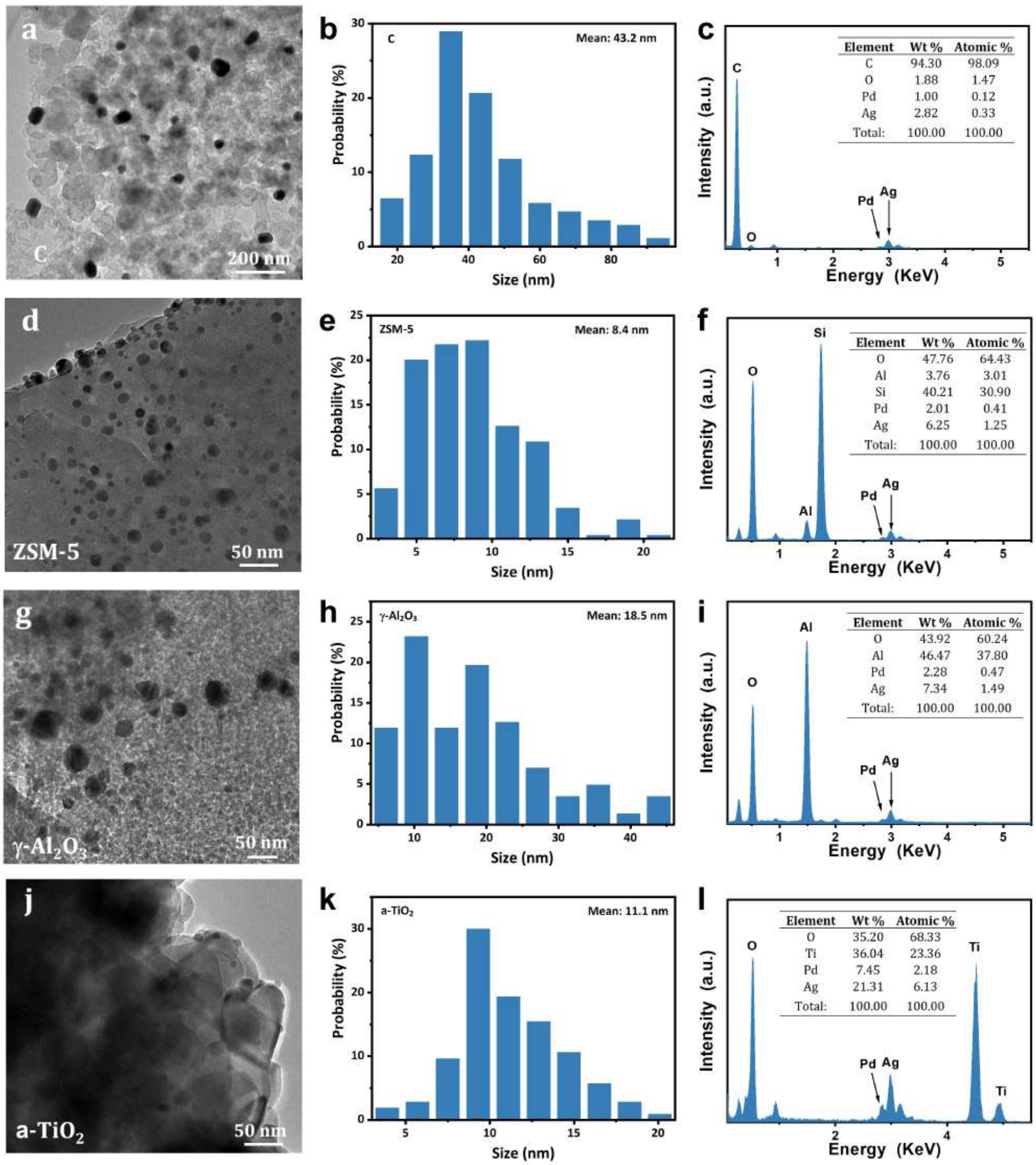

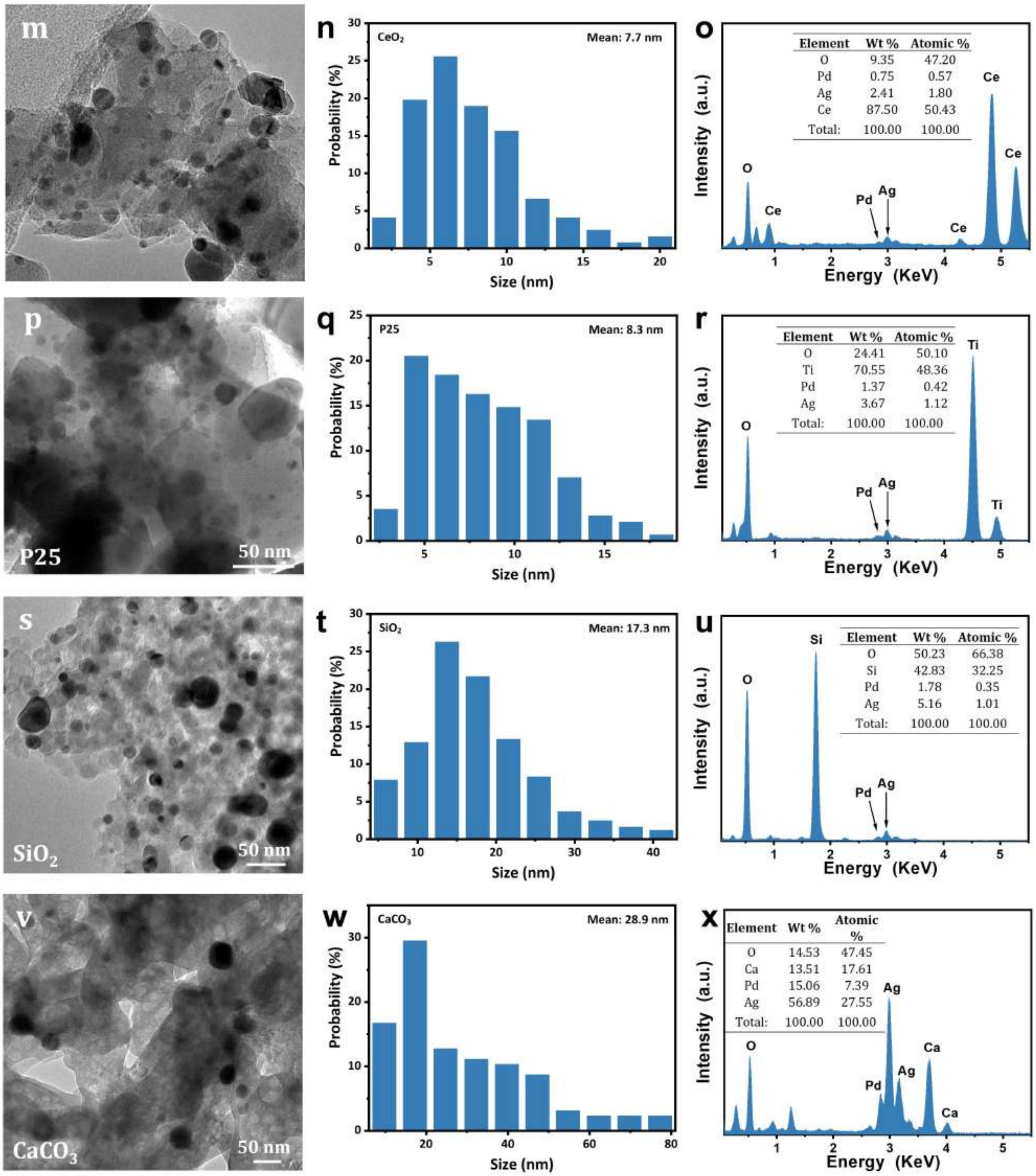
m
n
CeO2
Mean: 7.7 nm
Probability (%)
Size (nm)
o
Element Wt % Atomic %
O 9.35 47.20
Pd 0.75 0.57
Ag 2.41 1.80
Ce 87.50 50.43
Total: 100.00 100.00
Intensity (a.u.)
Energy (KeV)
O Ce Pd Ag Ce Ce Ce
p
P25
50 nm
q
P25
Mean: 8.3 nm
Probability (%)
Size (nm)
r
Element Wt % Atomic %
O 24.41 50.10
Ti 70.55 48.36
Pd 1.37 0.42
Ag 3.67 1.12
Total: 100.00 100.00
Intensity (a.u.)
Energy (KeV)
O Pd Ag Ti Ti
s
SiO2
50 nm
t
SiO2
Mean: 17.3 nm
Probability (%)
Size (nm)
u
Element Wt % Atomic %
O 50.23 66.38
Si 42.83 32.25
Pd 1.78 0.35
Ag 5.16 1.01
Total: 100.00 100.00
Intensity (a.u.)
Energy (KeV)
O Si Pd Ag
v
CaCO3
50 nm
w
CaCO3
Mean: 28.9 nm
Probability (%)
Size (nm)
x
Element Wt % Atomic %
O 14.53 47.45
Ca 13.51 17.61
Pd 15.06 7.39
Ag 56.89 27.55
Total: 100.00 100.00
Intensity (a.u.)
Energy (KeV)
O Pd Ag Ag Ca Ca

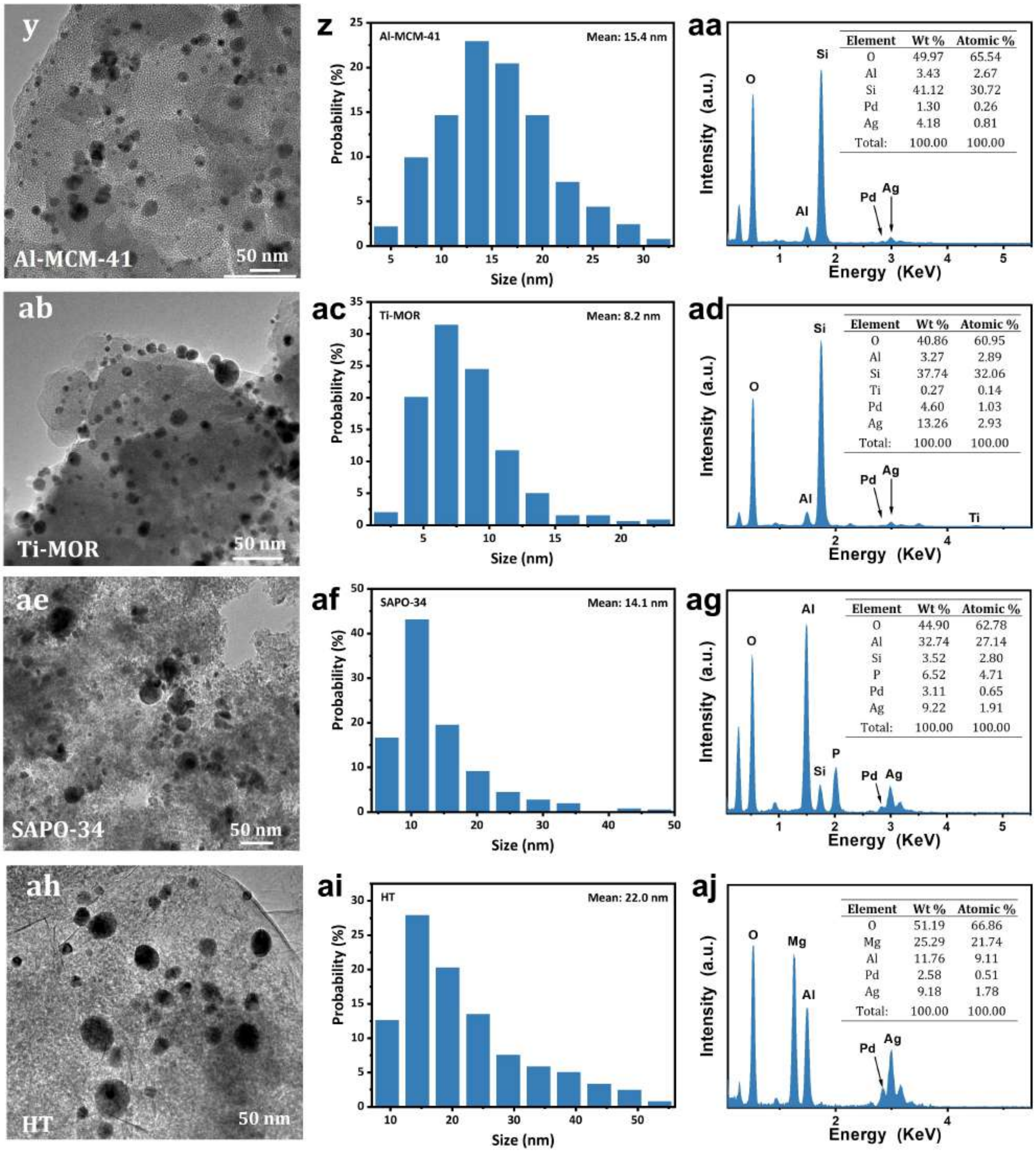

Figure S7. The TEM images, corresponding nanoparticle size distributions, and EDX of Pd_1Ag_3 on different supports at 750 ^{o}C annealing. (a,b,c) C; (d,e,f) ZSM-5; (g,h,i) γ-Al_2O_3; (j,k,l) a-TiO_2; (m,n,o) CeO_2; (p,q,l) P25; (o,p) SiO_2; (q,r) $CaCO_3$; (s,t) Al-MCM-41; (u,v) Ti-MOR; (w,x) SAPO-34; (y,z) HT.

6. Morphology of Pd_1Ag_3/r-TiO_2(T750) after the long-term hydrogenation experiment

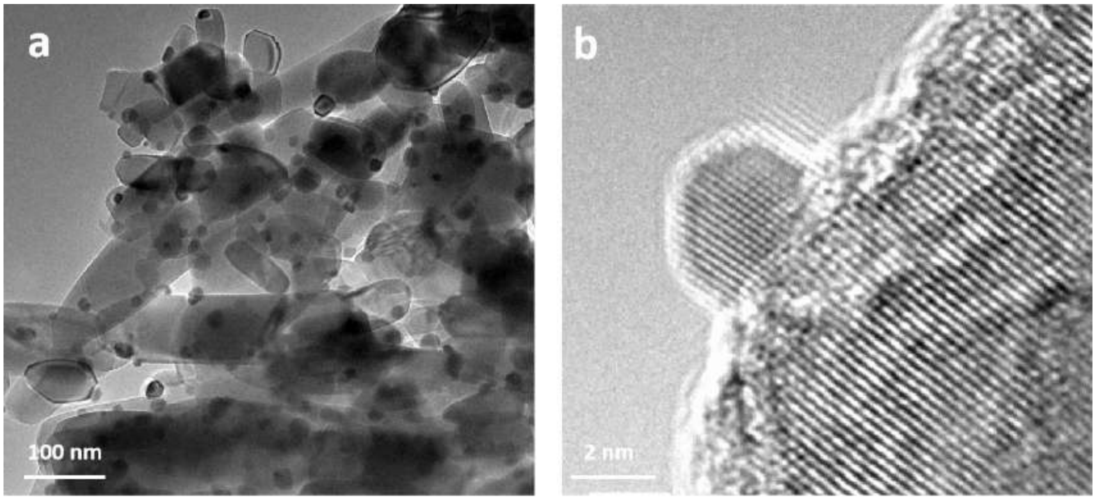

Figure S8. (a) TEM and (b) HR-TEM images of Pd_1Ag_3/r-TiO_2 (T750) after the long-term hydrogenation experiment for 120 h.

7. XRD spectra of Pd_1Ag_3/r-TiO_2

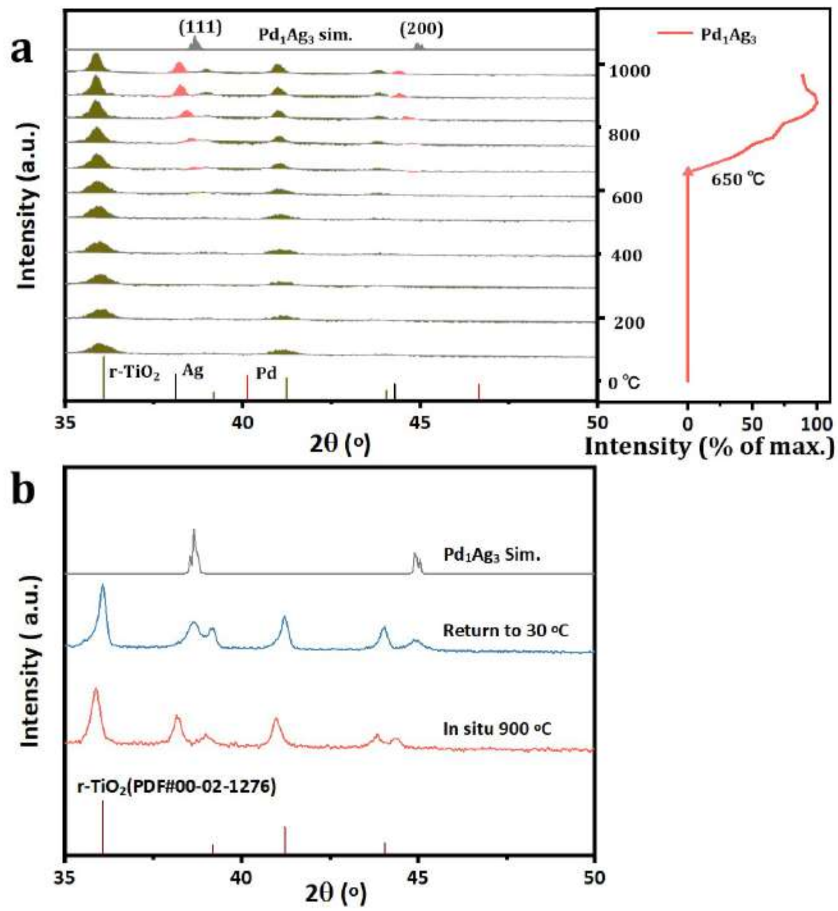

Figure S9. (a) In situ XRD patterns of a Pd_1Ag_3/r-TiO_2 sample during heating treatment from room temperature to 950 °C**. (b)** XRD pattern of Pd_1Ag_3/r-TiO_2. The standard patterns for pure Pd (JCPDS PDF # 00-046-1043) and Ag (JCPDS PDF # 00-04-0783) are attached at the bottom for comparison.

8. XRD patterns of Pd_1Ag_3 alloy on different supports

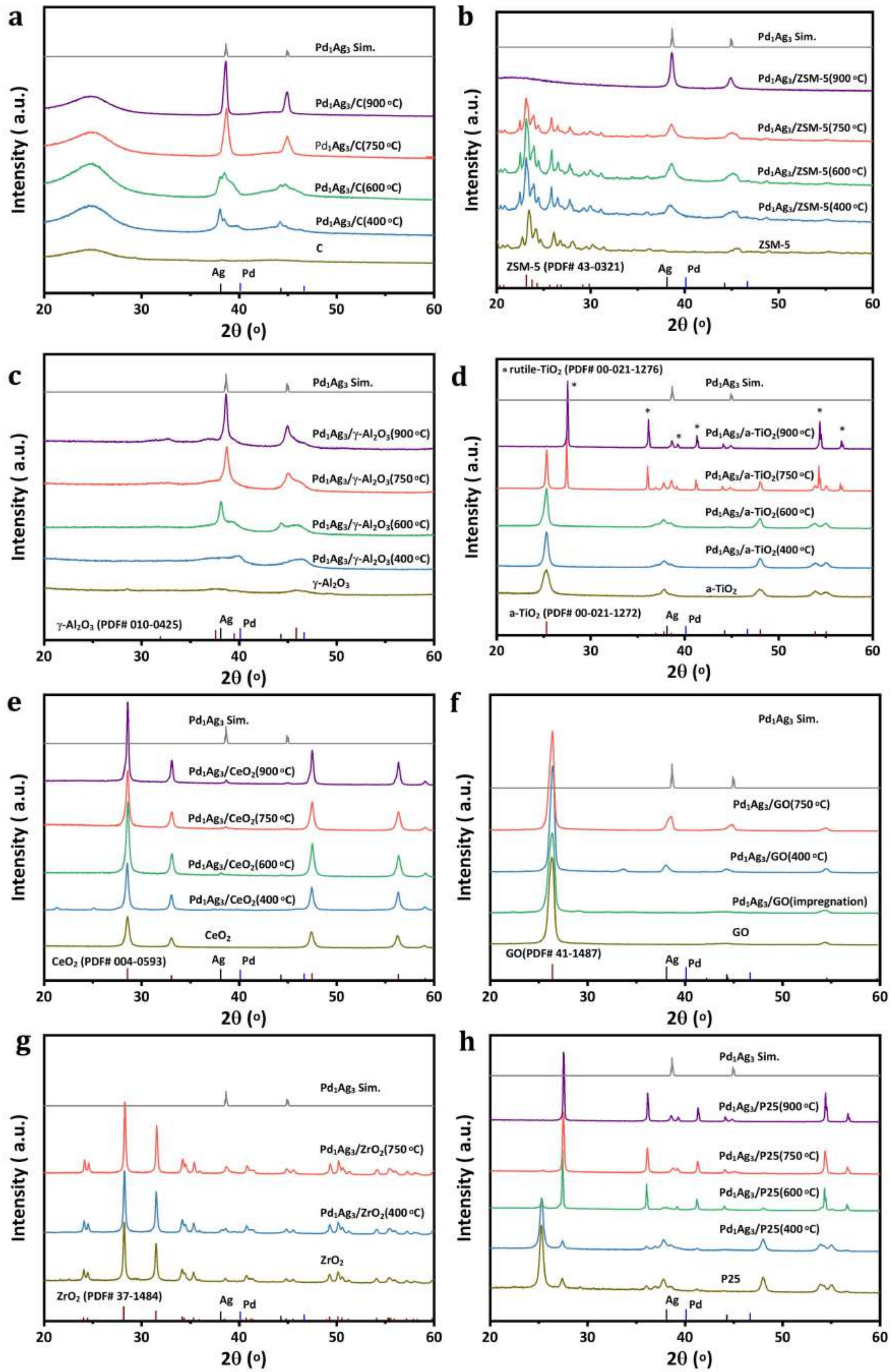

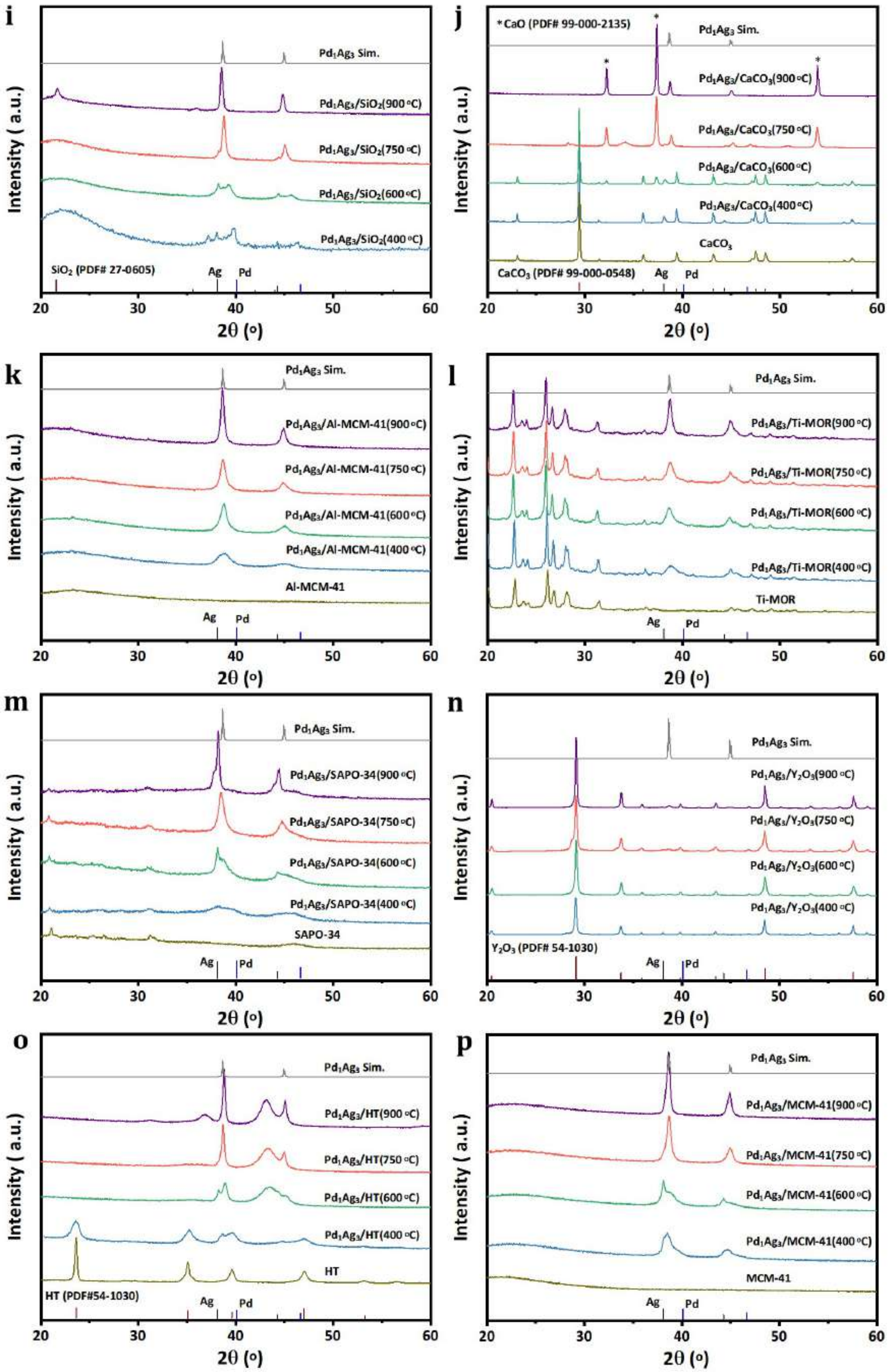
i
Pd_1Ag_3 Sim.
Pd_1Ag_3/SiO_2(900 °C)
Pd_1Ag_3/SiO_2(750 °C)
Pd_1Ag_3/SiO_2(600 °C)
Pd_1Ag_3/SiO_2(400 °C)
SiO_2 (PDF# 27-0605)
Ag
Pd
Intensity (a.u.)
2θ (°)
j
* CaO (PDF# 99-000-2135)
Pd_1Ag_3 Sim.
$Pd_1Ag_3/CaCO_3$(900 °C)
$Pd_1Ag_3/CaCO_3$(750 °C)
$Pd_1Ag_3/CaCO_3$(600 °C)
$Pd_1Ag_3/CaCO_3$(400 °C)
$CaCO_3$
$CaCO_3$ (PDF# 99-000-0548)
Ag
Pd
Intensity (a.u.)
2θ (°)
k
Pd_1Ag_3 Sim.
Pd_1Ag_3/Al-MCM-41(900 °C)
Pd_1Ag_3/Al-MCM-41(750 °C)
Pd_1Ag_3/Al-MCM-41(600 °C)
Pd_1Ag_3/Al-MCM-41(400 °C)
Al-MCM-41
Ag
Pd
Intensity (a.u.)
2θ (°)
l
Pd_1Ag_3 Sim.
Pd_1Ag_3/Ti-MOR(900 °C)
Pd_1Ag_3/Ti-MOR(750 °C)
Pd_1Ag_3/Ti-MOR(600 °C)
Pd_1Ag_3/Ti-MOR(400 °C)
Ti-MOR
Ag
Pd
Intensity (a.u.)
2θ (°)
m
Pd_1Ag_3 Sim.
Pd_1Ag_3/SAPO-34(900 °C)
Pd_1Ag_3/SAPO-34(750 °C)
Pd_1Ag_3/SAPO-34(600 °C)
Pd_1Ag_3/SAPO-34(400 °C)
SAPO-34
Ag
Pd
Intensity (a.u.)
2θ (°)
n
Pd_1Ag_3 Sim.
Pd_1Ag_3/Y_2O_3(900 °C)
Pd_1Ag_3/Y_2O_3(750 °C)
Pd_1Ag_3/Y_2O_3(600 °C)
Pd_1Ag_3/Y_2O_3(400 °C)
Y_2O_3 (PDF# 54-1030)
Ag
Pd
Intensity (a.u.)
2θ (°)
o
Pd_1Ag_3 Sim.
Pd_1Ag_3/HT(900 °C)
Pd_1Ag_3/HT(750 °C)
Pd_1Ag_3/HT(600 °C)
Pd_1Ag_3/HT(400 °C)
HT
HT (PDF#54-1030)
Ag
Pd
Intensity (a.u.)
2θ (°)
p
Pd_1Ag_3 Sim.
Pd_1Ag_3/MCM-41(900 °C)
Pd_1Ag_3/MCM-41(750 °C)
Pd_1Ag_3/MCM-41(600 °C)
Pd_1Ag_3/MCM-41(400 °C)
MCM-41
Ag
Pd
Intensity (a.u.)
2θ (°)

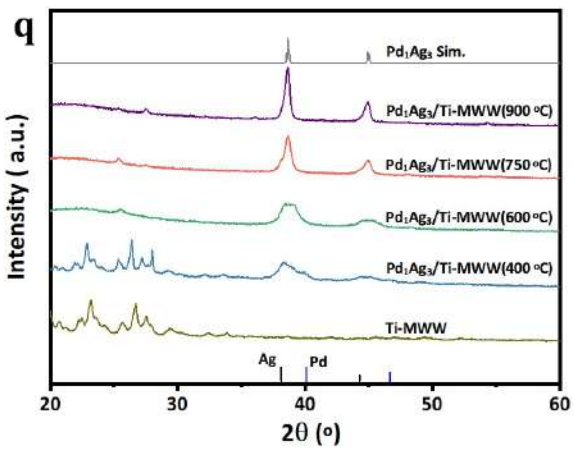

Figure S10. XRD patterns of Pd_1Ag_3 on different supports annealed at different temperatures. (a) C; (b) ZSM-5; (c) γ-Al_2O_3; (d) a-TiO_2; (e) CeO_2; (f) GO; (g) ZrO_2; (h) P25; (i) SiO_2; (j) $CaCO_3$; (k) Al-MCM-41; (l) Ti-MOR; (m) SAPO-34; (n) Y_2O_3; (o) HT; (p) MCM-41; (q) Ti-MWW. The standard patterns for pure Pd (JCPDS PDF # 46-1043) and Ag (JCPDS PDF # 04-0783 are attached at the bottom for comparison.

9. EXAFS results for the PdAg/r-TiO_2 (T750) catalyst

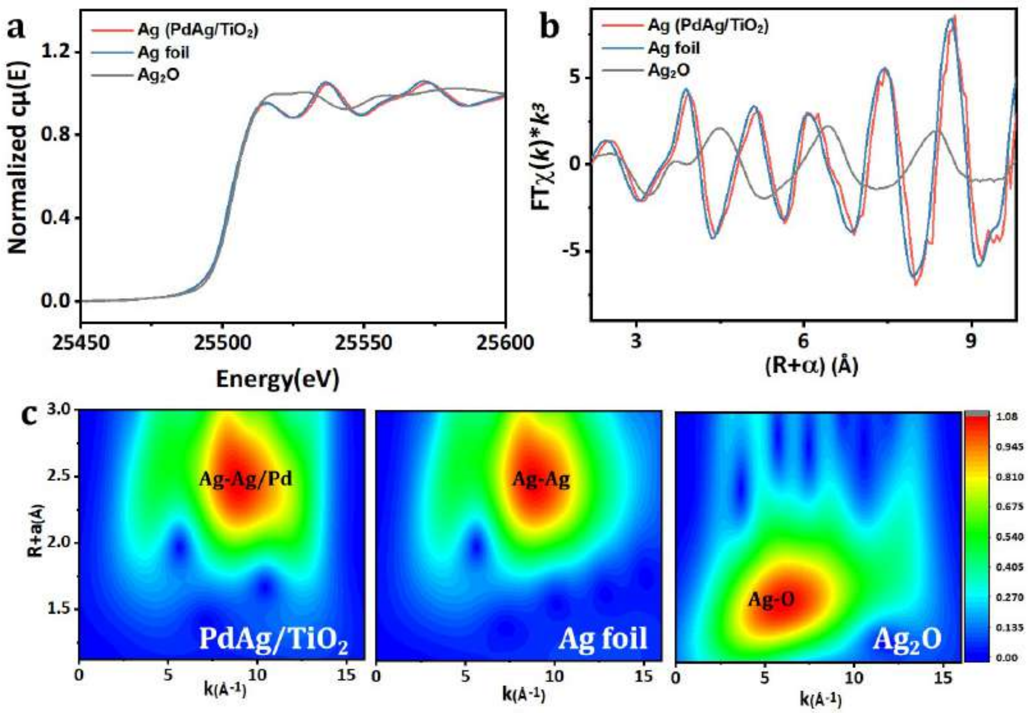

Figure S11. EXAFS results of the Ag species in Pd_1Ag_3 (T750) catalyst, Ag foil, and Ag_2O exposure to ambient conditions. (a) Normalized Ag K-edge, (b) the corresponding Fourier transforms of k^3-weighted EXAFS spectra and (c) wavelet transform EXAFS of T750, Ag foil, and Ag_2O exposure to ambient conditions.

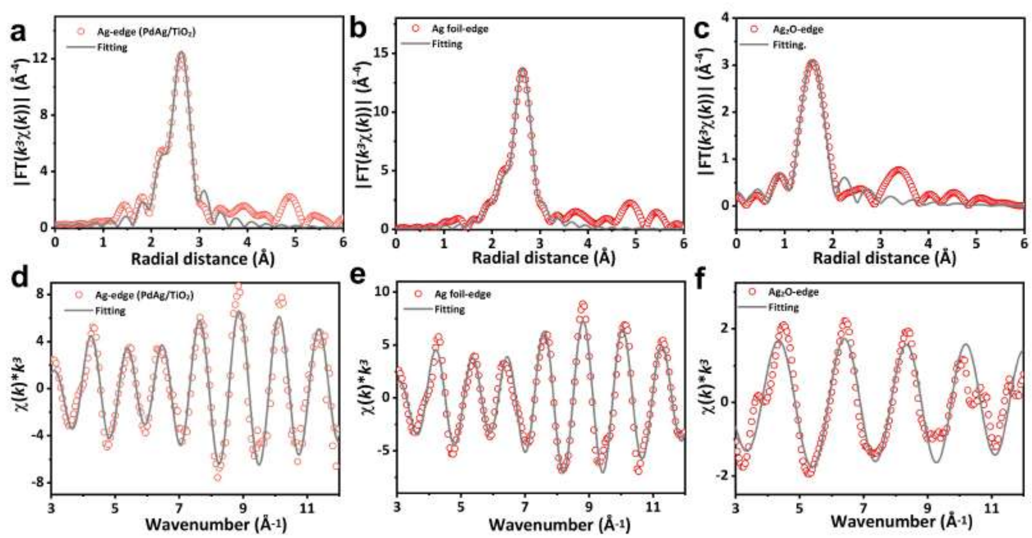

Figure 12. Ag K-edge EXAFS fitting plots. All fits performed in R-space (a-c) and oscillations in k-space (d-f) of Pd_1Ag_3/r-TiO_2 (T750), Ag foil, and Ag_2O exposure to ambient conditions.

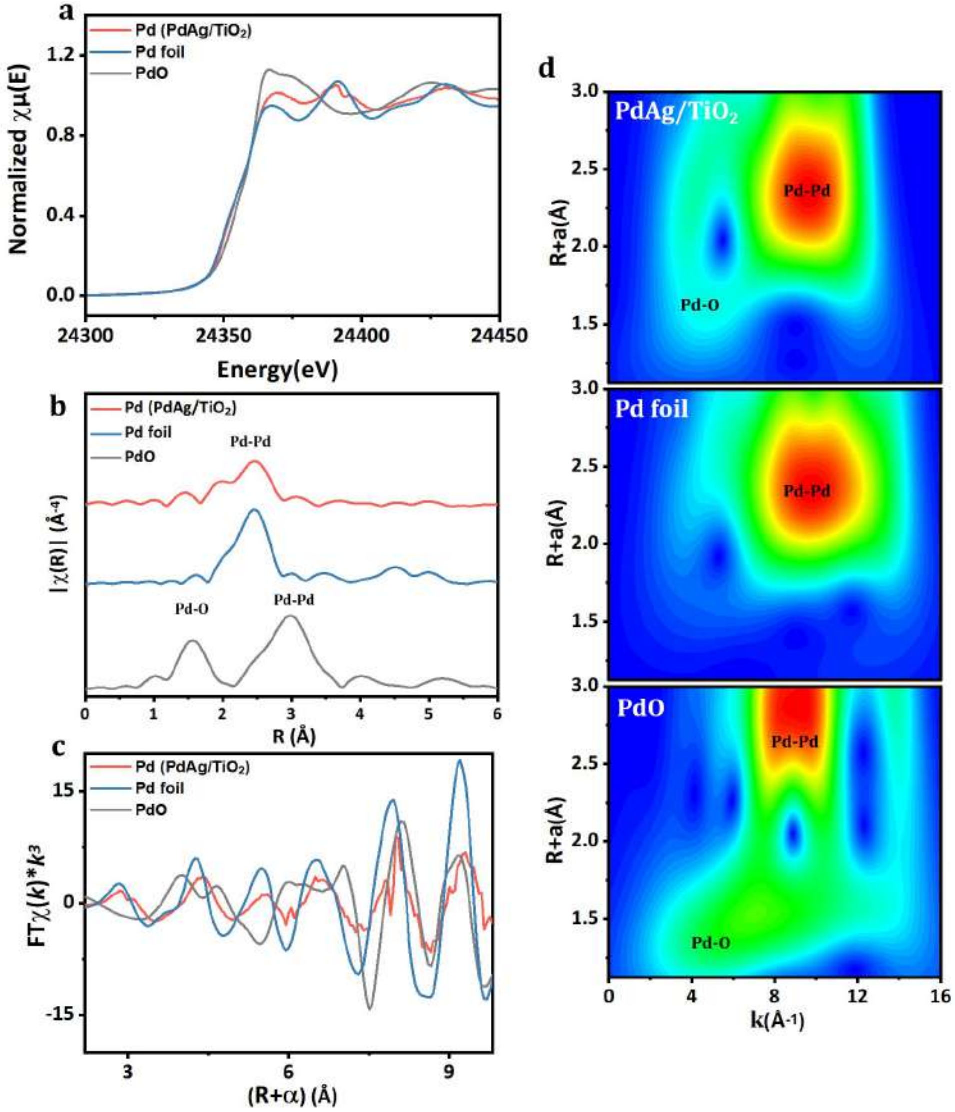

Figure S13. EXAFS results for the Pd species in Pd_1Ag_3 (T750) catalyst, Pd foil and PdO exposure to ambient conditions (a) Normalized Pd K-edge, b) Fourier transforms of k^3-weighted Pd K-edge; c) EXAFS oscillation functions at the Pd K-edge EXAFS spectra and (d) wavelet transform EXAFS of T750, Pd foil and PdO exposure to ambient conditions.

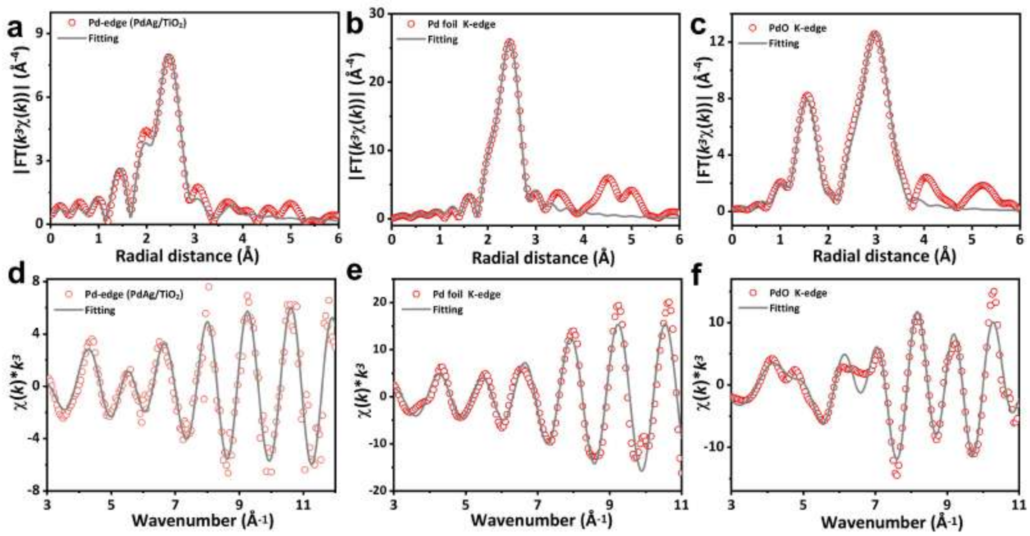

Figure S14. Pd K-edge EXAFS fitting plots. All fits performed in R-space (a-c) and oscillations in k-space (d-f) of Pd_1Ag_3/r-TiO_2 (T750), Pd foil, and PdO exposure to ambient conditions

10. Microkinetic simulations

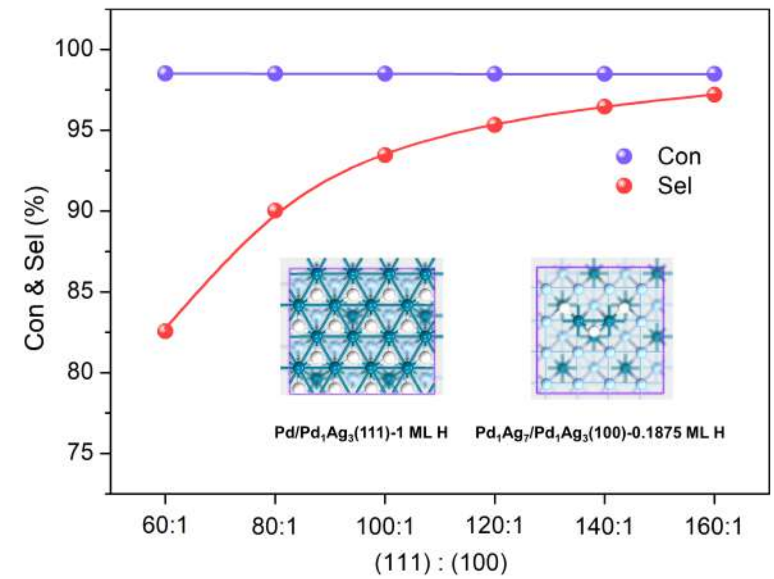

Figure S15. Microkinetic simulations for the hydrogenation reaction on two thermodynamic stable surfaces of Pd_1Ag_3, the Pd_1Ag_3(111) exposing all Pd atoms with 1 ML H adsorbed at the hollow sites and Pd_1Ag_3(100) exposed Pd_2 dimer sites with 3 adsorbed H atoms. The simulations at typical reaction conditions (i.e. 80 °C, $p(H_2)$: $p(C_2H_2)$: $p(C_2H_4)$ = 5 : 0.5 : 50) show that the increase of (111):(100) ratio from 60:1 to 160:1 can lift the ethylene selectivity from 82.56% to 97.19% (red curve).

11. Experimental dataset for RF ML.

Table S1. The experimental dataset for RF ML with detailed synthetic conditions and the catalytic performance.

Entry	Catalyst	Reaction Temp. (°C)	Yield (%)	Ann. Temp. (°C)	Reductant	Ann. Time (h)	Pre-Oxi.*	Load Pd# (%)	Load Ag# (%)	Support
1	Pd_1Ag_3/C	100	91.2	600	5% H_2	4	N	1	3	C
2	Pd_1Ag_3/Al-MCM-41	118	90.2	600	5% H_2	4	N	1	3	Al-MCM-41
3	Pd_1Ag_3/r-TiO_2	86	90.1	650	100% H_2	4	Y	1	3	r-TiO_2
4	Pd_1Ag_3/Ti-Mor	91	89.9	600	5% H_2	4	N	1	3	Ti-MOR
5	Pd_1Ag_3/a-TiO_2	82.5	89.8	450	5% H_2	4	Y	1	3	a-TiO_2
6	Pd_1Ag_3/r-TiO_2	83	89.7	650	100% H_2	4	Y	1	3	r-TiO_2
7	Pd_1Ag_3/r-TiO_2	82	89.4	650	100% H_2	4	Y	1	3	r-TiO_2
8	Pd_1Ag_3/a-TiO_2	90	89.3	450	5% H_2	4	Y	1	3	a-TiO_2
9	Pd_1Ag_3/r-TiO_2	68	89.1	600	5% H_2	4	N	1	3	r-TiO_2
10	Pd_1Ag_3/r-TiO_2	85	88.8	600	100% H_2	4	Y	1	3	r-TiO_2
11	Pd_1Ag_3/a-TiO_2	58	88.8	400	5% H_2	4	Y	1	3	a-TiO_2
12	Pd_1Ag_3/r-TiO_2	67.5	88.7	600	5% H_2	4	Y	1	3	r-TiO_2
13	Pd_1Ag_3/r-TiO_2	68	88.7	600	5% H_2	4	Y	1	3	r-TiO_2
14	Pd_1Ag_3/ZSM-5	95	88.6	600	5% H_2	4	N	1	3	ZSM-5
15	Pd_1Ag_3/a-TiO_2	60	88.4	400	5% H_2	4	N	1	3	a-TiO_2
16	Pd_1Ag_3/r-TiO_2	67	88.3	600	5% H_2	4	Y	1	3	r-TiO_2
17	Pd_1Ag_3/r-TiO_2	87	88.2	600	100% H_2	4	Y	1	3	r-TiO_2
18	Pd_1Ag_3/r-TiO_2	70	88.2	600	5% H_2	4	N	1	3	r-TiO_2
19	Pd_1Ag_3/C	80	88.0	600	5% H_2	4	N	1	3	C
20	Pd_1Ag_3/r-TiO_2	68	87.2	450	5% H_2	4	N	1	3	r-TiO_2
21	Pd_1Ag_3/r-TiO_2	80	87.2	600	100% H_2	4	Y	1	3	r-TiO_2
22	Pd_1Ag_3/r-TiO_2	72	87.0	600	5% H_2	4	Y	1	3	r-TiO_2
23	Pd_1Ag_3/a-TiO_2	75	87.0	400	5% H_2	4	Y	1	3	a-TiO_2
24	Pd_1Ag_3/r-TiO_2	70	86.9	600	5% H_2	4	Y	1	3	r-TiO_2
25	Pd_1Ag_3/a-TiO_2	92	86.6	400	5% H_2	4	Y	1	3	a-TiO_2
26	Pd_1Ag_3/P25	69	86.6	450	5% H_2	4	N	1	3	P25
27	Pd_1Ag_3Pb/HT	100	86.5	400	5% H_2	4	Y	1	3	HT
28	Pd_1Ag_3/CeO_2	90	86.3	600	5% H_2	4	N	1	3	CeO_2
29	Pd_1Ag_3/r-TiO_2	83	86.2	450	5% H_2	4	N	1	3	r-TiO_2
30	Pd_1Ag_3-Y/r-TiO_2	58	86.0	400	5% H_2	4	N	1	3	r-TiO_2
31	Pd_1Ag_3/r-TiO_2	76	86.0	450	100% H_2	4	Y	1	3	r-TiO_2
32	Pd_1Ag_3/r-TiO_2	60	85.9	450	100% H_2	4	Y	1	3	r-TiO_2
33	Pd_1Ag_3/HT	85	85.9	600	5% H_2	4	N	1	3	HT
34	Pd_1Ag_3/HT	80	85.6	600	5% H_2	4	N	1	3	HT
35	Pd_1Ag_3/r-TiO_2	70	85.4	450	100% H_2	4	Y	1	3	r-TiO_2
36	Pd_1Ag_3/r-TiO_2	65	85.3	450	100% H_2	4	Y	1	3	r-TiO_2
37	Pd_1Ag_3/a-TiO_2	105	85.3	400	5% H_2	4	Y	1	3	a-TiO_2
38	Pd_1Ag_3/r-TiO_2	75	85.3	450	100% H_2	4	Y	1	3	r-TiO_2
39	Pd_1Ag_3/r-TiO_2	79	85.1	400	5% H_2	4	N	1	3	r-TiO_2
40	Pd_1Ag_3B/r-TiO_2	85	85.0	400	5% H_2	4	Y	1	3	r-TiO_2
41	Pd_1Ag_3B/r-TiO_2	85	84.9	400	5% H_2	4	Y	1	3	r-TiO_2
42	Pd_1Ag_3/HT	85	84.9	600	5% H_2	4	N	1	3	HT

Supplementary Table 2. Continued from previous page.

43	Pd_1Ag_3/r-TiO_2	63	84.5	400	5% H_2	4	Y	1	3	r-TiO_2
44	Pd_1Ag_3/r-TiO_2	64	84.5	400	100% H_2	4	Y	1	3	r-TiO_2
45	Pd_1Ag_3/a-TiO_2	100	84.4	400	5% H_2	4	Y	1	3	a-TiO_2
46	Pd_1Ag_3/r-TiO_2	60	84.4	400	5% H_2	4	Y	1	3	r-TiO_2
47	Pd_1Ag_3/r-TiO_2	63	84.3	400	100% H_2	4	Y	1	3	r-TiO_2
48	$Pd_1Ag_3Y_1$/HT	75	84.0	600	5% H_2	4	N	1	3	HT
49	Pd_1Ag_3/HT	75	83.9	600	5% H_2	4	Y	1	3	HT
50	Pd_1Ag_3/r-TiO_2	80	83.9	450	Air	4	Y	1	3	r-TiO_2
51	Pd_1Ag_3/HT	60	83.8	600	5% H_2	4	Y	1	3	HT
52	Pd_1Ag_3/r-TiO_2	88	83.8	400	100% H_2	4	Y	1	3	r-TiO_2
53	Pd_1Ag_3/a-Al_2O_3	83	83.7	600	5% H_2	4	N	1	3	a-Al_2O_3
54	Pd_1Ag_3/γ-Al_2O_3	78	83.6	600	5% H_2	4	N	1	3	γ-Al_2O_3
55	Pd_1Ag_3/r-TiO_2	63	83.5	400	100% H_2	4	Y	1	3	r-TiO_2
56	Pd_1Ag_3Y/HT	60	83.4	400	5% H_2	4	Y	1	3	HT
57	Pd_1Ag_3/ZrO_2	53	83.4	450	5% H_2	4	N	1	3	ZrO_2
58	Pd_1Ag_3/HT	60	83.3	600	5% H_2	4	Y	1	3	HT
59	$Pd_1Ag_3Y_1$/HT	85	83.3	450	5% H_2	3	N	1	3	HT
60	Pd_1Ag_3/HT	80	83.3	600	5% H_2	4	Y	1	3	HT
61	Pd_1Ag_3/r-TiO_2	80	83.2	400	100% H_2	4	Y	1	3	r-TiO_2
62	Pd_1Ag_3/r-TiO_2	85	83.2	400	100% H_2	4	Y	1	3	r-TiO_2
63	Pd_1Ag_3/r-TiO_2	75	83.1	300	5% H_2	4	N	1	3	r-TiO_2
64	Pd_1Ag_3/HT	105	83.1	600	5% H_2	4	Y	5	15	HT
65	Pd_1Ag_3/P25	80	82.8	400	5% H_2	4	N	1	3	P25
66	Pd_1Ag_3/Y_2O_3	79	82.7	600	5% H_2	4	N	1	3	Y_2O_3
67	Pd_1Ag_3/r-TiO_2	69	82.6	300	5% H_2	4	N	1	3	r-TiO_2
68	Pd_1Ag_3/a-TiO_2	100	82.6	300	5% H_2	4	Y	1	3	a-TiO_2
69	Pd_1Ag_3/HT	53	82.6	600	5% H_2	4	Y	1	3	HT
70	Pd_1Ag_3/r-TiO_2	63	82.5	300	5% H_2	4	Y	1	3	r-TiO_2
71	Pd_1Ag_3/HT	63	82.5	600	5% H_2	4	Y	1	3	HT
72	Pd_1Ag_3/r-TiO_2	64	82.5	400	100% H_2	4	Y	1	3	r-TiO_2
73	Pd_1Ag_3/r-TiO_2	75	82.5	400	5% H_2	4	Y	0.2	0.6	r-TiO_2
74	$Pd_1Ag_3Y_2$/HT	80	82.4	250	5% H_2	4	N	1	3	HT
75	Pd_1Ag_3/γ-Al_2O_3	70	82.2	600	5% H_2	4	N	1	3	γ-Al_2O_3
76	Pd_1Ag_3/r-TiO_2	70	82.1	400	100% H_2	4	Y	1	3	r-TiO_2
77	Pd_1Ag_3/HT	68.5	82.1	600	5% H_2	4	Y	1	3	HT
78	Pd_1Ag_3/r-TiO_2	95	82.0	400	5% H_2	4	Y	0.01	0.03	r-TiO_2
79	Pd_1Ag_3/r-TiO_2	80	82.0	400	100% H_2	4	Y	1	3	r-TiO_2
80	Pd_1Ag_3/CeO_2	83	81.6	400	5% H_2	4	Y	1	3	CeO_2
81	Pd_1Ag_3/C	55	81.5	450	5% H_2	4	N	1	3	C
82	Pd_1Ag_3/P25	70	81.3	400	5% H_2	4	Y	1	3	P25
83	Pd_1Ag_3/P25	75	81.0	400	5% H_2	4	Y	1	3	P25
84	Pd_1Ag_3/r-TiO_2	95	81.0	400	5% H_2	4	Y	0.01	0.03	r-TiO_2
85	Pd_1Ag_3/r-TiO_2	80	80.9	300	100% H_2	4	Y	1	3	r-TiO_2
86	Pd_1Ag_3/a-TiO_2	115	80.9	300	5% H_2	4	Y	1	3	a-TiO_2
87	Pd_1Ag_3/a-TiO_2	62	80.9	300	5% H_2	4	N	1	3	a-TiO_2
88	Pd_1Ag_3/SiO_2	70	80.8	600	5% H_2	4	N	1	3	SiO_2
89	Pd_1Ag_3/r-TiO_2	70	80.8	450	Air	4	Y	1	3	r-TiO_2
90	Pd_1Ag_3/Y_2O_3	84	80.4	600	5% H_2	4	N	1	3	Y_2O_3
91	Pd_1Ag_3Y/r-TiO_2	65	80.3	400	5% H_2	4	N	1	3	r-TiO_2

Supplementary Table 2. Continued from previous page.

92	Pd_1Ag_3/Ti-Mor	70	80.1	300	5% H_2	4	N	1	3	Ti-MOR
93	Pd_1Ag_3/a-TiO_2	80	80.1	150	5% H_2	4	Y	1	3	a-TiO_2
94	Pd_1Ag_3/r-TiO_2	65	79.9	150	5% H_2	4	N	1	3	r-TiO_2
95	Pd_1Ag_3/a-TiO_2	55	79.7	150	5% H_2	4	N	1	3	a-TiO_2
96	$Pd_1Ag_3Y_1$/HT	85	79.7	350	5% H_2	3	N	1	3	HT
97	Pd_1Ag_3/MCM-41	58	79.5	600	5% H_2	4	N	1	3	MCM-41
98	Pd_1Ag_3/r-TiO_2	81	79.3	300	100% H_2	4	Y	1	3	r-TiO_2
99	Pd_1Ag_2/r-TiO_2	54	78.7	400	5% H_2	4	Y	1	2	r-TiO_2
100	Pd_1Ag_3/P25	72	78.7	300	5% H_2	4	N	1	3	P25
101	Pd_1Ag_3/r-TiO_2	80	78.7	400	5% H_2	4	Y	0.2	0.6	r-TiO_2
102	Pd_1Ag_3/HT	70	78.6	400	5% H_2	4	N	1	3	HT
103	Pd_1Ag_3/MCM-41	54	78.3	600	5% H_2	4	N	1	3	MCM-41
104	Pd_1Ag_3/r-TiO_2	72	78.2	150	5% H_2	4	N	1	3	r-TiO_2
105	Pd_1Ag_3/HT	60	78.0	400	5% H_2	4	N	1	3	HT
106	$Pd_1Ag_3Y_{0.5}$/HT	70	77.9	250	5% H_2	4	N	1	3	HT
107	Pd_1Ag_3/SAPO-34	83	77.9	600	5% H_2	4	N	1	3	SAPO-34
108	Pd_1Ag_3/P25	66	77.8	300	5% H_2	4	N	1	3	P25
109	Pd_1Ag_1/r-TiO_2	85	77.6	400	5% H_2	4	Y	1	1	r-TiO_2
110	$Pd_1Ag_3Y_1$/HT	40	77.5	400	5% H_2	5	Y	1	3	HT
111	Pd_1Ag_3/γ-Al_2O_3	60	77.4	450	5% H_2	4	N	1	3	γ-Al_2O_3
112	$Pd_1Ag_3Y_1$/r-TiO_2	75	77.3	400	5% H_2	4	Y	1	3	r-TiO_2
113	Pd_1Ag_3/HT	67	77.3	400	5% H_2	4	N	1	3	HT
114	Pd_1Ag_3/HT	60	77.2	400	5% H_2	4	N	1	3	HT
115	Pd_1Ag_3/r-TiO_2	66	77.2	150	5% H_2	4	N	1	3	r-TiO_2
116	Pd_1Ag_3/C	42	77.0	400	5% H_2	4	N	1	3	C
117	Pd_1Ag_3/r-TiO_2	67	76.9	150	5% H_2	4	N	1	3	r-TiO_2
118	$Pd_1Ag_3Y_1$/HT	75	76.3	550	5% H_2	4	N	1	3	HT
119	Pd_1Ag_4/r-TiO_2	85	76.2	400	5% H_2	4	Y	1	4	r-TiO_2
120	$Pd_1Ag_3Y_1$/HT	70	76.2	250	5% H_2	3	N	1	3	HT
121	Pd_1Ag_3/r-TiO_2	60	76.1	300	100% H_2	4	Y	1	3	r-TiO_2
122	Pd_1Ag_3/r-TiO_2	56	75.8	150	5% H_2	4	Y	1	3	r-TiO_2
123	Pd_1Ag_3/r-TiO_2	70	75.6	300	100% H_2	4	Y	1	3	r-TiO_2
124	Pd_1Ag_3/a-TiO_2	90	75.6	150	5% H_2	4	Y	5	15	a-TiO_2
125	Pd_1Ag_3/γ-Al_2O_3	60	75.3	450	5% H_2	4	Y	1	3	γ-Al_2O_3
126	Pd_1Ag_1/r-TiO_2	49	75.3	400	5% H_2	4	Y	1	1	r-TiO_2
127	Pd_1Ag_4/r-TiO_2	63	75.1	400	5% H_2	4	Y	1	4	r-TiO_2
128	Pd_1Ag_5/r-TiO_2	60	75.0	400	5% H_2	4	Y	1	5	r-TiO_2
129	$Pd_1Ag_3Y_1$/HT	65	74.9	350	5% H_2	4	N	1	3	HT
130	Pd_1Ag_3/CeO_2	70	74.9	300	5% H_2	4	N	1	3	CeO_2
131	Pd_1Ag_1/HT	35	74.5	600	5% H_2	4	N	1	1	HT
132	Pd_1Ag_3/r-TiO_2	85	74.5	400	100% H_2	4	Y	5	15	r-TiO_2
133	Pd_1Ag_3Bi/HT	130	74.3	400	5% H_2	4	Y	1	3	HT
134	Pd_1Ag_3/ZSM-5	65	74.2	400	5% H_2	4	Y	1	3	ZSM-5
135	Pd_1Ag_4/HT	75	73.9	600	5% H_2	4	Y	1	4	HT
136	Pd_1Ag_3/r-TiO_2	52	73.9	150	100% H_2	4	Y	1	3	r-TiO_2
137	Pd_1Ag_3/HT	60	73.5	300	5% H_2	4	Y	1	3	HT
138	Pd_1Ag_3/r-TiO_2	56	73.5	150	5% H_2	4	Y	1	3	r-TiO_2

Supplementary Table 2. Continued from previous page.

139	Pd_1Ag_3/Al-MCM-41	95	73.2	400	5% H_2	4	Y	1	3	Al-MCM-41
140	Pd_1Ag_3K/HT	90	73.1	400	5% H_2	4	Y	1	3	HT
141	Pd_1Ag_3/Ti-MWW	68	73.1	600	5% H_2	4	N	1	3	Ti-MWW
142	$Pd_1Ag_3Y_1$/HT	70	73.0	150	5% H_2	3	N	1	3	HT
143	Pd_1Ag_3/HT	55	72.8	300	5% H_2	4	Y	1	3	HT
144	$Pd_1Ag_3Y_1$/HT	60	72.7	150	5% H_2	3	N	1	3	HT
145	Pd_1Ag_3/HT	46	72.5	400	5% H_2	4	Y	1	3	HT
146	Pd_1Ag_3/r-TiO_2	85	72.5	400	5% H_2	4	Y	0.01	0.03	r-TiO_2
147	Pd_1Ag_3/HT	50	72.4	400	5% H_2	4	Y	1	3	HT
148	Pd_1Ag_3/HT	50	72.4	400	5% H_2	4	Y	1	3	HT
149	$Pd_1Ag_3Y_1$/HT	50	72.3	700	5% H_2	3	N	1	3	HT
150	Pd_1Ag_3/ZrO_2	56	72.3	300	5% H_2	4	N	1	3	ZrO_2
151	Pd_1Ag_3/r-TiO_2	90	72.2	400	100% H_2	4	Y	5	15	r-TiO_2
152	Pd_1Ag_3/r-TiO_2	70	72.2	150	100% H_2	4	Y	1	3	r-TiO_2
153	Pd_1Ag_3/SAPO-34	60	72.2	300	5% H_2	4	N	1	3	SAPO-34
154	Pd_1Ag_5/r-TiO_2	90	72.2	400	5% H_2	4	Y	1	5	r-TiO_2
155	Pd_1Ag_4/HT	70	72.1	600	5% H_2	4	Y	1	4	HT
156	Pd_1Ag_3/SiO_2	63	72.1	450	5% H_2	4	N	1	3	SiO_2
157	Pd_1Ag_2/HT	40	71.8	600	5% H_2	4	Y	1	2	HT
158	Pd_1Ag_3/a-Al_2O_3	67	71.6	400	5% H_2	4	Y	1	3	a-Al_2O_3
159	Pd_1Ag_3/r-TiO_2	70	71.6	150	100% H_2	4	Y	1	3	r-TiO_2
160	$Pd_1Ag_3Y_1$/HT	65	71.6	150	5% H_2	4	N	1	3	HT
161	Pd_1Ag_3/HT	65	71.5	400	5% H_2	4	Y	1	3	HT
162	$Pd_1Ag_3Y_1$/HT	65	70.8	250	5% H_2	4	N	1	3	HT
163	Pd_1Ag_3/$CaCO_3$	53	70.8	450	5% H_2	4	N	1	3	$CaCO_3$
164	Pd_1Ag_3/r-TiO_2	80	70.3	400	5% H_2	4	Y	0.2	0.6	r-TiO_2
165	Pd_1Ag_3/ZSM-5	80	70.0	300	5% H_2	4	N	1	3	ZSM-5
166	$Pd_1Ag_3Y_1$/HT	38	69.7	400	5% H_2	10	Y	1	3	HT
167	Pd_1Ag_3/MCM-41	50	69.7	450	5% H_2	4	N	1	3	MCM-41
168	Pd_1Ag_3/r-TiO_2	80	69.1	150	100% H_2	4	Y	1	3	r-TiO_2
169	Pd_1Ag_5/HT	75	68.9	600	5% H_2	4	Y	1	5	HT
170	Pd_1Ag_3/Al-MCM-41	74	68.8	300	5% H_2	4	N	1	3	Al-MCM-41
171	Pd_1Ag_3/a-Al_2O_3	56	68.8	300	5% H_2	4	N	1	3	a-Al_2O_3
172	Pd_1Ag_3/r-TiO_2	70	68.6	150	100% H_2	4	Y	1	3	r-TiO_2
173	Pd_1Ag_3/γ-Al_2O_3	55	68.4	150	5% H_2	4	N	1	3	γ-Al_2O_3
174	Pd_1Ag_3/C	50	68.2	300	5% H_2	4	N	1	3	C
175	Pd_1Ag_3/HT	55	67.8	300	5% H_2	4	Y	1	3	HT
176	Pd_1Ag_3/HT	50	67.2	300	5% H_2	4	Y	1	3	HT
177	Pd_1Ag_3/ZrO_2	49	67.0	150	5% H_2	4	N	1	3	ZrO_2
178	Pd_1Ag_3/r-TiO_2	72.5	67.0	150	100% H_2	4	Y	1	3	r-TiO_2
179	$Pd_1Ag_1Y_2$/HT	40	66.2	400	5% H_2	4	Y	1	1	HT
180	Pd_1Ag_3/HT	50	66.2	300	5% H_2	4	Y	1	3	HT
181	$Pd_1Ag_1Y_1$/HT	40	65.6	400	5% H_2	4	Y	1	1	HT
182	Pd_1Ag_2/HT	50	65.4	400	5% H_2	4	Y	1	2	HT
183	Pd_1Ag_3/HT	55	65.0	300	5% H_2	4	N	1	3	HT

Supplementary Table 2. Continued from previous page.

184	Pd_1Ag_3/Ti-MWW	70	64.6	400	5% H_2	4	Y	1	3	Ti-MWW
185	Pd_1Ag_3/HT	55	63.9	250	5% H_2	4	N	1	3	HT
186	Pd_1Ag_3/Ti-MWW	35	63.8	300	5% H_2	4	N	1	3	Ti-MWW
187	Pd_1Ag_3/HT	50	62.7	250	5% H_2	4	Y	1	3	HT
188	PdPb/$CaCO_3$	60	62.5	60	5% H_2	4	N	5	0	$CaCO_3$
189	Pd_1Ag_3/CeO_2	42	61.4	150	5% H_2	4	N	1	3	CeO_2
190	Pd_1Ag_3/P25	42	61.4	150	5% H_2	4	N	1	3	P25
191	$Pd_1Ag_{0.5}Y_{1.5}$/HT	35	61.3	400	5% H_2	4	Y	1	0.5	HT
192	Pd_1Ag_4/HT	50	61.3	400	5% H_2	4	Y	1	4	HT
193	Pd_1Ag_3/HT	55	61.1	250	5% H_2	4	Y	1	3	HT
194	Pd_1Ag_1/HT	42	61.0	450	5% H_2	4	Y	1	1	HT
195	Pd_1Ag_3/Y_2O_3	40	60.9	400	5% H_2	4	Y	1	3	Y_2O_3
196	Pd_1Ag_3/γ-Al_2O_3	70	59.7	400	5% H_2	4	Y	1	3	γ-Al_2O_3
197	$Pd_1Ag_{0.5}Y_{0.5}$/HT	35	59.2	400	5% H_2	4	Y	1	0.5	HT
198	Pd_1Ag_5/HT	70	59.2	400	5% H_2	4	Y	1	5	HT
199	Pd_1Ag_3/γ-Al_2O_3	65	58.1	400	5% H_2	4	Y	1	3	γ-Al_2O_3
200	Pd_1Ag_2/HT	60	57.9	150	5% H_2	4	Y	1	2	HT
201	PdxB/C	20	57.7	120	DMAB	12	N	10	0	C
202	Pd_1Ag_3/r-TiO_2	90	56.0	0	$NaBH_4$	1	N	1	3	r-TiO_2
203	Pd NS/C	40	55.8	200	5% H_2	2	N	10	0	C
204	Pd_1Ag_3/a-Al_2O_3	51	55.6	150	5% H_2	4	N	1	3	a-Al_2O_3
205	Pd_1Ag_3/MCM-41	44	55.6	400	5% H_2	4	Y	1	3	MCM-41
206	Pd_1Ag_4/HT	40	55.0	150	5% H_2	4	Y	1	4	HT
207	Pd_1Ag_3/HT	40	55.0	150	5% H_2	4	Y	1	3	HT
208	$Pd_1Pb_{0.3}$ NS/γ-Al_2O_3	40	54.7	150	5% H_2	2	N	1	0	γ-Al_2O_3
209	Pd_1Ag_3/SiO_2	50	54.1	150	5% H_2	4	N	1	3	SiO_2
210	Pd/r-TiO_2	25	54.0	600	5% H_2	4	N	1	0	r-TiO_2
211	Pd_1Ag_3/SiO_2	55	54.0	400	5% H_2	4	Y	1	3	SiO_2
212	Pd/HT	20	53.7	600	5% H_2	4	Y	1	0	HT
213	Pd_1Ag_3/$CaCO_3$	45	53.7	400	5% H_2	4	Y	1	3	$CaCO_3$
214	Pd_1Ag_3/$CaCO_3$	14	53.1	150	5% H_2	4	N	1	3	$CaCO_3$
215	Pd/HT	30	52.4	600	5% H_2	4	Y	1	0	HT
216	Pd_1Ag_3/r-TiO_2	120	52.2	400	5% H_2	4	Y	0.05	0.15	r-TiO_2
217	Pd_1Ag_2/r-TiO_2	60	51.7	400	5% H_2	4	Y	1	2	r-TiO_2
218	Pd/r-TiO_2	20	51.5	600	5% H_2	4	Y	1	0	r-TiO_2
219	Pd_1Ag_1/HT	45	51.5	400	5% H_2	4	Y	1	1	HT
220	Pd_1Ag_3/C	47	50.6	150	5% H_2	4	N	1	3	C
221	Pd_1Ag_3 NS/C	70	50.2	200	5% H_2	2	N	10	30	C
222	Pd_1Ag_5/HT	65	50.2	150	5% H_2	4	Y	1	5	HT
223	Pd_1Ag_3/r-TiO_2	85	50.1	0	$NaBH_4$	1	N	1	3	r-TiO_2
224	Pd_1Ag_3/r-TiO_2	65	48.4	60	Air	0	N	5	15	r-TiO_2
225	$Pd_1Ag_1Y_2$/HT	45	48.3	250	5% H_2	4	N	1	1	HT
226	Pd_1Ag_3/r-TiO_2	70	47.0	60	Air	0	N	5	15	r-TiO_2
227	Pd_1Ag_1/HT	60	47.0	300	5% H_2	4	Y	1	1	HT
228	Pd/r-TiO_2	25	46.5	400	5% H_2	4	N	1	0	r-TiO_2
229	Pd_1Ag_{10}/HT	70	44.2	400	5% H_2	4	Y	1	1	HT
230	Pd_1Ag_3/r-TiO_2	65	44.0	60	Air	0	N	5	15	r-TiO_2

Supplementary Table 2. Continued from previous page.

231	Pd_1Ag_3/r-TiO_2	120	43.6	400	5% H_2	4	N	0.05	0.15	r-TiO_2
232	Pd_1Ag_1/HT	35	42.5	150	5% H_2	4	N	1	1	HT
233	Pd/α-Al_2O_3	30	40.8	60	5% H_2	4	N	1	0	a-Al_2O_3
234	Pd_3Y_1/HT	25	40.6	250	5% H_2	4	Y	1	0	HT
235	Pd/HT	25	38.1	400	5% H_2	4	N	1	0	HT
236	Pd/HT	33	36.4	400	5% H_2	4	Y	1	0	HT
237	Pd_2B/C	5	30.6	120	DMAB	12	N	20	0	C
238	Pd_1Ag_3/r-TiO_2	125	26.0	400	5% H_2	4	Y	0.05	0.15	r-TiO_2
239	Pd_1Ag_3/MCM-41	40	25.9	300	5% H_2	4	N	1	3	MCM-41
240	Pd/r-TiO_2	15	25.1	400	5% H_2	4	Y	1	0	r-TiO_2
241	Pd/HT	40	24.4	150	5% H_2	4	Y	1	0	HT
242	Pd_1Ag_3/γ-Al_2O_3	50	21.0	400	5% H_2	4	Y	0.025	0.075	γ-Al_2O_3
243	Pd_1Ag_3 NS/$CaCO_3$	40	19.4	120	5% H_2	2	N	1	3	$CaCO_3$
244	Pd_1Ag_3/SnO_2	160	15.8	450	5% H_2	4	N	1	3	SnO_2
245	Pd NS/$CaCO_3$	30	12.8	150	CO	10	N	1	0	$CaCO_3$
246	r-TiO_2	150	8.4	30	Air	3	N	1	0	r-TiO_2
247	Pd NS/$CaCO_3$	30	7.2	150	CO	10	N	1	0	$CaCO_3$
248	Ag/HT	70	6.1	400	5% H_2	4	Y	0	100	HT
249	$Pd_1Pb_{0.01}$ NS/γ-Al_2O_3	15	5.7	150	5% H_2	2	N	1	0	γ-Al_2O_3
250	$Pd_1Ag_{0.01}$ NS/γ-Al_2O_3	10	3.6	150	5% H_2	2	N	1	0.01	γ-Al_2O_3
251	SiC	120	0.9	30	Air	0	N	0	0	SiC
252	SiC	65	0.5	30	Air	0	N	0	0	SiC
253	Pd NS/γ-Al_2O_3	5	-2.5	150	CO	10	N	10	0	γ-Al_2O_3
254	$Pd_1Ag_{0.3}$ NS/γ-Al_2O_3	20	-4.6	150	5% H_2	2	N	1	0.3	γ-Al_2O_3
255	PdB_2/γ-Al_2O_3	20	-14.8	120	DMAB	12	N	10	0	γ-Al_2O_3
256	Pd/C	20	-95.5	60	5% H_2	2	N	10	0	C
257	Pd/C	15	-106.1	150	5% H_2	4	N	10	0	C

Note: To reduce experimental errors, the reaction results of catalysts prepared under the same conditions but in some different batches are all listed in the table at the same time.

***: Y** means that after the catalyst was impregnated and dried, it was further calcined in air at 450°C for 4 hours and then reduced. **N** means the direct reduction after the catalyst was impregnated and dried.

#: The loading amount refers to the percentage of the input metal mass in the total mass at the beginning of synthesis.

12. Structural information of the global PES dataset for G-NN potential training

Table S2. Structural information of the global PES dataset for G-NN potential training. The listed data is the number of structures in the dataset, as distinguished by the chemical formula, the number of atoms per cell (N_{atm}), and the type of the structure, including cluster (N_{cls}), layer (N_{lay}), and bulk (N_{bul}). The total number of the structures (N_{tot}) is also summarized.

Chem. Formula	N_{atm}	N_{cls}	N_{lay}	N_{bul}	N_{tot}
Ag_{14}	14	0	3	30	33
Ag_{15}	15	84	5	724	813
Ag_{16}	16	0	1	6539	6540
Ag_{17}	17	0	0	19	19
Ag_{28}	28	0	0	34	34
Ag_{29}	29	0	15	0	15
Ag_{30}	30	0	31	32	63
Ag_{31}	31	0	0	74	74
Ag_{32}	32	0	2	93	95
Pd_1-Ag_1	2	0	0	77	77
Pd_1-Ag_3	4	0	0	1	1
Pd_1-Ag_{15}	16	0	0	19	19
Pd_2-Ag_2	4	0	0	1	1
Pd_2-Ag_6	8	0	0	36	36
Pd_2-Ag_{14}	16	1	0	5	6
Pd_2-Ag_{33}	35	0	8	0	8
Pd_2-Ag_{34}	36	0	53	0	53
Pd_3-Ag_1	4	0	0	3	3
Pd_3-Ag_3	6	0	31	4	35
Pd_3-Ag_{13}	16	1	0	10	11
Pd_4	4	2	2	23	27
Pd_4-Ag_4	8	0	3	0	3
Pd_4-Ag_{12}	16	5	0	10	15
Pd_4-Ag_{44}	48	0	7	0	7
Pd_5-Ag_{11}	16	1	0	84	85
Pd_5-Ag_{43}	48	0	9	0	9
Pd_6-Ag_{10}	16	2	0	85	87
Pd_7-Ag_9	16	2	0	8	10
Pd_8	8	0	4	41	45
Pd_8-Ag_8	16	2	0	70	72
Pd_8-Ag_{24}	32	0	7	0	7
Pd_8-Ag_{40}	48	0	6	0	6
Pd_8-Ag_{56}	64	0	5	0	5
Pd_9-Ag_7	16	0	0	29	29
Pd_{10}-Ag_6	16	3	0	74	77
Pd_{10}-Ag_{54}	64	0	22	0	22
Pd_{11}-Ag_5	16	2	0	10	12
Pd_{11}-Ag_{25}	36	107	72	0	179

Supplementary Table 2. Continued from previous page.

Pd_{12}-Ag_4	16	2	0	85	87
Pd_{12}-Ag_{12}	24	0	11	2	13
Pd_{12}-Ag_{20}	32	0	0	1	1
Pd_{12}-Ag_{52}	64	0	28	1	29
Pd_{13}-Ag_3	16	3	0	11	14
Pd_{14}-Ag_2	16	1	1	33	35
Pd_{14}-Ag_{50}	64	0	12	0	12
Pd_{15}	15	0	0	36	36
Pd_{15}-Ag_1	16	3	0	26	29
Pd_{16}	16	213	1	1342	1556
Pd_{16}-Ag_{16}	32	0	0	1	1
Pd_{16}-Ag_{32}	48	0	13	0	13
Pd_{16}-Ag_{48}	64	0	41	1	42
Pd_{18}-Ag_{14}	32	0	0	1	1
Pd_{18}-Ag_{46}	64	0	25	0	25
Pd_{19}-Ag_{13}	32	0	0	1	1
Pd_{20}-Ag_{44}	64	0	30	0	30
Pd_{21}-Ag_{14}	35	0	10	0	10
Pd_{22}-Ag_{14}	36	0	229	0	229
Pd_{22}-Ag_{42}	64	0	28	0	28
Pd_{23}-Ag_9	32	0	0	1	1
Pd_{24}-Ag_{24}	48	0	21	1	22
Pd_{24}-Ag_{40}	64	0	33	0	33
Pd_{26}-Ag_{38}	64	0	34	2	36
Pd_{28}-Ag_4	32	0	0	1	1
Pd_{28}-Ag_{36}	64	0	35	0	35
Pd_{29}	29	0	22	34	56
Pd_{30}-Ag_{34}	64	0	25	0	25
Pd_{31}	31	0	0	4	4
Pd_{32}	32	0	74	156	230
Pd_{32}-Ag_{16}	48	0	8	0	8
Pd_{32}-Ag_{32}	64	0	94	12	106
Pd_{33}-Ag_2	35	0	4	0	4
Pd_{34}-Ag_2	36	0	21	0	21
Pd_{34}-Ag_{30}	64	0	35	0	35
Pd_{36}-Ag_{28}	64	0	29	0	29
Pd_{38}-Ag_{26}	64	0	22	1	23
Pd_{40}-Ag_{24}	64	0	29	0	29
Pd_{42}-Ag_{22}	64	0	16	2	18
Pd_{44}-Ag_{20}	64	0	8	0	8
Pd_{46}-Ag_{18}	64	0	5	0	5
Pd_{48}	48	0	9	0	9
Pd_{48}-Ag_{16}	64	0	9	0	9
Pd_{52}-Ag_{12}	64	0	3	0	3

Supplementary Table 2. Continued from previous page.

Pd_{54}	54	0	10	6	16
Pd_{56}-Ag_8	64	0	8	1	9
Pd_{58}	58	0	69	38	107
Pd_{60}	60	0	88	28	116
Pd_{60}-Ag_4	64	0	11	0	11
Pd_{64}	64	0	909	618	1527
O_1	1	1	0	0	1
O_2	2	5	0	0	5
O_4	4	0	15	0	15
O_6-Ti_4	10	0	0	44	44
O_7-Ti_4	11	0	13	3937	3950
O_7-Ti_4-Ag_2	13	0	27	3	30
O_7-Ti_4-Ag_5	16	0	120	3	123
O_7-Ti_4-Pd_1-Ag_1	13	0	38	0	38
O_7-Ti_4-Pd_1-Ag_4	16	0	8	0	8
O_7-Ti_4-Pd_2	13	0	46	5	51
O_7-Ti_4-Pd_2-Ag_3	16	0	23	6	29
O_7-Ti_4-Pd_3-Ag_2	16	0	33	0	33
O_7-Ti_4-Pd_4-Ag_1	16	0	15	0	15
O_7-Ti_4-Pd_5	16	0	116	8	124
O_8-Ti_4	12	2115	190	12144	14449
O_8-Ti_4-Ag_2	14	0	71	4	75
O_8-Ti_4-Ag_5	17	0	123	7	130
O_8-Ti_4-Pd_1-Ag_1	14	0	29	0	29
O_8-Ti_4-Pd_1-Ag_4	17	0	8	0	8
O_8-Ti_4-Pd_2	14	0	35	5	40
O_8-Ti_4-Pd_2-Ag_3	17	0	17	1	18
O_8-Ti_4-Pd_3-Ag_2	17	0	29	0	29
O_8-Ti_4-Pd_4-Ag_1	17	0	17	1	18
O_8-Ti_4-Pd_5	17	0	138	11	149
O_9-Ti_4-Ag_1	14	0	77	1	78
O_9-Ti_4-Ag_5	18	0	89	0	89
O_9-Ti_4-Pd_1	14	0	59	6	65
O_9-Ti_4-Pd_1-Ag_4	18	0	1	0	1
O_9-Ti_4-Pd_2-Ag_3	18	0	16	2	18
O_9-Ti_4-Pd_3-Ag_2	18	0	11	6	17
O_9-Ti_4-Pd_4-Ag_1	18	0	11	0	11
O_9-Ti_4-Pd_5	18	0	70	30	100
O_{10}-Ti_5-Ag_9	24	0	312	28	340
O_{10}-Ti_5-Pd_1-Ag_8	24	0	5	1	6
O_{10}-Ti_5-Pd_2-Ag_7	24	0	51	22	73
O_{10}-Ti_5-Pd_3-Ag_6	24	0	17	6	23
O_{10}-Ti_5-Pd_4-Ag_5	24	0	10	2	12
O_{10}-Ti_5-Pd_5-Ag_4	24	0	4	0	4

Supplementary Table 2. Continued from previous page.

O_{10}-Ti_5-Pd_6-Ag_3	24	0	25	3	28
O_{10}-Ti_5-Pd_7-Ag_2	24	0	5	3	8
O_{10}-Ti_5-Pd_8-Ag_1	24	0	23	9	32
O_{10}-Ti_5-Pd_9	24	0	234	125	359
O_{11}	11	0	77	24	101
O_{11}-Ti_5-Ag_8	24	0	271	35	306
O_{11}-Ti_5-Pd_1-Ag_7	24	0	24	6	30
O_{11}-Ti_5-Pd_2-Ag_6	24	0	46	3	49
O_{11}-Ti_5-Pd_3-Ag_5	24	0	20	3	23
O_{11}-Ti_5-Pd_4-Ag_4	24	0	32	3	35
O_{11}-Ti_5-Pd_5-Ag_3	24	0	12	4	16
O_{11}-Ti_5-Pd_6-Ag_2	24	0	27	1	28
O_{11}-Ti_5-Pd_7-Ag_1	24	0	29	2	31
O_{11}-Ti_5-Pd_8	24	0	256	112	368
O_{11}-Ti_6-Ag_2	19	0	44	6	50
O_{11}-Ti_6-Ag_5	22	0	33	3	36
O_{11}-Ti_6-Pd_1-Ag_1	19	0	14	1	15
O_{11}-Ti_6-Pd_1-Ag_4	22	0	11	1	12
O_{11}-Ti_6-Pd_2	19	0	37	13	50
O_{11}-Ti_6-Pd_2-Ag_3	22	0	1	0	1
O_{11}-Ti_6-Pd_3-Ag_2	22	0	1	0	1
O_{11}-Ti_6-Pd_4-Ag_1	22	0	4	0	4
O_{11}-Ti_6-Pd_5	22	0	24	4	28
O_{12}-Ti_4-Ag_8	24	0	483	41	524
O_{12}-Ti_4-Pd_1-Ag_7	24	0	26	5	31
O_{12}-Ti_4-Pd_2-Ag_6	24	0	29	1	30
O_{12}-Ti_4-Pd_3-Ag_5	24	0	12	5	17
O_{12}-Ti_4-Pd_4-Ag_4	24	0	35	16	51
O_{12}-Ti_4-Pd_5-Ag_3	24	0	57	4	61
O_{12}-Ti_4-Pd_6-Ag_2	24	0	22	2	24
O_{12}-Ti_4-Pd_7-Ag_1	24	0	28	3	31
O_{12}-Ti_4-Pd_8	24	0	332	144	476
O_{12}-Ti_6-Ag_1	19	0	63	9	72
O_{12}-Ti_6-Ag_5	23	0	100	9	109
O_{12}-Ti_6-Pd_1	19	0	57	21	78
O_{12}-Ti_6-Pd_1-Ag_4	23	0	8	0	8
O_{12}-Ti_6-Pd_2-Ag_3	23	0	29	0	29
O_{12}-Ti_6-Pd_3-Ag_2	23	0	8	0	8
O_{12}-Ti_6-Pd_4-Ag_1	23	0	8	1	9
O_{12}-Ti_6-Pd_5	23	0	90	26	116
O_{12}-Ti_8	20	0	0	378	378
O_{13}-Ti_6	19	0	144	476	620
O_{13}-Ti_6-Ag_1	20	0	62	8	70
O_{13}-Ti_6-Ag_5	24	0	532	50	582

Supplementary Table 2. Continued from previous page.

O_{13}-Ti_6-Pd_1	20	0	50	22	72
O_{13}-Ti_6-Pd_1-Ag_4	24	0	74	19	93
O_{13}-Ti_6-Pd_2-Ag_3	24	0	104	8	112
O_{13}-Ti_6-Pd_3-Ag_2	24	0	76	19	95
O_{13}-Ti_6-Pd_4-Ag_1	24	0	115	28	143
O_{13}-Ti_6-Pd_5	24	0	485	184	669
O_{13}-Ti_7	20	0	40	19	59
O_{14}-Ti_7	21	0	0	1	1
O_{14}-Ti_8	22	0	0	198	198
O_{14}-Ti_8-Ag_4	26	0	8	0	8
O_{14}-Ti_8-Ag_{10}	32	0	2	0	2
O_{14}-Ti_8-Pd_3-Ag_7	32	0	13	0	13
O_{14}-Ti_8-Pd_4	26	0	3	0	3
O_{14}-Ti_8-Pd_{10}	32	0	6	0	6
O_{15}-Ti_9	24	0	2	283	285
O_{16}-Ti_8	24	0	127	676	803
O_{16}-Ti_8-Ag_{10}	34	0	9	0	9
O_{16}-Ti_8-Pd_6-Ag_4	34	0	1	0	1
O_{16}-Ti_8-Pd_9-Ag_1	34	0	1	0	1
O_{16}-Ti_8-Pd_{10}	34	0	5	0	5
O_{18}-Ti_7	25	0	0	1	1
O_{18}-Ti_8	26	0	0	3	3
O_{18}-Ti_8-Ag_2	28	0	1	0	1
O_{18}-Ti_8-Pd_2	28	0	4	0	4
O_{18}-Ti_8-Pd_{10}	36	0	2	0	2
O_{18}-Ti_{12}	30	0	349	17	366
O_{20}-Ti_{10}-Ag_{18}	48	0	467	1	468
O_{20}-Ti_{10}-Pd_1-Ag_{17}	48	0	2	0	2
O_{20}-Ti_{10}-Pd_2-Ag_{16}	48	0	24	10	34
O_{20}-Ti_{10}-Pd_3-Ag_{15}	48	0	37	5	42
O_{20}-Ti_{10}-Pd_4-Ag_{14}	48	0	41	3	44
O_{20}-Ti_{10}-Pd_5-Ag_{13}	48	0	28	8	36
O_{20}-Ti_{10}-Pd_6-Ag_{12}	48	0	15	3	18
O_{20}-Ti_{10}-Pd_7-Ag_{11}	48	0	46	7	53
O_{20}-Ti_{10}-Pd_8-Ag_{10}	48	0	7	4	11
O_{20}-Ti_{10}-Pd_9-Ag_9	48	0	8	6	14
O_{20}-Ti_{10}-Pd_{10}-Ag_8	48	0	18	3	21
O_{20}-Ti_{10}-Pd_{11}-Ag_7	48	0	11	5	16
O_{20}-Ti_{10}-Pd_{12}-Ag_6	48	0	13	1	14
O_{20}-Ti_{10}-Pd_{13}-Ag_5	48	0	35	6	41
O_{20}-Ti_{10}-Pd_{14}-Ag_4	48	0	11	3	14
O_{20}-Ti_{10}-Pd_{15}-Ag_3	48	0	14	7	21
O_{20}-Ti_{10}-Pd_{16}-Ag_2	48	0	25	4	29
O_{20}-Ti_{10}-Pd_{17}-Ag_1	48	0	18	2	20

Supplementary Table 2. Continued from previous page.

O_{20}-Ti_{10}-Pd_{18}	48	0	649	335	984
O_{22}-Ti_{10}-Ag_{16}	48	0	523	1	524
O_{22}-Ti_{10}-Pd_1-Ag_{15}	48	0	11	6	17
O_{22}-Ti_{10}-Pd_2-Ag_{14}	48	0	32	3	35
O_{22}-Ti_{10}-Pd_3-Ag_{13}	48	0	25	11	36
O_{22}-Ti_{10}-Pd_4-Ag_{12}	48	0	20	5	25
O_{22}-Ti_{10}-Pd_5-Ag_{11}	48	0	11	9	20
O_{22}-Ti_{10}-Pd_6-Ag_{10}	48	0	31	13	44
O_{22}-Ti_{10}-Pd_7-Ag_9	48	0	38	22	60
O_{22}-Ti_{10}-Pd_8-Ag_8	48	0	14	0	14
O_{22}-Ti_{10}-Pd_9-Ag_7	48	0	9	8	17
O_{22}-Ti_{10}-Pd_{10}-Ag_6	48	0	18	1	19
O_{22}-Ti_{10}-Pd_{11}-Ag_5	48	0	43	8	51
O_{22}-Ti_{10}-Pd_{12}-Ag_4	48	0	37	13	50
O_{22}-Ti_{10}-Pd_{13}-Ag_3	48	0	21	4	25
O_{22}-Ti_{10}-Pd_{14}-Ag_2	48	0	28	3	31
O_{22}-Ti_{10}-Pd_{15}-Ag_1	48	0	24	10	34
O_{22}-Ti_{10}-Pd_{16}	48	0	671	396	1067
O_{22}-Ti_{12}-Ag_{10}	44	0	43	0	43
O_{22}-Ti_{12}-Pd_1-Ag_9	44	0	3	4	7
O_{22}-Ti_{12}-Pd_2-Ag_8	44	0	7	1	8
O_{22}-Ti_{12}-Pd_4	38	0	3	0	3
O_{22}-Ti_{12}-Pd_4-Ag_6	44	0	2	1	3
O_{22}-Ti_{12}-Pd_6-Ag_4	44	0	4	0	4
O_{22}-Ti_{12}-Pd_7-Ag_3	44	0	1	0	1
O_{22}-Ti_{12}-Pd_8-Ag_2	44	0	4	2	6
O_{22}-Ti_{12}-Pd_9-Ag_1	44	0	17	4	21
O_{22}-Ti_{12}-Pd_{10}	44	0	43	45	88
O_{24}-Ti_8-Ag_{16}	48	0	725	0	725
O_{24}-Ti_8-Pd_1-Ag_{15}	48	0	20	6	26
O_{24}-Ti_8-Pd_2-Ag_{14}	48	0	26	25	51
O_{24}-Ti_8-Pd_3-Ag_{13}	48	0	43	14	57
O_{24}-Ti_8-Pd_4-Ag_{12}	48	0	50	10	60
O_{24}-Ti_8-Pd_5-Ag_{11}	48	0	80	14	94
O_{24}-Ti_8-Pd_6-Ag_{10}	48	0	32	27	59
O_{24}-Ti_8-Pd_7-Ag_9	48	0	25	8	33
O_{24}-Ti_8-Pd_8-Ag_8	48	0	53	10	63
O_{24}-Ti_8-Pd_9-Ag_7	48	0	40	9	49
O_{24}-Ti_8-Pd_{10}-Ag_6	48	0	38	7	45
O_{24}-Ti_8-Pd_{11}-Ag_5	48	0	48	17	65
O_{24}-Ti_8-Pd_{12}-Ag_4	48	0	30	9	39
O_{24}-Ti_8-Pd_{13}-Ag_3	48	0	29	4	33
O_{24}-Ti_8-Pd_{14}-Ag_2	48	0	58	25	83
O_{24}-Ti_8-Pd_{15}-Ag_1	48	0	46	22	68

Supplementary Table 2. Continued from previous page.

O_{24}-Ti_8-Pd_{16}	48	0	868	590	1458
O_{24}-Ti_{12}-Ag_2	38	0	15	0	15
O_{24}-Ti_{12}-Ag_{10}	46	0	174	0	174
O_{24}-Ti_{12}-Pd_1-Ag_9	46	0	18	0	18
O_{24}-Ti_{12}-Pd_2	38	0	6	0	6
O_{24}-Ti_{12}-Pd_2-Ag_8	46	0	13	7	20
O_{24}-Ti_{12}-Pd_3-Ag_7	46	0	13	0	13
O_{24}-Ti_{12}-Pd_4-Ag_6	46	0	6	0	6
O_{24}-Ti_{12}-Pd_5-Ag_5	46	0	8	7	15
O_{24}-Ti_{12}-Pd_6-Ag_4	46	0	3	1	4
O_{24}-Ti_{12}-Pd_7-Ag_3	46	0	6	2	8
O_{24}-Ti_{12}-Pd_8-Ag_2	46	0	6	6	12
O_{24}-Ti_{12}-Pd_9-Ag_1	46	0	0	2	2
O_{24}-Ti_{12}-Pd_{10}	46	0	201	139	340
O_{26}-Ti_{12}-Ag_{10}	48	0	804	0	804
O_{26}-Ti_{12}-Pd_1-Ag_1	40	0	5	0	5
O_{26}-Ti_{12}-Pd_1-Ag_9	48	0	57	19	76
O_{26}-Ti_{12}-Pd_2	40	0	4	0	4
O_{26}-Ti_{12}-Pd_2-Ag_8	48	0	118	25	143
O_{26}-Ti_{12}-Pd_3-Ag_7	48	0	75	27	102
O_{26}-Ti_{12}-Pd_4-Ag_6	48	0	36	17	53
O_{26}-Ti_{12}-Pd_5-Ag_5	48	0	58	12	70
O_{26}-Ti_{12}-Pd_6-Ag_4	48	0	78	14	92
O_{26}-Ti_{12}-Pd_7-Ag_3	48	0	50	15	65
O_{26}-Ti_{12}-Pd_8-Ag_2	48	0	106	36	142
O_{26}-Ti_{12}-Pd_9-Ag_1	48	0	82	25	107
O_{26}-Ti_{12}-Pd_{10}	48	0	1160	743	1903
O_{28}-Ti_{16}-Ag_8	52	0	47	0	47
O_{28}-Ti_{16}-Ag_{20}	64	0	143	2	145
O_{28}-Ti_{16}-Pd_1-Ag_7	52	0	4	0	4
O_{28}-Ti_{16}-Pd_1-Ag_{19}	64	0	8	1	9
O_{28}-Ti_{16}-Pd_2-Ag_6	52	0	0	1	1
O_{28}-Ti_{16}-Pd_2-Ag_{18}	64	0	7	4	11
O_{28}-Ti_{16}-Pd_3-Ag_5	52	0	12	0	12
O_{28}-Ti_{16}-Pd_3-Ag_{17}	64	0	2	0	2
O_{28}-Ti_{16}-Pd_4-Ag_4	52	0	0	8	8
O_{28}-Ti_{16}-Pd_4-Ag_{16}	64	0	4	4	8
O_{28}-Ti_{16}-Pd_5-Ag_3	52	0	7	3	10
O_{28}-Ti_{16}-Pd_5-Ag_{15}	64	0	7	4	11
O_{28}-Ti_{16}-Pd_6-Ag_2	52	0	2	0	2
O_{28}-Ti_{16}-Pd_6-Ag_{14}	64	0	7	1	8
O_{28}-Ti_{16}-Pd_7-Ag_{13}	64	0	12	0	12
O_{28}-Ti_{16}-Pd_8	52	0	66	27	93
O_{28}-Ti_{16}-Pd_8-Ag_{12}	64	0	14	1	15

Supplementary Table 2. Continued from previous page.

O_{28}-Ti_{16}-Pd_9-Ag_{11}	64	0	3	0	3
O_{28}-Ti_{16}-Pd_{10}-Ag_{10}	64	0	2	0	2
O_{28}-Ti_{16}-Pd_{11}-Ag_9	64	0	2	1	3
O_{28}-Ti_{16}-Pd_{12}-Ag_8	64	0	15	1	16
O_{28}-Ti_{16}-Pd_{13}-Ag_7	64	0	11	0	11
O_{28}-Ti_{16}-Pd_{14}-Ag_6	64	0	3	4	7
O_{28}-Ti_{16}-Pd_{15}-Ag_5	64	0	14	2	16
O_{28}-Ti_{16}-Pd_{16}-Ag_4	64	0	3	0	3
O_{28}-Ti_{16}-Pd_{17}-Ag_3	64	0	12	1	13
O_{28}-Ti_{16}-Pd_{18}-Ag_2	64	0	5	7	12
O_{28}-Ti_{16}-Pd_{19}-Ag_1	64	0	3	1	4
O_{28}-Ti_{16}-Pd_{20}	64	0	225	158	383
O_{31}-Ti_{16}-Ag_4	51	0	45	1	46
O_{31}-Ti_{16}-Ag_8	55	0	16	0	16
O_{31}-Ti_{16}-Pd_1-Ag_3	51	0	5	0	5
O_{31}-Ti_{16}-Pd_1-Ag_7	55	0	7	0	7
O_{31}-Ti_{16}-Pd_2-Ag_2	51	0	10	3	13
O_{31}-Ti_{16}-Pd_2-Ag_6	55	0	6	0	6
O_{31}-Ti_{16}-Pd_3-Ag_1	51	0	10	2	12
O_{31}-Ti_{16}-Pd_3-Ag_5	55	0	0	2	2
O_{31}-Ti_{16}-Pd_4	51	0	82	18	100
O_{31}-Ti_{16}-Pd_4-Ag_4	55	0	1	0	1
O_{31}-Ti_{16}-Pd_5-Ag_3	55	0	2	0	2
O_{31}-Ti_{16}-Pd_6-Ag_2	55	0	10	0	10
O_{31}-Ti_{16}-Pd_8	55	0	59	22	81
O_{32}-Ti_{16}	48	0	130	0	130
O_{32}-Ti_{16}-Ag_4	52	0	82	1	83
O_{32}-Ti_{16}-Ag_8	56	0	73	0	73
O_{32}-Ti_{16}-Ag_{20}	68	0	161	0	161
O_{32}-Ti_{16}-Pd_1-Ag_3	52	0	25	1	26
O_{32}-Ti_{16}-Pd_1-Ag_{19}	68	0	2	0	2
O_{32}-Ti_{16}-Pd_2-Ag_2	52	0	14	6	20
O_{32}-Ti_{16}-Pd_2-Ag_6	56	0	12	7	19
O_{32}-Ti_{16}-Pd_2-Ag_{18}	68	0	12	1	13
O_{32}-Ti_{16}-Pd_3-Ag_1	52	0	6	0	6
O_{32}-Ti_{16}-Pd_3-Ag_5	56	0	1	1	2
O_{32}-Ti_{16}-Pd_3-Ag_{17}	68	0	6	2	8
O_{32}-Ti_{16}-Pd_4	52	0	96	41	137
O_{32}-Ti_{16}-Pd_4-Ag_4	56	0	6	1	7
O_{32}-Ti_{16}-Pd_4-Ag_{16}	68	0	2	0	2
O_{32}-Ti_{16}-Pd_5-Ag_3	56	0	5	2	7
O_{32}-Ti_{16}-Pd_5-Ag_{15}	68	0	8	1	9
O_{32}-Ti_{16}-Pd_6-Ag_2	56	0	12	0	12
O_{32}-Ti_{16}-Pd_6-Ag_{14}	68	0	14	0	14

Supplementary Table 2. Continued from previous page.

O_{32}-Ti_{16}-Pd_7-Ag_1	56	0	7	1	8
O_{32}-Ti_{16}-Pd_7-Ag_{13}	68	0	2	3	5
O_{32}-Ti_{16}-Pd_8	56	0	81	48	129
O_{32}-Ti_{16}-Pd_8-Ag_{12}	68	0	7	0	7
O_{32}-Ti_{16}-Pd_9-Ag_{11}	68	0	2	2	4
O_{32}-Ti_{16}-Pd_{10}-Ag_{10}	68	0	5	3	8
O_{32}-Ti_{16}-Pd_{11}-Ag_9	68	0	5	0	5
O_{32}-Ti_{16}-Pd_{12}-Ag_8	68	0	8	3	11
O_{32}-Ti_{16}-Pd_{13}-Ag_7	68	0	1	3	4
O_{32}-Ti_{16}-Pd_{14}-Ag_6	68	0	5	4	9
O_{32}-Ti_{16}-Pd_{15}-Ag_5	68	0	5	0	5
O_{32}-Ti_{16}-Pd_{17}-Ag_3	68	0	6	1	7
O_{32}-Ti_{16}-Pd_{18}-Ag_2	68	0	13	2	15
O_{32}-Ti_{16}-Pd_{19}-Ag_1	68	0	9	5	14
O_{32}-Ti_{16}-Pd_{20}	68	0	248	149	397
O_{33}-Ti_{16}-Ag_5	54	0	81	2	83
O_{33}-Ti_{16}-Ag_7	56	0	33	1	34
O_{33}-Ti_{16}-Pd_1-Ag_4	54	0	32	1	33
O_{33}-Ti_{16}-Pd_2-Ag_3	54	0	19	3	22
O_{33}-Ti_{16}-Pd_2-Ag_5	56	0	1	0	1
O_{33}-Ti_{16}-Pd_3-Ag_2	54	0	16	2	18
O_{33}-Ti_{16}-Pd_4-Ag_1	54	0	15	8	23
O_{33}-Ti_{16}-Pd_4-Ag_3	56	0	1	0	1
O_{33}-Ti_{16}-Pd_5	54	0	162	84	246
O_{33}-Ti_{16}-Pd_5-Ag_2	56	0	1	0	1
O_{33}-Ti_{16}-Pd_7	56	0	24	0	24
O_{36}-Ti_{16}-Ag_4	56	0	68	0	68
O_{36}-Ti_{16}-Ag_{20}	72	0	119	1	120
O_{36}-Ti_{16}-Pd_1-Ag_3	56	0	30	0	30
O_{36}-Ti_{16}-Pd_1-Ag_{19}	72	0	4	0	4
O_{36}-Ti_{16}-Pd_2-Ag_2	56	0	8	0	8
O_{36}-Ti_{16}-Pd_3-Ag_1	56	0	4	4	8
O_{36}-Ti_{16}-Pd_3-Ag_{17}	72	0	4	2	6
O_{36}-Ti_{16}-Pd_4	56	0	119	76	195
O_{36}-Ti_{16}-Pd_4-Ag_{16}	72	0	5	2	7
O_{36}-Ti_{16}-Pd_5-Ag_{15}	72	0	0	2	2
O_{36}-Ti_{16}-Pd_6-Ag_{14}	72	0	4	5	9
O_{36}-Ti_{16}-Pd_7-Ag_{13}	72	0	1	0	1
O_{36}-Ti_{16}-Pd_8-Ag_{12}	72	0	6	0	6
O_{36}-Ti_{16}-Pd_9-Ag_{11}	72	0	3	0	3
O_{36}-Ti_{16}-Pd_{10}-Ag_{10}	72	0	13	3	16
O_{36}-Ti_{16}-Pd_{12}-Ag_8	72	0	3	0	3
O_{36}-Ti_{16}-Pd_{13}-Ag_7	72	0	9	4	13
O_{36}-Ti_{16}-Pd_{14}-Ag_6	72	0	2	0	2

Supplementary Table 2. Continued from previous page.

O_{36}-Ti_{16}-Pd_{15}-Ag_5	72	0	7	1	8
O_{36}-Ti_{16}-Pd_{16}-Ag_4	72	0	9	1	10
O_{36}-Ti_{16}-Pd_{17}-Ag_3	72	0	6	0	6
O_{36}-Ti_{16}-Pd_{18}-Ag_2	72	0	2	11	13
O_{36}-Ti_{16}-Pd_{19}-Ag_1	72	0	2	2	4
O_{36}-Ti_{16}-Pd_{20}	72	0	201	111	312
O_{40}-Ti_{20}	60	0	84	0	84
O_{44}-Ti_{24}-Ag_8	76	0	46	0	46
O_{44}-Ti_{24}-Pd_1-Ag_7	76	0	2	0	2
O_{44}-Ti_{24}-Pd_2-Ag_6	76	0	7	1	8
O_{44}-Ti_{24}-Pd_3-Ag_5	76	0	17	1	18
O_{44}-Ti_{24}-Pd_4-Ag_4	76	0	0	1	1
O_{44}-Ti_{24}-Pd_5-Ag_3	76	0	4	0	4
O_{44}-Ti_{24}-Pd_6-Ag_2	76	0	7	0	7
O_{44}-Ti_{24}-Pd_7-Ag_1	76	0	9	4	13
O_{44}-Ti_{24}-Pd_8	76	0	94	49	143
O_{46}-Ti_{23}-Ag_2	71	0	4	0	4
O_{46}-Ti_{23}-Ag_3	72	0	10	3	13
O_{46}-Ti_{23}-Pd_1-Ag_2	72	0	4	0	4
O_{46}-Ti_{23}-Pd_2	71	0	8	4	12
O_{46}-Ti_{23}-Pd_3	72	0	9	4	13
O_{46}-Ti_{24}-Ag_2	72	0	32	1	33
O_{46}-Ti_{24}-Pd_1-Ag_1	72	0	6	2	8
O_{46}-Ti_{24}-Pd_2	72	0	16	14	30
O_{47}-Ti_{23}-Ag_2	72	0	8	0	8
O_{47}-Ti_{23}-Ag_4	74	0	5	0	5
O_{47}-Ti_{23}-Pd_1-Ag_1	72	0	1	3	4
O_{47}-Ti_{23}-Pd_1-Ag_3	74	0	5	1	6
O_{47}-Ti_{23}-Pd_2	72	0	13	12	25
O_{47}-Ti_{23}-Pd_2-Ag_2	74	0	1	3	4
O_{47}-Ti_{23}-Pd_4	74	0	21	21	42
O_{47}-Ti_{24}-Ag_2	73	0	19	3	22
O_{47}-Ti_{24}-Ag_8	79	0	4	0	4
O_{47}-Ti_{24}-Pd_1-Ag_1	73	0	3	1	4
O_{47}-Ti_{24}-Pd_1-Ag_7	79	0	8	0	8
O_{47}-Ti_{24}-Pd_2	73	0	18	19	37
O_{47}-Ti_{24}-Pd_2-Ag_6	79	0	2	1	3
O_{47}-Ti_{24}-Pd_6-Ag_2	79	0	1	0	1
O_{47}-Ti_{24}-Pd_7-Ag_1	79	0	3	1	4
O_{47}-Ti_{24}-Pd_8	79	0	21	13	34
O_{48}-Ti_{24}	72	0	119	0	119
O_{48}-Ti_{24}-Ag_4	76	0	75	4	79
O_{48}-Ti_{24}-Ag_8	80	0	1	0	1
O_{48}-Ti_{24}-Pd_1-Ag_1	74	0	1	1	2

Supplementary Table 2. Continued from previous page.

O_{48}-Ti_{24}-Pd_1-Ag_3	76	0	17	7	24
O_{48}-Ti_{24}-Pd_2	74	0	15	27	42
O_{48}-Ti_{24}-Pd_2-Ag_2	76	0	4	5	9
O_{48}-Ti_{24}-Pd_3-Ag_1	76	0	19	7	26
O_{48}-Ti_{24}-Pd_4	76	0	179	115	294
O_{48}-Ti_{24}-Pd_4-Ag_4	80	0	1	0	1
O_{48}-Ti_{24}-Pd_6-Ag_2	80	0	1	0	1
O_{48}-Ti_{24}-Pd_7-Ag_1	80	0	2	0	2
O_{48}-Ti_{24}-Pd_8	80	0	18	14	32
O_{49}-Ti_{24}-Ag_1	74	0	7	2	9
O_{49}-Ti_{24}-Ag_3	76	0	7	2	9
O_{49}-Ti_{24}-Ag_6	79	0	14	1	15
O_{49}-Ti_{24}-Ag_7	80	0	7	0	7
O_{49}-Ti_{24}-Pd_1	74	0	27	17	44
O_{49}-Ti_{24}-Pd_1-Ag_2	76	0	7	0	7
O_{49}-Ti_{24}-Pd_2-Ag_1	76	0	3	0	3
O_{49}-Ti_{24}-Pd_2-Ag_4	79	0	1	0	1
O_{49}-Ti_{24}-Pd_3	76	0	27	5	32
O_{49}-Ti_{24}-Pd_4-Ag_3	80	0	1	2	3
O_{49}-Ti_{24}-Pd_6	79	0	19	1	20
O_{49}-Ti_{24}-Pd_6-Ag_1	80	0	2	1	3
O_{49}-Ti_{24}-Pd_7	80	0	14	4	18
O_{52}-Ti_{24}-Ag_4	80	0	97	0	97
O_{52}-Ti_{24}-Pd_1-Ag_3	80	0	38	13	51
O_{52}-Ti_{24}-Pd_2-Ag_2	80	0	70	5	75
O_{52}-Ti_{24}-Pd_3-Ag_1	80	0	16	12	28
O_{52}-Ti_{24}-Pd_4	80	0	203	55	258
O_{56}-Ti_{28}	84	0	137	0	137
O_{62}-Ti_{32}-Pd_8	102	0	2	4	6
O_{62}-Ti_{32}-Pd_{10}-Ag_6	110	0	2	0	2
O_{62}-Ti_{32}-Pd_{16}	110	0	9	0	9
O_{64}-Ti_{32}	96	0	147	0	147
O_{64}-Ti_{32}-Pd_2-Ag_6	104	0	0	4	4
O_{64}-Ti_{32}-Pd_3-Ag_5	104	0	3	1	4
O_{64}-Ti_{32}-Pd_4-Ag_4	104	0	1	0	1
O_{64}-Ti_{32}-Pd_6-Ag_2	104	0	1	1	2
O_{64}-Ti_{32}-Pd_7-Ag_1	104	0	0	1	1
O_{64}-Ti_{32}-Pd_8	104	0	14	7	21
O_{66}-Ti_{32}-Ag_{14}	112	0	3	0	3
O_{66}-Ti_{32}-Pd_4-Ag_6	108	0	2	0	2
O_{66}-Ti_{32}-Pd_{10}	108	0	16	0	16
O_{66}-Ti_{32}-Pd_{14}	112	0	1	0	1
O_{94}-Ti_{48}-Ag_4	146	0	12	0	12
O_{94}-Ti_{48}-Ag_{16}	158	0	3	0	3

Supplementary Table 2. Continued from previous page.

O_{94}-Ti_{48}-Pd_4-Ag_{12}	158	0	8	0	8
O_{94}-Ti_{48}-Pd_{16}	158	0	1	0	1
O_{95}-Ti_{48}-Ag_5	148	0	2	0	2
O_{95}-Ti_{48}-Ag_8	151	0	1	0	1
O_{95}-Ti_{48}-Pd_{16}	159	0	2	0	2
O_{96}-Ti_{48}-Ag_6	150	0	5	0	5
O_{96}-Ti_{48}-Ag_7	151	0	1	0	1
O_{96}-Ti_{48}-Ag_9	153	0	5	0	5
O_{96}-Ti_{48}-Ag_{14}	158	0	8	0	8
O_{96}-Ti_{48}-Pd_1-Ag_7	152	0	1	0	1
O_{96}-Ti_{48}-Pd_2-Ag_6	152	0	3	0	3
O_{96}-Ti_{48}-Pd_3-Ag_9	156	0	1	0	1
O_{96}-Ti_{48}-Pd_4-Ag_{10}	158	0	19	0	19
O_{96}-Ti_{48}-Pd_6-Ag_2	152	0	16	0	16
O_{96}-Ti_{48}-Pd_7-Ag_1	152	0	15	0	15
O_{96}-Ti_{48}-Pd_8	152	0	8	0	8
O_{96}-Ti_{48}-Pd_8-Ag_6	158	0	15	0	15
O_{96}-Ti_{48}-Pd_{10}	154	0	1	0	1
O_{96}-Ti_{48}-Pd_{12}	156	0	1	0	1
O_{96}-Ti_{48}-Pd_{14}	158	0	3	0	3
O_{96}-Ti_{48}-Pd_{15}-Ag_1	160	0	1	0	1
O_{96}-Ti_{48}-Pd_{16}	160	0	1	0	1
O_{97}-Ti_{48}-Ag_2	147	0	12	0	12
O_{97}-Ti_{48}-Ag_5	150	0	6	0	6
O_{97}-Ti_{48}-Ag_6	151	0	1	3	4
O_{97}-Ti_{48}-Ag_7	152	0	10	0	10
O_{97}-Ti_{48}-Ag_8	153	0	1	0	1
O_{97}-Ti_{48}-Ag_{12}	157	0	13	0	13
O_{97}-Ti_{48}-Ag_{13}	158	0	9	0	9
O_{97}-Ti_{48}-Pd_4-Ag_{10}	159	0	6	0	6
O_{97}-Ti_{48}-Pd_5-Ag_3	153	0	14	0	14
O_{97}-Ti_{48}-Pd_6-Ag_6	157	0	18	0	18
O_{97}-Ti_{48}-Pd_6-Ag_7	158	0	20	0	20
O_{97}-Ti_{48}-Pd_9-Ag_3	157	0	1	0	1
O_{97}-Ti_{48}-Pd_9-Ag_5	159	0	6	0	6
O_{97}-Ti_{48}-Pd_{10}-Ag_2	157	0	9	0	9
O_{97}-Ti_{48}-Pd_{10}-Ag_3	158	0	21	0	21
O_{97}-Ti_{48}-Pd_{12}	157	0	2	0	2
O_{97}-Ti_{48}-Pd_{13}	158	0	4	0	4
O_{97}-Ti_{48}-Pd_{14}	159	0	1	0	1
O_{97}-Ti_{48}-Pd_{15}	160	0	2	0	2
O_{98}-Ti_{48}-Ag_3	149	0	5	0	5
O_{98}-Ti_{48}-Ag_6	152	0	13	0	13
O_{98}-Ti_{48}-Pd_{11}-Ag_3	160	0	1	0	1

Supplementary Table 2. Continued from previous page.

O_{98}-Ti_{48}-Pd_{14}	160	0	1	0	1
O_{99}-Ti_{48}-Ag_{5}	152	0	3	0	3
O_{99}-Ti_{48}-Ag_{10}	157	0	6	0	6
O_{99}-Ti_{48}-Ag_{11}	158	0	6	0	6
O_{100}-Ti_{48}-Ag_{10}	158	0	9	0	9
O_{101}-Ti_{48}-Ag_{9}	158	0	14	0	14
O_{112}-Ti_{56}	168	0	47	0	47
O_{128}-Ti_{64}	192	0	80	0	80
O_{160}-Ti_{80}	240	0	161	0	161
O_{224}-Ti_{112}	336	0	2	0	2
O_{240}-Ti_{120}	360	0	1	0	1
O_{240}-Ti_{120}-Pd_{1}-Ag_{3}	364	0	1	0	1
O_{240}-Ti_{120}-Pd_{2}-Ag_{6}	368	0	1	0	1
O_{240}-Ti_{120}-Pd_{3}-Ag_{9}	372	0	2	0	2
O_{240}-Ti_{120}-Pd_{4}-Ag_{12}	376	0	1	0	1
O_{240}-Ti_{120}-Pd_{5}-Ag_{15}	380	0	1	0	1
O_{240}-Ti_{120}-Pd_{6}-Ag_{18}	384	0	1	0	1
O_{240}-Ti_{120}-Pd_{7}-Ag_{21}	388	0	1	0	1
O_{240}-Ti_{120}-Pd_{8}-Ag_{24}	392	0	1	0	1
O_{240}-Ti_{120}-Pd_{9}-Ag_{27}	396	0	1	0	1
O_{240}-Ti_{120}-Pd_{10}-Ag_{30}	400	0	1	0	1
O_{240}-Ti_{120}-Pd_{13}-Ag_{39}	412	0	1	0	1
O_{252}-Ti_{126}	378	0	2	0	2
O_{252}-Ti_{126}-Pd_{1}-Ag_{3}	382	0	2	0	2
O_{252}-Ti_{126}-Pd_{2}-Ag_{6}	386	0	1	0	1
O_{252}-Ti_{126}-Pd_{3}-Ag_{9}	390	0	1	0	1
O_{252}-Ti_{126}-Pd_{4}-Ag_{12}	394	0	1	0	1
O_{252}-Ti_{126}-Pd_{5}-Ag_{15}	398	0	1	0	1
O_{252}-Ti_{126}-Pd_{6}-Ag_{18}	402	0	1	0	1
O_{252}-Ti_{126}-Pd_{7}-Ag_{21}	406	0	1	0	1
O_{252}-Ti_{126}-Pd_{8}-Ag_{24}	410	0	1	0	1
O_{252}-Ti_{126}-Pd_{9}-Ag_{27}	414	0	1	0	1
O_{252}-Ti_{126}-Pd_{10}-Ag_{30}	418	0	1	0	1
O_{252}-Ti_{126}-Pd_{13}-Ag_{39}	430	0	1	0	1
H_{1}	1	0	1	0	1
H_{1}-Ag_{16}	17	0	9	16	25
H_{1}-Pd_{1}-Ag_{15}	17	0	16	0	16
H_{1}-Pd_{2}-Ag_{13}	16	0	0	1	1
H_{1}-Pd_{3}-Ag_{12}	16	0	0	1	1
H_{1}-Pd_{4}-Ag_{11}	16	0	0	4	4
H_{1}-Pd_{5}-Ag_{10}	16	0	0	2	2
H_{1}-Pd_{5}-Ag_{18}	24	0	1	1	2
H_{1}-Pd_{6}-Ag_{9}	16	0	0	2	2
H_{1}-Pd_{6}-Ag_{20}	27	0	1	0	1

Supplementary Table 2. Continued from previous page.

H_1-Pd_7-Ag_8	16	0	0	3	3
H_1-Pd_7-Ag_{20}	28	0	1	0	1
H_1-Pd_8-Ag_7	16	0	0	2	2
H_1-Pd_9-Ag_6	16	0	0	3	3
H_1-Pd_{10}-Ag_{13}	24	0	1	0	1
H_1-Pd_{10}-Ag_{25}	36	10	0	0	10
H_1-Pd_{11}-Ag_4	16	0	0	6	6
H_1-Pd_{11}-Ag_{12}	24	0	0	1	1
H_1-Pd_{12}-Ag_3	16	0	0	7	7
H_1-Pd_{13}-Ag_2	16	0	0	3	3
H_1-Pd_{13}-Ag_{13}	27	0	1	0	1
H_1-Pd_{14}-Ag_1	16	0	0	1	1
H_1-Pd_{14}-Ag_2	17	0	19	0	19
H_1-Pd_{15}	16	0	0	365	365
H_1-Pd_{16}-Ag_{11}	28	0	1	0	1
H_1-Pd_{19}-Ag_7	27	0	1	0	1
H_1-Pd_{21}-Ag_5	27	0	1	0	1
H_1-Pd_{22}-Ag_4	27	0	1	0	1
H_1-Pd_{23}	24	0	33	17	50
H_1-Pd_{24}-Ag_3	28	0	1	0	1
H_1-Pd_{26}	27	0	81	0	81
H_1-Pd_{27}	28	0	32	0	32
H_1-Pd_{28}-Ag_3	32	0	0	1	1
H_1-Pd_{31}	32	1	0	16	17
H_1-Ti_{15}	16	0	0	1188	1188
H_1-O_1	2	0	3	0	3
H_1-O_8-Ti_4	13	0	0	13813	13813
H_1-O_{10}-Ti_5-Pd_2-Ag_6	24	0	202	24	226
H_1-O_{12}-Ti_6	19	0	290	220	510
H_1-O_{20}-Ti_{10}-Pd_4-Ag_{13}	48	0	174	42	216
H_1-O_{20}-Ti_{10}-Pd_5-Ag_{12}	48	0	31	13	44
H_1-O_{32}-Ti_{16}-Pd_5-Ag_{14}	68	0	11	7	18
H_1-O_{32}-Ti_{16}-Pd_6-Ag_{13}	68	0	9	2	11
H_1-O_{64}-Ti_{32}-Ag_3	100	0	1	1	2
H_1-O_{64}-Ti_{32}-Pd_1-Ag_2	100	0	5	7	12
H_1-O_{64}-Ti_{32}-Pd_1-Ag_3	101	0	1	4	5
H_1-O_{64}-Ti_{32}-Pd_1-Ag_6	104	0	0	1	1
H_1-O_{64}-Ti_{32}-Pd_2-Ag_1	100	0	0	14	14
H_1-O_{64}-Ti_{32}-Pd_2-Ag_2	101	0	3	1	4
H_1-O_{64}-Ti_{32}-Pd_2-Ag_5	104	0	0	2	2
H_1-O_{64}-Ti_{32}-Pd_2-Ag_6	105	0	4	1	5
H_1-O_{64}-Ti_{32}-Pd_2-Ag_9	108	0	1	2	3
H_1-O_{64}-Ti_{32}-Pd_3-Ag_4	104	0	1	5	6
H_1-O_{64}-Ti_{32}-Pd_3-Ag_9	109	0	1	4	5

Supplementary Table 2. Continued from previous page.

H_1-O_{64}-Ti_{32}-Pd_3-Ag_{12}	112	0	4	3	7
H_1-O_{64}-Ti_{32}-Pd_4-Ag_3	104	0	1	1	2
H_1-O_{64}-Ti_{32}-Pd_4-Ag_4	105	0	2	1	3
H_1-O_{64}-Ti_{32}-Pd_4-Ag_{11}	112	0	3	0	3
H_1-O_{64}-Ti_{32}-Pd_4-Ag_{12}	113	0	1	3	4
H_1-O_{64}-Ti_{32}-Pd_4-Ag_{15}	116	0	2	1	3
H_1-O_{64}-Ti_{32}-Pd_5-Ag_6	108	0	4	1	5
H_1-O_{64}-Ti_{32}-Pd_5-Ag_{14}	116	0	1	2	3
H_1-O_{64}-Ti_{32}-Pd_5-Ag_{15}	117	0	0	1	1
H_1-O_{64}-Ti_{32}-Pd_6-Ag_5	108	0	0	1	1
H_1-O_{64}-Ti_{32}-Pd_6-Ag_6	109	0	3	3	6
H_1-O_{72}-Ti_{36}-Ag_3	112	0	6	0	6
H_1-O_{72}-Ti_{36}-Ag_4	113	0	2	0	2
H_1-O_{72}-Ti_{36}-Ag_8	117	0	3	0	3
H_1-O_{72}-Ti_{36}-Ag_{12}	121	0	10	0	10
H_1-O_{72}-Ti_{36}-Ag_{16}	125	0	1	0	1
H_1-O_{72}-Ti_{36}-Pd_1-Ag_3	113	0	1	0	1
H_1-O_{72}-Ti_{36}-Pd_1-Ag_7	117	0	1	0	1
H_1-O_{72}-Ti_{36}-Pd_1-Ag_{15}	125	0	1	0	1
H_1-O_{72}-Ti_{36}-Pd_2-Ag_6	117	0	5	0	5
H_1-O_{72}-Ti_{36}-Pd_2-Ag_9	120	0	4	0	4
H_1-O_{72}-Ti_{36}-Pd_3-Ag_5	117	0	1	0	1
H_1-O_{72}-Ti_{36}-Pd_3-Ag_8	120	0	2	0	2
H_1-O_{72}-Ti_{36}-Pd_3-Ag_9	121	0	2	0	2
H_1-O_{72}-Ti_{36}-Pd_3-Ag_{13}	125	0	2	0	2
H_1-O_{72}-Ti_{36}-Pd_4	113	0	4	0	4
H_1-O_{72}-Ti_{36}-Pd_4-Ag_4	117	0	2	0	2
H_1-O_{72}-Ti_{36}-Pd_4-Ag_{12}	125	0	1	0	1
H_1-O_{72}-Ti_{36}-Pd_4-Ag_{15}	128	0	1	0	1
H_1-O_{72}-Ti_{36}-Pd_5-Ag_{13}	127	0	1	0	1
H_1-O_{72}-Ti_{36}-Pd_5-Ag_{14}	128	0	3	0	3
H_1-O_{72}-Ti_{36}-Pd_5-Ag_{15}	129	0	2	0	2
H_1-O_{72}-Ti_{36}-Pd_6-Ag_6	121	0	3	0	3
H_1-O_{72}-Ti_{36}-Pd_6-Ag_{10}	125	0	1	0	1
H_1-O_{72}-Ti_{36}-Pd_7-Ag_5	121	0	1	0	1
H_1-O_{72}-Ti_{36}-Pd_7-Ag_9	125	0	1	0	1
H_1-O_{72}-Ti_{36}-Pd_8-Ag_4	121	0	2	0	2
H_1-O_{72}-Ti_{36}-Pd_9-Ag_{11}	129	0	7	0	7
H_1-O_{72}-Ti_{36}-Pd_{11}-Ag_1	121	0	1	0	1
H_1-O_{72}-Ti_{36}-Pd_{12}	121	0	2	0	2
H_1-O_{72}-Ti_{36}-Pd_{12}-Ag_4	125	0	1	0	1
H_1-O_{72}-Ti_{36}-Pd_{12}-Ag_8	129	0	1	0	1
H_1-O_{72}-Ti_{36}-Pd_{13}-Ag_3	125	0	1	0	1
H_1-O_{72}-Ti_{36}-Pd_{15}-Ag_1	125	0	2	0	2

Supplementary Table 2. Continued from previous page.

H_1-O_{72}-Ti_{36}-Pd_{16}	125	0	3	0	3
H_1-O_{72}-Ti_{36}-Pd_{18}-Ag_2	129	0	2	0	2
H_1-O_{72}-Ti_{36}-Pd_{20}	129	0	3	0	3
H_1-O_{96}-Ti_{48}	145	0	1	0	1
H_1-O_{96}-Ti_{48}-Ag_{12}	157	0	2	0	2
H_1-O_{96}-Ti_{48}-Ag_{16}	161	0	3	0	3
H_1-O_{96}-Ti_{48}-Pd_1-Ag_3	149	0	2	0	2
H_1-O_{96}-Ti_{48}-Pd_1-Ag_{15}	161	0	1	0	1
H_1-O_{96}-Ti_{48}-Pd_2-Ag_4	151	0	1	0	1
H_1-O_{96}-Ti_{48}-Pd_2-Ag_5	152	0	1	0	1
H_1-O_{96}-Ti_{48}-Pd_2-Ag_6	153	0	3	0	3
H_1-O_{96}-Ti_{48}-Pd_2-Ag_9	156	0	1	0	1
H_1-O_{96}-Ti_{48}-Pd_2-Ag_{14}	161	0	2	0	2
H_1-O_{96}-Ti_{48}-Pd_3-Ag_5	153	0	6	0	6
H_1-O_{96}-Ti_{48}-Pd_3-Ag_7	155	0	1	0	1
H_1-O_{96}-Ti_{48}-Pd_3-Ag_9	157	0	1	0	1
H_1-O_{96}-Ti_{48}-Pd_4	149	0	6	0	6
H_1-O_{96}-Ti_{48}-Pd_4-Ag_4	153	0	1	0	1
H_1-O_{96}-Ti_{48}-Pd_4-Ag_{10}	159	0	1	0	1
H_1-O_{96}-Ti_{48}-Pd_4-Ag_{11}	160	0	3	0	3
H_1-O_{96}-Ti_{48}-Pd_4-Ag_{12}	161	0	2	0	2
H_1-O_{96}-Ti_{48}-Pd_5-Ag_3	153	0	3	0	3
H_1-O_{96}-Ti_{48}-Pd_5-Ag_7	157	0	3	0	3
H_1-O_{96}-Ti_{48}-Pd_5-Ag_{13}	163	0	1	0	1
H_1-O_{96}-Ti_{48}-Pd_5-Ag_{15}	165	0	3	0	3
H_1-O_{96}-Ti_{48}-Pd_6-Ag_2	153	0	1	0	1
H_1-O_{96}-Ti_{48}-Pd_6-Ag_{10}	161	0	3	0	3
H_1-O_{96}-Ti_{48}-Pd_6-Ag_{14}	165	0	1	0	1
H_1-O_{96}-Ti_{48}-Pd_7-Ag_5	157	0	1	0	1
H_1-O_{96}-Ti_{48}-Pd_8	153	0	2	0	2
H_1-O_{96}-Ti_{48}-Pd_9-Ag_3	157	0	2	0	2
H_1-O_{96}-Ti_{48}-Pd_9-Ag_7	161	0	2	0	2
H_1-O_{96}-Ti_{48}-Pd_9-Ag_{11}	165	0	1	0	1
H_1-O_{96}-Ti_{48}-Pd_{10}-Ag_2	157	0	1	0	1
H_1-O_{96}-Ti_{48}-Pd_{10}-Ag_6	161	0	2	0	2
H_1-O_{96}-Ti_{48}-Pd_{11}-Ag_5	161	0	2	0	2
H_1-O_{96}-Ti_{48}-Pd_{12}-Ag_8	165	0	1	0	1
H_1-O_{96}-Ti_{48}-Pd_{13}-Ag_3	161	0	1	0	1
H_1-O_{96}-Ti_{48}-Pd_{14}-Ag_2	161	0	1	0	1
H_1-O_{96}-Ti_{48}-Pd_{15}-Ag_5	165	0	1	0	1
H_1-O_{96}-Ti_{48}-Pd_{18}-Ag_2	165	0	1	0	1
H_1-O_{96}-Ti_{48}-Pd_{20}	165	0	1	0	1
H_1-O_{224}-Ti_{112}	337	0	2	0	2
H_1-O_{240}-Ti_{120}-Pd_1-Ag_3	365	0	1	0	1

Supplementary Table 2. Continued from previous page.

H_1-O_{240}-Ti_{120}-Pd_2-Ag_6	369	0	2	0	2
H_1-O_{240}-Ti_{120}-Pd_3-Ag_9	373	0	1	0	1
H_1-O_{240}-Ti_{120}-Pd_4-Ag_{12}	377	0	1	0	1
H_1-O_{240}-Ti_{120}-Pd_5-Ag_{15}	381	0	1	0	1
H_1-O_{240}-Ti_{120}-Pd_6-Ag_{18}	385	0	2	0	2
H_1-O_{240}-Ti_{120}-Pd_7-Ag_{21}	389	0	1	0	1
H_1-O_{240}-Ti_{120}-Pd_8-Ag_{24}	393	0	2	0	2
H_1-O_{240}-Ti_{120}-Pd_9-Ag_{27}	397	0	1	0	1
H_1-O_{240}-Ti_{120}-Pd_{10}-Ag_{30}	401	0	2	0	2
H_1-O_{252}-Ti_{126}-Pd_1-Ag_3	383	0	4	0	4
H_1-O_{252}-Ti_{126}-Pd_2-Ag_6	387	0	1	0	1
H_1-O_{252}-Ti_{126}-Pd_3-Ag_9	391	0	1	0	1
H_1-O_{252}-Ti_{126}-Pd_4-Ag_{12}	395	0	2	0	2
H_1-O_{252}-Ti_{126}-Pd_5-Ag_{15}	399	0	1	0	1
H_1-O_{252}-Ti_{126}-Pd_6-Ag_{18}	403	0	2	0	2
H_1-O_{252}-Ti_{126}-Pd_7-Ag_{21}	407	0	2	0	2
H_1-O_{252}-Ti_{126}-Pd_8-Ag_{24}	411	0	2	0	2
H_1-O_{252}-Ti_{126}-Pd_9-Ag_{27}	415	0	3	0	3
H_1-O_{252}-Ti_{126}-Pd_{10}-Ag_{30}	419	0	2	0	2
H_2	2	0	9	0	9
H_2-Ag_{16}	18	0	3	240	243
H_2-Pd_1-Ag_{15}	18	0	67	0	67
H_2-Pd_2-Ag_{12}	16	0	0	2	2
H_2-Pd_2-Ag_{14}	18	0	0	19	19
H_2-Pd_3-Ag_{11}	16	0	2	6	8
H_2-Pd_4-Ag_{10}	16	0	0	4	4
H_2-Pd_4-Ag_{23}	29	0	0	1	1
H_2-Pd_5-Ag_9	16	0	1	3	4
H_2-Pd_5-Ag_{17}	24	0	1	0	1
H_2-Pd_6-Ag_8	16	0	0	6	6
H_2-Pd_6-Ag_{21}	29	0	1	0	1
H_2-Pd_6-Ag_{42}	50	0	2	0	2
H_2-Pd_7-Ag_7	16	0	0	5	5
H_2-Pd_7-Ag_{20}	29	0	0	1	1
H_2-Pd_8-Ag_6	16	0	1	9	10
H_2-Pd_8-Ag_{14}	24	0	1	0	1

Supplementary Table 2. Continued from previous page.

H_2-Pd_8-Ag_{19}	29	0	0	1	1
H_2-Pd_9-Ag_5	16	0	2	7	9
H_2-Pd_9-Ag_{19}	30	0	1	0	1
H_2-Pd_{10}-Ag_4	16	0	0	6	6
H_2-Pd_{11}-Ag_3	16	0	1	5	6
H_2-Pd_{12}-Ag_2	16	0	0	13	13
H_2-Pd_{13}-Ag_1	16	0	0	7	7
H_2-Pd_{13}-Ag_{17}	32	0	0	1	1
H_2-Pd_{14}	16	0	69	626	695
H_2-Pd_{14}-Ag_2	18	0	36	102	138
H_2-Pd_{14}-Ag_{13}	29	0	2	1	3
H_2-Pd_{14}-Ag_{14}	30	0	1	0	1
H_2-Pd_{15}-Ag_1	18	0	0	154	154
H_2-Pd_{15}-Ag_{12}	29	0	0	2	2
H_2-Pd_{15}-Ag_{13}	30	0	1	0	1
H_2-Pd_{19}-Ag_9	30	0	1	0	1
H_2-Pd_{20}-Ag_8	30	0	1	0	1
H_2-Pd_{21}-Ag_6	29	0	0	1	1
H_2-Pd_{22}	24	0	29	0	29
H_2-Pd_{22}-Ag_5	29	0	1	0	1
H_2-Pd_{23}-Ag_4	29	0	1	0	1
H_2-Pd_{23}-Ag_5	30	0	1	0	1
H_2-Pd_{24}-Ag_4	30	0	1	0	1
H_2-Pd_{25}-Ag_2	29	0	0	1	1
H_2-Pd_{26}-Ag_1	29	0	1	0	1
H_2-Pd_{26}-Ag_2	30	0	1	0	1
H_2-Pd_{27}	29	3	51	74	128
H_2-Pd_{28}	30	0	64	0	64
H_2-Pd_{29}-Ag_1	32	0	0	1	1
H_2-Pd_{30}	32	2	0	16	18
H_2-Ti_{14}	16	0	19	1535	1554
H_2-O_1-Ti_{26}	29	0	11	0	11
H_2-O_4-Ti_{23}	29	0	19	0	19
H_2-O_8-Ti_4	14	429	1361	14571	16361
H_2-O_{10}-Ti_5-Pd_2-Ag_5	24	0	16	0	16
H_2-O_{12}-Ti_6	20	0	267	133	400
H_2-O_{14}-Ti_8	24	0	39	0	39
H_2-O_{16}-Ti_8	26	0	3	44	47
H_2-O_{17}-Ti_8	27	0	22	0	22
H_2-O_{19}-Ti_8	29	0	54	0	54
H_2-O_{20}-Ti_{10}-Pd_4-Ag_{12}	48	0	103	35	138
H_2-O_{20}-Ti_{10}-Pd_5-Ag_{11}	48	0	99	20	119
H_2-O_{24}-Ti_{12}-Pd_2-Ag_6	46	0	32	10	42
H_2-O_{32}-Ti_{16}-Pd_5-Ag_{13}	68	0	57	18	75

Supplementary Table 2. Continued from previous page.

H_2-O_{64}-Ti_{32}-Pd_1-Ag_2	101	0	1	1	2
H_2-O_{64}-Ti_{32}-Pd_1-Ag_6	105	0	2	2	4
H_2-O_{64}-Ti_{32}-Pd_2-Ag_1	101	0	1	0	1
H_2-O_{64}-Ti_{32}-Pd_2-Ag_2	102	0	5	2	7
H_2-O_{64}-Ti_{32}-Pd_2-Ag_5	105	0	2	2	4
H_2-O_{64}-Ti_{32}-Pd_2-Ag_6	106	0	1	0	1
H_2-O_{64}-Ti_{32}-Pd_2-Ag_9	109	0	1	5	6
H_2-O_{64}-Ti_{32}-Pd_3-Ag_4	105	0	2	1	3
H_2-O_{64}-Ti_{32}-Pd_3-Ag_8	109	0	1	5	6
H_2-O_{64}-Ti_{32}-Pd_3-Ag_9	110	0	2	1	3
H_2-O_{64}-Ti_{32}-Pd_3-Ag_{12}	113	0	2	4	6
H_2-O_{64}-Ti_{32}-Pd_4-Ag_3	105	0	0	2	2
H_2-O_{64}-Ti_{32}-Pd_4-Ag_4	106	0	2	3	5
H_2-O_{64}-Ti_{32}-Pd_4-Ag_{11}	113	0	3	1	4
H_2-O_{64}-Ti_{32}-Pd_4-Ag_{12}	114	0	2	1	3
H_2-O_{64}-Ti_{32}-Pd_4-Ag_{15}	117	0	2	5	7
H_2-O_{64}-Ti_{32}-Pd_5-Ag_6	109	0	0	3	3
H_2-O_{64}-Ti_{32}-Pd_5-Ag_{14}	117	0	3	3	6
H_2-O_{64}-Ti_{32}-Pd_5-Ag_{15}	118	0	2	2	4
H_2-O_{64}-Ti_{32}-Pd_6-Ag_5	109	0	1	4	5
H_2-O_{64}-Ti_{32}-Pd_6-Ag_6	110	0	3	3	6
H_2-O_{72}-Ti_{36}-Ag_{12}	122	0	1	0	1
H_2-O_{72}-Ti_{36}-Ag_{16}	126	0	1	0	1
H_2-O_{72}-Ti_{36}-Pd_1-Ag_2	113	0	1	0	1
H_2-O_{72}-Ti_{36}-Pd_1-Ag_3	114	0	1	0	1
H_2-O_{72}-Ti_{36}-Pd_1-Ag_{15}	126	0	1	0	1
H_2-O_{72}-Ti_{36}-Pd_2-Ag_6	118	0	1	0	1
H_2-O_{72}-Ti_{36}-Pd_2-Ag_9	121	0	1	0	1
H_2-O_{72}-Ti_{36}-Pd_2-Ag_{10}	122	0	2	0	2
H_2-O_{72}-Ti_{36}-Pd_3-Ag_7	120	0	3	0	3
H_2-O_{72}-Ti_{36}-Pd_3-Ag_9	122	0	3	0	3
H_2-O_{72}-Ti_{36}-Pd_3-Ag_{12}	125	0	3	0	3
H_2-O_{72}-Ti_{36}-Pd_3-Ag_{17}	130	0	3	0	3
H_2-O_{72}-Ti_{36}-Pd_4-Ag_{10}	124	0	1	0	1
H_2-O_{72}-Ti_{36}-Pd_4-Ag_{12}	126	0	12	0	12
H_2-O_{72}-Ti_{36}-Pd_4-Ag_{15}	129	0	1	0	1
H_2-O_{72}-Ti_{36}-Pd_5-Ag_3	118	0	2	0	2
H_2-O_{72}-Ti_{36}-Pd_5-Ag_7	122	0	1	0	1
H_2-O_{72}-Ti_{36}-Pd_5-Ag_{11}	126	0	1	0	1
H_2-O_{72}-Ti_{36}-Pd_6-Ag_6	122	0	1	0	1
H_2-O_{72}-Ti_{36}-Pd_7-Ag_9	126	0	2	0	2
H_2-O_{72}-Ti_{36}-Pd_{10}-Ag_2	122	0	3	0	3
H_2-O_{72}-Ti_{36}-Pd_{11}-Ag_1	122	0	1	0	1
H_2-O_{72}-Ti_{36}-Pd_{11}-Ag_5	126	0	4	0	4

Supplementary Table 2. Continued from previous page.

H_2-O_{72}-Ti_{36}-Pd_{12}	122	0	1	0	1
H_2-O_{72}-Ti_{36}-Pd_{12}-Ag_8	130	0	2	0	2
H_2-O_{72}-Ti_{36}-Pd_{15}-Ag_1	126	0	1	0	1
H_2-O_{72}-Ti_{36}-Pd_{15}-Ag_5	130	0	1	0	1
H_2-O_{72}-Ti_{36}-Pd_{16}	126	0	2	0	2
H_2-O_{96}-Ti_{48}	146	0	1	0	1
H_2-O_{96}-Ti_{48}-Ag_3	149	0	1	0	1
H_2-O_{96}-Ti_{48}-Ag_8	154	0	1	0	1
H_2-O_{96}-Ti_{48}-Ag_{12}	158	0	2	0	2
H_2-O_{96}-Ti_{48}-Ag_{16}	162	0	5	0	5
H_2-O_{96}-Ti_{48}-Pd_1-Ag_6	153	0	2	0	2
H_2-O_{96}-Ti_{48}-Pd_2-Ag_6	154	0	1	0	1
H_2-O_{96}-Ti_{48}-Pd_2-Ag_9	157	0	1	0	1
H_2-O_{96}-Ti_{48}-Pd_2-Ag_{10}	158	0	2	0	2
H_2-O_{96}-Ti_{48}-Pd_3-Ag_8	157	0	3	0	3
H_2-O_{96}-Ti_{48}-Pd_3-Ag_{13}	162	0	1	0	1
H_2-O_{96}-Ti_{48}-Pd_3-Ag_{17}	166	0	2	0	2
H_2-O_{96}-Ti_{48}-Pd_4-Ag_4	154	0	2	0	2
H_2-O_{96}-Ti_{48}-Pd_4-Ag_8	158	0	4	0	4
H_2-O_{96}-Ti_{48}-Pd_4-Ag_{11}	161	0	3	0	3
H_2-O_{96}-Ti_{48}-Pd_4-Ag_{12}	162	0	2	0	2
H_2-O_{96}-Ti_{48}-Pd_5-Ag_3	154	0	1	0	1
H_2-O_{96}-Ti_{48}-Pd_5-Ag_{11}	162	0	2	0	2
H_2-O_{96}-Ti_{48}-Pd_5-Ag_{15}	166	0	6	0	6
H_2-O_{96}-Ti_{48}-Pd_6-Ag_{10}	162	0	2	0	2
H_2-O_{96}-Ti_{48}-Pd_7-Ag_5	158	0	1	0	1
H_2-O_{96}-Ti_{48}-Pd_7-Ag_9	162	0	2	0	2
H_2-O_{96}-Ti_{48}-Pd_8	154	0	1	0	1
H_2-O_{96}-Ti_{48}-Pd_8-Ag_8	162	0	1	0	1
H_2-O_{96}-Ti_{48}-Pd_9-Ag_3	158	0	1	0	1
H_2-O_{96}-Ti_{48}-Pd_9-Ag_7	162	0	3	0	3
H_2-O_{96}-Ti_{48}-Pd_9-Ag_{11}	166	0	1	0	1
H_2-O_{96}-Ti_{48}-Pd_{10}-Ag_2	158	0	1	0	1
H_2-O_{96}-Ti_{48}-Pd_{11}-Ag_1	158	0	2	0	2
H_2-O_{96}-Ti_{48}-Pd_{12}	158	0	1	0	1
H_2-O_{96}-Ti_{48}-Pd_{12}-Ag_8	166	0	1	0	1
H_2-O_{96}-Ti_{48}-Pd_{14}-Ag_2	162	0	2	0	2
H_2-O_{96}-Ti_{48}-Pd_{15}-Ag_1	162	0	2	0	2
H_2-O_{96}-Ti_{48}-Pd_{16}	162	0	3	0	3
H_2-O_{96}-Ti_{48}-Pd_{18}-Ag_2	166	0	1	0	1
H_2-O_{160}-Ti_{80}	242	0	1	0	1
H_2-O_{224}-Ti_{112}	338	0	2	0	2
H_2-O_{240}-Ti_{120}-Pd_4-Ag_{12}	378	0	4	0	4
H_3-Ag_{16}	19	0	74	175	249

Supplementary Table 2. Continued from previous page.

H_3-Pd_4-Ag_{12}	19	0	13	0	13
H_3-Pd_4-Ag_{25}	32	0	0	1	1
H_3-Pd_5-Ag_{21}	29	0	1	0	1
H_3-Pd_6-Ag_{20}	29	0	1	0	1
H_3-Pd_6-Ag_{23}	32	0	0	1	1
H_3-Pd_7-Ag_{19}	29	0	1	0	1
H_3-Pd_{10}-Ag_{16}	29	0	2	0	2
H_3-Pd_{12}-Ag_{14}	29	0	1	0	1
H_3-Pd_{12}-Ag_{17}	32	1	0	0	1
H_3-Pd_{18}-Ag_8	29	0	1	0	1
H_3-Pd_{19}-Ag_7	29	0	1	0	1
H_3-Pd_{20}-Ag_6	29	0	1	0	1
H_3-Pd_{21}-Ag_5	29	0	3	0	3
H_3-Pd_{22}-Ag_4	29	0	2	0	2
H_3-Pd_{23}-Ag_3	29	0	1	0	1
H_3-Pd_{26}	29	0	120	0	120
H_3-Pd_{26}-Ag_3	32	0	0	1	1
H_3-Pd_{27}-Ag_2	32	0	0	1	1
H_3-Pd_{28}	31	1	0	11	12
H_3-Pd_{29}	32	2	0	23	25
H_3-Pd_{32}-Ag_7	42	0	141	0	141
H_3-O_6-Ti_{20}	29	0	20	0	20
H_3-O_8-Ti_4	15	0	1	2350	2351
H_3-O_{12}-Ti_6	21	0	316	176	492
H_3-O_{15}-Ti_8	26	0	15	0	15
H_3-O_{16}-Ti_8	27	0	8	0	8
H_3-O_{18}-Ti_8	29	0	3	0	3
H_3-O_{19}-Ti_8	30	0	107	0	107
H_3-O_{20}-Ti_{10}-Pd_4-Ag_{11}	48	0	25	6	31
H_3-O_{32}-Ti_{16}-Pd_5-Ag_{12}	68	0	17	4	21
H_3-O_{64}-Ti_{32}-Pd_2-Ag_9	110	0	2	3	5
H_3-O_{64}-Ti_{32}-Pd_3-Ag_4	106	0	1	6	7
H_3-O_{64}-Ti_{32}-Pd_3-Ag_8	110	0	1	2	3
H_3-O_{64}-Ti_{32}-Pd_3-Ag_9	111	0	1	7	8
H_3-O_{64}-Ti_{32}-Pd_3-Ag_{12}	114	0	1	1	2
H_3-O_{64}-Ti_{32}-Pd_4-Ag_3	106	0	1	1	2
H_3-O_{64}-Ti_{32}-Pd_4-Ag_4	107	0	5	2	7
H_3-O_{64}-Ti_{32}-Pd_4-Ag_{11}	114	0	2	1	3
H_3-O_{64}-Ti_{32}-Pd_4-Ag_{12}	115	0	1	4	5
H_3-O_{64}-Ti_{32}-Pd_4-Ag_{15}	118	0	1	6	7
H_3-O_{64}-Ti_{32}-Pd_5-Ag_6	110	0	4	1	5
H_3-O_{64}-Ti_{32}-Pd_5-Ag_{14}	118	0	1	3	4
H_3-O_{64}-Ti_{32}-Pd_5-Ag_{15}	119	0	0	1	1
H_3-O_{64}-Ti_{32}-Pd_6-Ag_5	110	0	1	4	5

Supplementary Table 2. Continued from previous page.

H_3-O_{64}-Ti_{32}-Pd_6-Ag_6	111	0	2	1	3
H_3-O_{224}-Ti_{112}	339	0	2	0	2
H_3-O_{240}-Ti_{120}-Pd_4-Ag_{12}	379	0	1	0	1
H_3-O_{252}-Ti_{126}-Pd_4-Ag_{12}	397	0	1	0	1
H_4-Ag_{12}	16	1	0	0	1
H_4-Pd_1-Ag_{11}	16	2	0	2	4
H_4-Pd_1-Ag_{15}	20	0	3	203	206
H_4-Pd_2-Ag_{10}	16	13	0	2	15
H_4-Pd_2-Ag_{15}	21	0	0	1	1
H_4-Pd_2-Ag_{22}	28	0	1	0	1
H_4-Pd_3-Ag_9	16	16	0	2	18
H_4-Pd_3-Ag_{14}	21	0	0	1	1
H_4-Pd_4-Ag_8	16	27	0	3	30
H_4-Pd_4-Ag_{20}	28	0	1	0	1
H_4-Pd_5-Ag_7	16	14	0	4	18
H_4-Pd_6-Ag_6	16	18	0	5	23
H_4-Pd_6-Ag_{11}	21	0	0	2	2
H_4-Pd_7-Ag_5	16	20	0	1	21
H_4-Pd_7-Ag_{10}	21	0	0	1	1
H_4-Pd_8-Ag_4	16	18	0	0	18
H_4-Pd_8-Ag_8	20	0	0	16	16
H_4-Pd_8-Ag_{12}	24	0	1	0	1
H_4-Pd_8-Ag_{40}	52	0	1	0	1
H_4-Pd_9-Ag_3	16	16	0	1	17
H_4-Pd_9-Ag_8	21	0	0	2	2
H_4-Pd_{10}-Ag_2	16	29	0	1	30
H_4-Pd_{11}-Ag_1	16	35	0	2	37
H_4-Pd_{11}-Ag_6	21	0	0	1	1
H_4-Pd_{11}-Ag_{13}	28	0	1	0	1
H_4-Pd_{12}	16	2122	0	256	2378
H_4-Pd_{12}-Ag_4	20	0	10	0	10
H_4-Pd_{13}-Ag_4	21	0	0	2	2
H_4-Pd_{13}-Ag_7	24	0	1	0	1
H_4-Pd_{13}-Ag_{11}	28	0	1	0	1
H_4-Pd_{14}-Ag_2	20	0	14	0	14
H_4-Pd_{15}-Ag_2	21	0	0	2	2
H_4-Pd_{16}-Ag_1	21	0	0	4	4
H_4-Pd_{17}	21	0	0	170	170
H_4-Pd_{17}-Ag_7	28	0	1	0	1
H_4-Pd_{18}-Ag_2	24	0	1	0	1
H_4-Pd_{18}-Ag_6	28	0	1	0	1
H_4-Pd_{19}-Ag_5	28	0	1	0	1
H_4-Pd_{20}	24	0	24	0	24
H_4-Pd_{22}-Ag_2	28	0	1	0	1

Supplementary Table 2. Continued from previous page.

H_4-Pd_{24}	28	0	45	0	45
H_4-Pd_{26}-Ag_{10}	40	0	319	0	319
H_4-Pd_{31}-Ag_5	40	0	168	0	168
H_4-Pd_{31}-Ag_7	42	0	3	0	3
H_4-Pd_{35}-Ag_2	41	0	11	0	11
H_4-Pd_{36}-Ag_2	42	0	149	0	149
H_4-Ti_{12}	16	1479	0	730	2209
H_4-Ti_{17}	21	0	18	469	487
H_4-O_4-Ti_8	16	0	0	676	676
H_4-O_5-Ti_{20}	29	0	24	0	24
H_4-O_8-Ti_4	16	35	403	2521	2959
H_4-O_{16}-Ti_8	28	0	14	624	638
H_4-O_{19}-Ti_8	31	0	89	0	89
H_4-O_{32}-Ti_{16}-Pd_4-Ag_{12}	68	0	18	0	18
H_4-O_{32}-Ti_{16}-Pd_5-Ag_{11}	68	0	10	2	12
H_4-O_{64}-Ti_{32}-Pd_3-Ag_4	107	0	6	2	8
H_4-O_{64}-Ti_{32}-Pd_3-Ag_{12}	115	0	0	6	6
H_4-O_{64}-Ti_{32}-Pd_4-Ag_3	107	0	4	1	5
H_4-O_{64}-Ti_{32}-Pd_4-Ag_4	108	0	2	0	2
H_4-O_{64}-Ti_{32}-Pd_4-Ag_{12}	116	0	3	1	4
H_4-O_{64}-Ti_{32}-Pd_4-Ag_{15}	119	0	1	0	1
H_4-O_{64}-Ti_{32}-Pd_5-Ag_6	111	0	0	1	1
H_4-O_{64}-Ti_{32}-Pd_5-Ag_{14}	119	0	2	6	8
H_4-O_{64}-Ti_{32}-Pd_5-Ag_{15}	120	0	5	1	6
H_4-O_{64}-Ti_{32}-Pd_6-Ag_5	111	0	1	2	3
H_4-O_{64}-Ti_{32}-Pd_6-Ag_6	112	0	1	0	1
H_4-O_{160}-Ti_{80}	244	0	2	0	2
H_4-O_{224}-Ti_{112}	340	0	2	0	2
H_4-O_{240}-Ti_{120}-Pd_4-Ag_{12}	380	0	3	0	3
H_4-O_{252}-Ti_{126}-Pd_4-Ag_{12}	398	0	1	0	1
H_4-O_{252}-Ti_{126}-Pd_{10}-Ag_{30}	422	0	2	0	2
H_5-Pd_3-Ag_{13}	21	0	1	0	1
H_5-Pd_4-Ag_{12}	21	0	76	154	230
H_5-Pd_5-Ag_{11}	21	0	1	1	2
H_5-Pd_5-Ag_{30}	40	9	0	0	9
H_5-Pd_6-Ag_{10}	21	0	1	2	3
H_5-Pd_8-Ag_8	21	0	1	0	1
H_5-Pd_9-Ag_7	21	0	2	0	2
H_5-Pd_{10}-Ag_6	21	0	1	0	1
H_5-Pd_{11}-Ag_5	21	0	4	1	5
H_5-Pd_{12}-Ag_4	21	0	1	0	1
H_5-Pd_{13}-Ag_3	21	0	4	1	5
H_5-Pd_{14}-Ag_2	21	0	2	1	3

Supplementary Table 2. Continued from previous page.

H_5-Pd_{15}-Ag_1	21	0	1	0	1
H_5-Pd_{16}	21	0	182	38	220
H_5-Pd_{25}-Ag_{10}	40	0	4	0	4
H_5-Ti_{16}	21	0	364	26	390
H_5-O_{10}-Ti_5-Pd_1-Ag_3	24	0	21	8	29
H_5-O_{19}-Ti_8	32	0	70	0	70
H_5-O_{20}-Ti_{10}-Pd_3-Ag_{10}	48	0	30	4	34
H_5-O_{20}-Ti_{10}-Pd_4-Ag_9	48	0	12	3	15
H_5-O_{64}-Ti_{32}-Pd_4-Ag_{15}	120	0	4	1	5
H_5-O_{64}-Ti_{32}-Pd_5-Ag_6	112	0	1	0	1
H_5-O_{64}-Ti_{32}-Pd_5-Ag_{14}	120	0	4	2	6
H_5-O_{64}-Ti_{32}-Pd_5-Ag_{15}	121	0	4	3	7
H_5-O_{64}-Ti_{32}-Pd_6-Ag_5	112	0	5	2	7
H_5-O_{64}-Ti_{32}-Pd_6-Ag_6	113	0	2	1	3
H_5-O_{96}-Ti_{48}	149	0	1	0	1
H_5-O_{160}-Ti_{80}	245	0	2	0	2
H_5-O_{224}-Ti_{112}	341	0	2	0	2
H_5-O_{240}-Ti_{120}-Pd_{10}-Ag_{30}	405	0	2	0	2
H_6-Pd_1-Ag_9	16	0	0	1	1
H_6-Pd_1-Ag_{14}	21	0	1	0	1
H_6-Pd_2-Ag_8	16	0	0	3	3
H_6-Pd_2-Ag_{13}	21	0	1	0	1
H_6-Pd_3-Ag_7	16	0	0	5	5
H_6-Pd_3-Ag_{12}	21	0	2	0	2
H_6-Pd_3-Ag_{23}	32	1	0	0	1
H_6-Pd_4-Ag_6	16	0	0	6	6
H_6-Pd_4-Ag_{22}	32	0	0	1	1
H_6-Pd_5-Ag_5	16	0	0	8	8
H_6-Pd_5-Ag_{10}	21	0	4	0	4
H_6-Pd_5-Ag_{20}	31	0	1	0	1
H_6-Pd_5-Ag_{31}	42	38	0	0	38
H_6-Pd_6-Ag_4	16	0	0	3	3
H_6-Pd_6-Ag_9	21	0	5	0	5
H_6-Pd_7-Ag_3	16	0	0	9	9
H_6-Pd_7-Ag_8	21	0	2	0	2
H_6-Pd_7-Ag_{19}	32	0	0	1	1
H_6-Pd_8-Ag_2	16	0	0	7	7
H_6-Pd_8-Ag_7	21	0	4	0	4
H_6-Pd_8-Ag_{18}	32	0	1	0	1
H_6-Pd_8-Ag_{28}	42	0	155	0	155
H_6-Pd_9-Ag_1	16	0	0	5	5
H_6-Pd_9-Ag_{17}	32	0	0	1	1
H_6-Pd_{10}	16	0	0	360	360
H_6-Pd_{10}-Ag_5	21	0	1	0	1

Supplementary Table 2. Continued from previous page.

H_6-Pd_{10}-Ag_{16}	32	0	1	1	2
H_6-Pd_{10}-Ag_{38}	54	0	2	0	2
H_6-Pd_{11}-Ag_4	21	0	4	0	4
H_6-Pd_{11}-Ag_{15}	32	0	0	1	1
H_6-Pd_{11}-Ag_{37}	54	0	3	0	3
H_6-Pd_{12}-Ag_3	21	0	3	0	3
H_6-Pd_{12}-Ag_{13}	31	0	1	0	1
H_6-Pd_{12}-Ag_{14}	32	0	1	1	2
H_6-Pd_{12}-Ag_{36}	54	0	5	0	5
H_6-Pd_{13}-Ag_2	21	0	1	0	1
H_6-Pd_{14}-Ag_1	21	0	3	0	3
H_6-Pd_{14}-Ag_{11}	31	0	1	0	1
H_6-Pd_{14}-Ag_{12}	32	0	0	1	1
H_6-Pd_{15}	21	0	286	5	291
H_6-Pd_{15}-Ag_{10}	31	0	3	0	3
H_6-Pd_{15}-Ag_{19}	40	5	0	0	5
H_6-Pd_{15}-Ag_{21}	42	85	0	0	85
H_6-Pd_{16}-Ag_9	31	0	1	0	1
H_6-Pd_{16}-Ag_{10}	32	0	1	0	1
H_6-Pd_{16}-Ag_{20}	42	0	79	0	79
H_6-Pd_{17}-Ag_9	32	1	0	0	1
H_6-Pd_{18}-Ag_7	31	0	2	0	2
H_6-Pd_{19}-Ag_7	32	1	1	0	2
H_6-Pd_{20}-Ag_6	32	1	2	2	5
H_6-Pd_{21}-Ag_4	31	0	1	0	1
H_6-Pd_{21}-Ag_5	32	0	1	1	2
H_6-Pd_{22}-Ag_3	31	0	1	0	1
H_6-Pd_{22}-Ag_4	32	0	0	2	2
H_6-Pd_{23}-Ag_3	32	1	0	0	1
H_6-Pd_{24}-Ag_2	32	2	1	0	3
H_6-Pd_{25}	31	0	80	0	80
H_6-Pd_{25}-Ag_1	32	1	1	1	3
H_6-Pd_{26}	32	108	77	106	291
H_6-Pd_{27}-Ag_9	42	90	0	0	90
H_6-Pd_{32}-Ag_4	42	0	56	0	56
H_6-Pd_{35}-Ag_1	42	96	70	0	166
H_6-Ti_{10}	16	0	5	870	875
H_6-Ti_{15}	21	0	464	1	465
H_6-Ti_{25}	31	0	23	0	23
H_6-Ti_{26}	32	108	77	106	291
H_6-O_{19}-Ti_8	33	0	99	27	126
H_6-O_{64}-Ti_{32}-Pd_5-Ag_6	113	0	1	1	2
H_6-O_{64}-Ti_{32}-Pd_6-Ag_5	113	0	1	1	2
H_6-O_{64}-Ti_{32}-Pd_6-Ag_6	114	0	0	1	1

Supplementary Table 2. Continued from previous page.

H_6-O_{96}-Ti_{48}	150	0	3	0	3
H_6-O_{160}-Ti_{80}	246	0	5	0	5
H_6-O_{224}-Ti_{112}	342	0	2	0	2
H_6-O_{240}-Ti_{120}-Pd_7-Ag_{21}	394	0	2	0	2
H_6-O_{252}-Ti_{126}-Pd_7-Ag_{21}	412	0	3	0	3
H_7-Pd_5-Ag_{20}	32	0	0	1	1
H_7-Pd_8-Ag_{17}	32	0	0	1	1
H_7-Pd_8-Ag_{27}	42	0	4	0	4
H_7-Pd_{12}-Ag_{13}	32	0	0	1	1
H_7-Pd_{13}-Ag_{12}	32	0	0	1	1
H_7-Pd_{17}-Ag_8	32	0	0	1	1
H_7-Pd_{22}-Ag_3	32	0	0	2	2
H_7-Pd_{23}-Ag_2	32	0	0	2	2
H_7-Pd_{24}-Ag_1	32	0	0	3	3
H_7-Pd_{25}	32	0	0	68	68
H_7-Ti_{25}	32	0	0	35	35
H_7-O_{16}-Ti_8	31	0	26	0	26
H_7-O_{18}-Ti_8	33	0	6	0	6
H_7-O_{96}-Ti_{48}	151	0	3	0	3
H_7-O_{160}-Ti_{80}	247	0	2	0	2
H_7-O_{224}-Ti_{112}	343	0	2	0	2
H_7-O_{240}-Ti_{120}-Pd_7-Ag_{21}	395	0	1	0	1
H_7-O_{240}-Ti_{120}-Pd_{10}-Ag_{30}	407	0	2	0	2
H_7-O_{252}-Ti_{126}-Pd_7-Ag_{21}	413	0	4	0	4
H_8-Ag_8	16	9	0	7	16
H_8-Pd_1-Ag_7	16	33	0	8	41
H_8-Pd_2-Ag_6	16	31	0	19	50
H_8-Pd_2-Ag_{14}	24	0	2	188	190
H_8-Pd_3-Ag_5	16	37	0	21	58
H_8-Pd_3-Ag_{13}	24	0	1	0	1
H_8-Pd_4-Ag_4	16	43	0	17	60
H_8-Pd_5-Ag_3	16	37	0	17	54
H_8-Pd_5-Ag_{11}	24	0	2	0	2
H_8-Pd_6-Ag_2	16	61	0	21	82
H_8-Pd_7-Ag_1	16	57	0	30	87
H_8-Pd_7-Ag_9	24	0	1	0	1
H_8-Pd_8	16	2986	0	1462	4448
H_8-Pd_8-Ag_8	24	0	0	199	199
H_8-Pd_8-Ag_{12}	28	0	1	0	1
H_8-Pd_{10}-Ag_6	24	0	1	0	1
H_8-Pd_{11}-Ag_9	28	0	1	0	1
H_8-Pd_{12}-Ag_4	24	0	60	169	229

Supplementary Table 2. Continued from previous page.

H_8-Pd_{12}-Ag_8	28	0	1	0	1
H_8-Pd_{12}-Ag_{36}	56	0	3	0	3
H_8-Pd_{13}-Ag_7	28	0	1	0	1
H_8-Pd_{13}-Ag_{35}	56	0	3	0	3
H_8-Pd_{14}-Ag_2	24	0	65	155	220
H_8-Pd_{15}-Ag_1	24	0	2	0	2
H_8-Pd_{16}	24	0	53	0	53
H_8-Pd_{16}-Ag_4	28	0	1	0	1
H_8-Pd_{16}-Ag_{32}	56	0	1	0	1
H_8-Pd_{17}-Ag_3	28	0	1	0	1
H_8-Pd_{20}	28	0	28	0	28
H_8-Ti_8	16	1517	59	2827	4403
H_8-O_{19}-Ti_8	35	0	108	55	163
H_8-O_{36}-Ti_{16}	60	0	61	0	61
H_8-O_{44}-Ti_{20}	72	0	99	0	99
H_8-O_{52}-Ti_{24}	84	0	90	0	90
H_8-O_{68}-Ti_{32}	108	0	10	0	10
H_8-O_{96}-Ti_{48}	152	0	4	0	4
H_8-O_{160}-Ti_{80}	248	0	3	0	3
H_8-O_{224}-Ti_{112}	344	0	2	0	2
H_8-O_{240}-Ti_{120}-Pd_7-Ag_{21}	396	0	2	0	2
H_8-O_{240}-Ti_{120}-Pd_{10}-Ag_{30}	408	0	4	0	4
H_8-O_{240}-Ti_{120}-Pd_{13}-Ag_{39}	420	0	1	0	1
H_8-O_{252}-Ti_{126}-Pd_7-Ag_{21}	414	0	2	0	2
H_8-O_{252}-Ti_{126}-Pd_{10}-Ag_{30}	426	0	1	0	1
H_9-Pd_5-Ag_{18}	32	1	0	0	1
H_9-Pd_7-Ag_{16}	32	1	0	0	1
H_9-Pd_9-Ag_{14}	32	1	0	0	1
H_9-Pd_{10}-Ag_{13}	32	1	0	0	1
H_9-Pd_{13}-Ag_{10}	32	1	0	0	1
H_9-Pd_{14}-Ag_9	32	2	0	0	2
H_9-Pd_{21}-Ag_2	32	1	0	0	1
H_9-Pd_{22}-Ag_1	32	1	0	0	1
H_9-Pd_{23}	32	96	0	0	96
H_9-Pd_{27}-Ag_4	40	0	6	0	6
H_9-Ti_{23}	32	50	0	0	50
H_9-O_{240}-Ti_{120}-Pd_{10}-Ag_{30}	409	0	4	0	4
H_9-O_{252}-Ti_{126}-Pd_{10}-Ag_{30}	427	0	2	0	2
H_9-O_{252}-Ti_{126}-Pd_{13}-Ag_{39}	439	0	1	0	1
H_{10}-Pd_3-Ag_{19}	32	0	2	0	2
H_{10}-Pd_4-Ag_{18}	32	0	1	0	1

Supplementary Table 2. Continued from previous page.

H_{10}-Pd_5-Ag_{17}	32	0	0	2	2
H_{10}-Pd_6-Ag_{15}	31	0	2	0	2
H_{10}-Pd_6-Ag_{16}	32	0	0	2	2
H_{10}-Pd_7-Ag_{14}	31	0	1	0	1
H_{10}-Pd_7-Ag_{15}	32	0	1	2	3
H_{10}-Pd_8-Ag_{14}	32	0	1	2	3
H_{10}-Pd_9-Ag_{12}	31	0	1	0	1
H_{10}-Pd_{10}-Ag_{11}	31	0	2	0	2
H_{10}-Pd_{10}-Ag_{12}	32	0	0	3	3
H_{10}-Pd_{12}-Ag_{10}	32	0	0	1	1
H_{10}-Pd_{12}-Ag_{36}	58	0	3	0	3
H_{10}-Pd_{13}-Ag_{35}	58	0	1	0	1
H_{10}-Pd_{14}-Ag_7	31	0	1	0	1
H_{10}-Pd_{16}-Ag_5	31	0	1	0	1
H_{10}-Pd_{16}-Ag_6	32	0	0	2	2
H_{10}-Pd_{17}-Ag_5	32	0	2	1	3
H_{10}-Pd_{19}-Ag_3	32	0	0	3	3
H_{10}-Pd_{20}-Ag_1	31	0	1	0	1
H_{10}-Pd_{20}-Ag_2	32	0	0	3	3
H_{10}-Pd_{21}	31	0	92	0	92
H_{10}-Pd_{21}-Ag_1	32	0	1	1	2
H_{10}-Pd_{22}	32	0	64	207	271
H_{10}-Ti_{21}	31	0	25	0	25
H_{10}-Ti_{22}	32	0	64	207	271
H_{10}-O_1-Ti_{18}	29	0	20	0	20
H_{10}-O_{20}-Ti_8	38	0	55	11	66
H_{10}-O_{21}-Ti_8	39	0	40	6	46
H_{10}-O_{72}-Ti_{36}-Pd_1-Ag_{19}	138	0	1	0	1
H_{10}-O_{72}-Ti_{36}-Pd_2-Ag_{18}	138	0	2	0	2
H_{10}-O_{72}-Ti_{36}-Pd_4-Ag_{16}	138	0	2	0	2
H_{10}-O_{72}-Ti_{36}-Pd_5-Ag_{15}	138	0	1	0	1
H_{10}-O_{72}-Ti_{36}-Pd_6-Ag_{14}	138	0	1	0	1
H_{10}-O_{72}-Ti_{36}-Pd_7-Ag_{13}	138	0	4	0	4
H_{10}-O_{72}-Ti_{36}-Pd_9-Ag_{11}	138	0	1	0	1
H_{10}-O_{72}-Ti_{36}-Pd_{10}-Ag_{10}	138	0	1	0	1
H_{10}-O_{72}-Ti_{36}-Pd_{11}-Ag_9	138	0	2	0	2
H_{10}-O_{72}-Ti_{36}-Pd_{17}-Ag_3	138	0	4	0	4
H_{10}-O_{72}-Ti_{36}-Pd_{19}-Ag_1	138	0	3	0	3
H_{10}-O_{96}-Ti_{48}-Pd_{13}-Ag_7	174	0	4	0	4

Supplementary Table 2. Continued from previous page.

H_{10}-O_{96}-Ti_{48}-Pd_{16}-Ag_4	174	0	1	0	1
H_{10}-O_{96}-Ti_{48}-Pd_{18}-Ag_2	174	0	2	0	2
H_{10}-O_{240}-Ti_{120}-Pd_{10}-Ag_{30}	410	0	5	0	5
H_{10}-O_{252}-Ti_{126}-Pd_{10}-Ag_{30}	428	0	1	0	1
H_{10}-O_{252}-Ti_{126}-Pd_{13}-Ag_{39}	440	0	2	0	2
H_{11}-Ag_5	16	0	0	10	10
H_{11}-Pd_1-Ag_4	16	0	2	25	27
H_{11}-Pd_2-Ag_3	16	0	2	26	28
H_{11}-Pd_3-Ag_2	16	0	2	23	25
H_{11}-Pd_3-Ag_{18}	32	0	0	3	3
H_{11}-Pd_4-Ag_1	16	0	2	40	42
H_{11}-Pd_4-Ag_{17}	32	0	0	1	1
H_{11}-Pd_5	16	0	41	1334	1375
H_{11}-Pd_6-Ag_{15}	32	0	0	1	1
H_{11}-Pd_9-Ag_{12}	32	0	0	2	2
H_{11}-Pd_{10}-Ag_{11}	32	0	0	1	1
H_{11}-Pd_{11}-Ag_{10}	32	0	0	1	1
H_{11}-Pd_{12}-Ag_9	32	0	0	1	1
H_{11}-Pd_{14}-Ag_7	32	0	0	1	1
H_{11}-Pd_{15}-Ag_6	32	0	0	4	4
H_{11}-Pd_{16}-Ag_5	32	0	0	1	1
H_{11}-Pd_{18}-Ag_3	32	0	0	1	1
H_{11}-Pd_{19}-Ag_2	32	0	0	1	1
H_{11}-Pd_{20}-Ag_1	32	0	0	2	2
H_{11}-Pd_{21}	32	0	0	176	176
H_{11}-Ti_5	16	0	17	1610	1627
H_{11}-Ti_{18}	29	0	17	0	17
H_{11}-Ti_{21}	32	0	0	75	75
H_{11}-O_{240}-Ti_{120}-Pd_{13}-Ag_{39}	423	0	1	0	1
H_{11}-O_{252}-Ti_{126}-Pd_{13}-Ag_{39}	441	0	8	0	8
H_{12}-Pd_{16}-Ag_{32}	60	0	3	0	3
H_{12}-O_{240}-Ti_{120}-Pd_{10}-Ag_{30}	412	0	2	0	2
H_{12}-O_{240}-Ti_{120}-Pd_{13}-Ag_{39}	424	0	4	0	4
H_{12}-O_{252}-Ti_{126}-Pd_{13}-Ag_{39}	442	0	1	0	1
H_{13}-Pd_6-Ag_{13}	32	0	0	1	1
H_{13}-Pd_9-Ag_{10}	32	0	0	1	1
H_{13}-Pd_{17}-Ag_2	32	0	0	1	1
H_{13}-Pd_{19}	32	0	0	53	53
H_{13}-Ti_{19}	32	0	0	53	53

Supplementary Table 2. Continued from previous page.

H_{13}-O_{240}-Ti_{120}-Pd_{13}-Ag_{39}	425	0	3	0	3
H_{14}-Pd_{2}-Ag_{15}	31	0	0	2	2
H_{14}-Pd_{4}-Ag_{13}	31	0	0	3	3
H_{14}-Pd_{5}-Ag_{12}	31	0	0	2	2
H_{14}-Pd_{5}-Ag_{13}	32	0	0	2	2
H_{14}-Pd_{7}-Ag_{10}	31	0	0	1	1
H_{14}-Pd_{8}-Ag_{9}	31	0	0	1	1
H_{14}-Pd_{9}-Ag_{8}	31	0	0	1	1
H_{14}-Pd_{10}-Ag_{7}	31	0	0	1	1
H_{14}-Pd_{10}-Ag_{8}	32	0	0	1	1
H_{14}-Pd_{11}-Ag_{6}	31	0	0	1	1
H_{14}-Pd_{11}-Ag_{7}	32	0	0	1	1
H_{14}-Pd_{12}-Ag_{5}	31	0	0	1	1
H_{14}-Pd_{12}-Ag_{6}	32	0	0	1	1
H_{14}-Pd_{13}-Ag_{4}	31	0	0	1	1
H_{14}-Pd_{14}-Ag_{3}	31	0	0	2	2
H_{14}-Pd_{14}-Ag_{4}	32	0	0	1	1
H_{14}-Pd_{15}-Ag_{3}	32	0	0	2	2
H_{14}-Pd_{16}-Ag_{1}	31	0	0	1	1
H_{14}-Pd_{17}	31	0	0	126	126
H_{14}-Pd_{17}-Ag_{1}	32	0	0	1	1
H_{14}-Pd_{17}-Ag_{31}	62	0	2	0	2
H_{14}-Pd_{18}	32	0	0	84	84
H_{14}-Ti_{17}	31	0	0	60	60
H_{14}-Ti_{18}	32	0	0	41	41
H_{14}-O_{7}	21	0	1	808	809
H_{14}-O_{21}-Ti_{8}	43	0	18	17	35
H_{15}-Ag_{6}	21	0	1	0	1
H_{15}-Pd_{1}-Ag_{5}	21	0	8	0	8
H_{15}-Pd_{1}-Ag_{16}	32	0	0	1	1
H_{15}-Pd_{2}-Ag_{4}	21	0	10	0	10
H_{15}-Pd_{2}-Ag_{14}	31	0	0	1	1
H_{15}-Pd_{2}-Ag_{15}	32	0	0	1	1
H_{15}-Pd_{3}-Ag_{3}	21	0	5	0	5
H_{15}-Pd_{3}-Ag_{14}	32	0	0	1	1
H_{15}-Pd_{4}-Ag_{2}	21	0	17	0	17
H_{15}-Pd_{4}-Ag_{12}	31	0	0	2	2
H_{15}-Pd_{4}-Ag_{13}	32	0	0	1	1
H_{15}-Pd_{5}-Ag_{1}	21	0	16	0	16
H_{15}-Pd_{5}-Ag_{11}	31	0	0	2	2
H_{15}-Pd_{5}-Ag_{12}	32	0	0	1	1
H_{15}-Pd_{6}	21	0	650	0	650
H_{15}-Pd_{6}-Ag_{11}	32	0	0	1	1
H_{15}-Pd_{7}-Ag_{9}	31	0	0	1	1

Supplementary Table 2. Continued from previous page.

H_{15}-Pd_7-Ag_{10}	32	0	0	1	1
H_{15}-Pd_8-Ag_8	31	0	0	1	1
H_{15}-Pd_9-Ag_8	32	0	0	1	1
H_{15}-Pd_{10}-Ag_6	31	0	0	1	1
H_{15}-Pd_{10}-Ag_7	32	0	0	2	2
H_{15}-Pd_{11}-Ag_6	32	0	0	3	3
H_{15}-Pd_{12}-Ag_5	32	0	0	2	2
H_{15}-Pd_{13}-Ag_4	32	0	0	1	1
H_{15}-Pd_{14}-Ag_2	31	0	0	1	1
H_{15}-Pd_{14}-Ag_3	32	0	0	8	8
H_{15}-Pd_{15}-Ag_1	31	0	0	2	2
H_{15}-Pd_{15}-Ag_2	32	0	0	5	5
H_{15}-Pd_{16}	31	0	0	165	165
H_{15}-Pd_{16}-Ag_1	32	0	0	2	2
H_{15}-Pd_{17}	32	0	0	259	259
H_{15}-Ti_6	21	0	974	0	974
H_{15}-Ti_{16}	31	0	0	67	67
H_{15}-Ti_{17}	32	0	0	259	259
H_{16}-Ag_5	21	0	4	0	4
H_{16}-Pd_1-Ag_4	21	0	17	3	20
H_{16}-Pd_2-Ag_3	21	0	21	2	23
H_{16}-Pd_3-Ag_2	21	0	27	0	27
H_{16}-Pd_3-Ag_{13}	32	0	0	1	1
H_{16}-Pd_4-Ag_1	21	0	24	1	25
H_{16}-Pd_4-Ag_{12}	32	0	0	5	5
H_{16}-Pd_5	21	0	950	58	1008
H_{16}-Pd_5-Ag_{11}	32	0	0	2	2
H_{16}-Pd_6-Ag_{10}	32	0	0	2	2
H_{16}-Pd_7-Ag_9	32	0	0	3	3
H_{16}-Pd_8-Ag_8	32	0	0	2	2
H_{16}-Pd_9-Ag_7	32	0	0	5	5
H_{16}-Pd_{10}-Ag_6	32	0	0	6	6
H_{16}-Pd_{11}-Ag_5	32	0	0	5	5
H_{16}-Pd_{12}-Ag_4	32	0	0	10	10
H_{16}-Pd_{13}-Ag_3	32	0	0	8	8
H_{16}-Pd_{14}-Ag_2	32	0	0	6	6
H_{16}-Pd_{16}	32	0	1	459	460
H_{16}-Pd_{18}-Ag_{30}	64	0	1	0	1
H_{16}-Pd_{20}-Ag_{28}	64	0	2	0	2
H_{16}-Ti_5	21	0	1262	0	1262
H_{16}-Ti_{16}	32	0	1	428	429
H_{16}-O_8	24	0	14	3955	3969
H_{17}-Pd_3-Ag_{12}	32	0	0	2	2
H_{17}-Pd_4-Ag_{11}	32	0	0	2	2

Supplementary Table 2. Continued from previous page.

H_{17}-Pd_5-Ag_{10}	32	0	0	1	1
H_{17}-Pd_6-Ag_9	32	0	0	2	2
H_{17}-Pd_7-Ag_8	32	0	0	2	2
H_{17}-Pd_8-Ag_7	32	0	0	3	3
H_{17}-Pd_9-Ag_6	32	0	0	1	1
H_{17}-Pd_{10}-Ag_5	32	0	0	2	2
H_{17}-Pd_{13}-Ag_2	32	0	0	2	2
H_{17}-Pd_{14}-Ag_1	32	0	0	3	3
H_{17}-Pd_{15}	32	0	0	103	103
H_{17}-Ti_{15}	32	0	0	45	45
H_{18}-Pd_6-Ag_7	31	0	0	3	3
H_{18}-Pd_7-Ag_6	31	0	0	1	1
H_{18}-Pd_{11}-Ag_2	31	0	0	1	1
H_{18}-Pd_{12}-Ag_1	31	0	0	1	1
H_{18}-Pd_{13}	31	0	0	50	50
H_{18}-Ti_{13}	31	0	0	19	19
H_{19}-Pd_3-Ag_{10}	32	0	0	2	2
H_{19}-Pd_5-Ag_8	32	0	0	1	1
H_{19}-Pd_{10}-Ag_3	32	0	0	1	1
H_{19}-Pd_{11}-Ag_2	32	0	0	1	1
H_{19}-Pd_{13}	32	0	0	64	64
H_{19}-Ti_{13}	32	0	0	64	64
H_{23}-Ag_9	32	0	2	0	2
H_{23}-Pd_1-Ag_7	31	0	1	0	1
H_{23}-Pd_1-Ag_8	32	0	3	2	5
H_{23}-Pd_2-Ag_6	31	0	4	0	4
H_{23}-Pd_2-Ag_7	32	0	2	0	2
H_{23}-Pd_3-Ag_5	31	0	1	0	1
H_{23}-Pd_3-Ag_6	32	0	3	0	3
H_{23}-Pd_4-Ag_4	31	0	1	0	1
H_{23}-Pd_4-Ag_5	32	0	7	1	8
H_{23}-Pd_5-Ag_3	31	0	2	1	3
H_{23}-Pd_5-Ag_4	32	0	2	1	3
H_{23}-Pd_6-Ag_2	31	0	4	1	5
H_{23}-Pd_6-Ag_3	32	0	2	0	2
H_{23}-Pd_7-Ag_1	31	0	1	2	3
H_{23}-Pd_7-Ag_2	32	0	1	2	3
H_{23}-Pd_8	31	0	149	68	217
H_{23}-Pd_8-Ag_1	32	0	1	2	3
H_{23}-Pd_9	32	0	235	139	374
H_{23}-Ti_8	31	0	58	6	64
H_{23}-Ti_9	32	0	235	140	375
H_{24}-Pd_1-Ag_7	32	0	0	1	1
H_{24}-Pd_2-Ag_6	32	0	0	3	3

Supplementary Table 2. Continued from previous page.

H_{24}-Pd_3-Ag_5	32	0	0	1	1
H_{24}-Pd_4-Ag_4	32	0	3	0	3
H_{24}-Pd_7-Ag_1	32	0	1	1	2
H_{24}-Pd_8	32	0	41	71	112
H_{24}-Ti_8	32	0	0	23	23
H_{30}-O_{15}	45	124	4	94	222
H_{32}-Pd_{32}	64	99	0	22	121
Total	--	12585	37444	95092	145121

13. Statistics for MD simulations of PdAg nanoparticles on TiO_2 at different temperatures

Supplementary Table 3. Statistics of the number of bonds between Pd_{208}-Ag_{208} nanoparticle and the surface O atoms of rutile TiO_2(110) in the isothermal Nose-Hoover molecular simulations at different temperatures.

Temperature	**Number of bonds**			
	$N_{Pd\text{-}O}$	$N_{Pd\text{-}Obr}$	$N_{Ag\text{-}O}$	$N_{Ag\text{-}Obr}$
327 °C	6	19	2	19
527 °C	5	14	2	17
727 °C	2	6	2	17

14. Experimental results guided by multi-scale ML

Table S4. Experimental results guided by multi-scale ML with detailed synthetic conditions and the catalytic performance in acetylene semi-hydrogenation.

Entry	Catalyst	Reaction Temp. (°C)	Yield (%)	Ann. Temp. (°C)	Reductant	Ann. Time (h)	Pre-Oxi.*	Load Pd# (%)	Load Ag# (%)	Support	Process **
1	Pd_1Ag_3/r-TiO_2	98.0	97.2	750	5% H_2	4	N	1	3	r-TiO_2	1
2	Pd_1Ag_3/r-TiO_x	97.0	97.1	750	5% H_2	4	N	1	3	r-TiO_x	2
3	Pd_1Ag_3/r-TiO_x	95.0	97.1	750	5% H_2	4	N	1	3	r-TiO_x	1
4	Pd_1Ag_3/r-TiO_2	77.5	97.0	750	5% H_2	4	N	1	3	r-TiO_2	1
5	Pd_1Ag_3/r-TiO_2	82.0	97.0	750	5% H_2	4	Y	1	3	r-TiO_2	1
6	Pd_1Ag_3/r-TiO_2	98.0	97.0	750	5% H_2	4	N	1	3	r-TiO_2	1
7	Pd_1Ag_3/r-TiO_2	86.0	96.9	750	5% H_2	4	Y	1	3	r-TiO_2	1
8	Pd_1Ag_3/r-TiO_2	96.0	96.9	750	5% H_2	4	N	1	3	r-TiO_2	1
9	Pd_1Ag_3/r-TiO_2	80.0	96.8	750	5% H_2	4	Y	1	3	r-TiO_2	1
10	Pd_1Ag_3/r-TiO_2	95.0	96.8	750	5% H_2	4	N	1	3	r-TiO_2	1
11	Pd_1Ag_3/r-TiO_2	97.0	96.7	750	5% H_2	4	N	1	3	r-TiO_2	1
12	Pd_1Ag_3/r-TiO_2	97.0	96.7	750	5% H_2	4	N	1	3	r-TiO_2	1
13	Pd_1Ag_3/r-TiO_2	97.0	96.7	750	5% H_2	4	Y	1	3	r-TiO_2	1
14	Pd_1Ag_3/r-TiO_2	91.0	96.6	750	5% H_2	4	N	1	3	r-TiO_2	1
15	Pd_1Ag_3/r-TiO_2	100.0	96.6	750	5% H_2	4	N	1	3	r-TiO_2	1
16	Pd_1Ag_3/r-TiO_2	110.0	96.6	900	N_2	0	N	1	3	r-TiO_2	2
17	Pd_1Ag_3/r-TiO_2	101.0	96.4	750	5% H_2	4	N	1	3	r-TiO_2	1
18	Pd_1Ag_3/r-TiO_2	93.0	96.2	750	5% H_2	4	N	0.2	0.6	r-TiO_2	1
19	Pd_1Ag_3/r-TiO_2	91.0	96.1	750	5% H_2	4	Y	1	3	r-TiO_2	1
20	Pd_1Ag_3/r-TiO_x	98.0	95.7	750	5% H_2	4	N	1	3	r-TiO_x	2
21	Pd_1Ag_3/r-TiO_2	88.0	95.6	750	5% H_2+N_2	4	N	1	3	r-TiO_2	1
22	Pd_1Ag_3/r-TiO_2	79.0	95.5	750	5% H_2	4	Y	1	3	r-TiO_2	1
23	Pd_1Ag_3/r-TiO_2	98.0	95.4	750	N_2	4	N	1	3	r-TiO_2	1
24	Pd_1Ag_3/r-TiO_2	85.0	95.4	750	5% H_2+N_2	4	N	1	3	r-TiO_2	1
25	Pd_1Ag_3/r-TiO_2	85.0	95.4	650	5% H_2	40	Y	1	3	r-TiO_2	1
26	Pd_1Ag_3/r-TiO_2	85.0	95.4	650	5% H_2	40	Y	1	3	r-TiO_2	1
27	Pd_1Ag_3/C	104.0	95.4	750	5% H_2	4	N	1	3	C	1
28	Pd_1Ag_3/r-TiO_2	104.0	95.3	750	5% H_2	4	N	0.05	0.15	r-TiO_2	1
29	Pd_1Ag_3/C	108.0	95.3	750	5% H_2	4	N	1	3	C	1
30	Pd_1Ag_3/C	106.0	95.3	750	5% H_2	4	N	10	30	C	1
31	Pd_1Ag_3/C	117.0	95.2	1000	5% H_2	4	N	10	30	C	2
32	Pd_1Ag_3/C	82.0	95.2	650	5% H_2	40	N	1	3	C	1
33	Pd_1Ag_3/C	93.0	95.2	750	N_2	4	N	1	3	C	1
34	Pd_1Ag_3/r-TiO_2	81.0	95.1	700	5% H_2	4	N	1	3	r-TiO_2	2
35	Pd_1Ag_3/r-TiO_x	102.0	95.0	900	5% H_2	4	N	1	3	r-TiO_x	1
36	Pd_1Ag_3/r-TiO_2	81.0	95.0	700	5% H_2	4	Y	1	3	r-TiO_2	1
37	Pd_1Ag_3/r-TiO_2	92.0	95.0	750	N_2	4	N	1	3	r-TiO_2	1
38	Pd_1Ag_3/ZSM-5	105.0	94.9	750	5% H_2	4	N	1	3	ZSM-5	1
39	Pd_1Ag_3/r-TiO_2	81.0	94.9	750	100% H_2	4	Y	1	3	r-TiO_2	1
40	Pd_1Ag_3/r-TiO_2	81.0	94.9	750	100% H_2	4	Y	1	3	r-TiO_2	1
41	Pd_1Ag_3/$CaCO_3$	100.0	94.7	900	5% H_2	4	N	1	3	$CaCO_3$	1
42	Pd_1Ag_3/r-TiO_2	82.0	94.6	700	5% H_2	4	Y	1	3	r-TiO_2	1
43	Pd_1Ag_3/C	85.0	94.6	700	5% H_2	4	N	1	3	C	1

Supplementary Table 4. Continued from previous page.

44	Pd_1Ag_3/r-TiO_2	81.0	94.6	650	5% H_2	40	N	1	3	r-TiO_2	1
45	Pd_1Ag_3/SiO_2	115.0	94.5	900	5% H_2	4	N	1	3	SiO_2	1
46	Pd_1Ag_3/γ-Al_2O_3	105.5	94.5	750	5% H_2	4	N	1	3	γ-Al_2O_3	1
47	Pd_1Ag_3/r-TiO_2	104.0	94.5	700	5% H_2	4	N	1	3	r-TiO_2	1
48	Pd_1Ag_3/r-TiO_2	83.0	94.4	750	100% H_2	4	Y	1	3	r-TiO_2	1
49	Pd_1Ag_3/r-TiO_2	84.0	94.4	650	5% H_2	40	N	1	3	r-TiO_2	1
50	Pd_1Ag_3/r-TiO_2	85.0	94.1	700	5% H_2	4	N	1	3	r-TiO_2	1
51	Pd_1Ag_3/r-TiO_2	78.0	94.1	650	5% H_2	4	N	1	3	r-TiO_2	1
52	Pd_1Ag_3/r-TiO_2	82.0	94.1	750	100% H_2	4	Y	1	3	r-TiO_2	1
53	Pd_1Ag_3/r-TiO_2	81.0	94.1	650	5% H_2	4	Y	1	3	r-TiO_2	1
54	Pd_1Ag_3/r-TiO_2	85.0	93.9	600	5% H_2	4	N	1	3	r-TiO_2	1
55	Pd_1Ag_3/CeO_2	90.0	93.7	750	5% H_2	4	N	1	3	CeO_2	1
56	Pd_1Ag_3/Al-MCM-41	107.0	93.7	750	5% H_2	4	N	1	3	Al-MCM-41	1
57	Pd_1Ag_3/a-TiO_2	100.0	93.7	750	5% H_2	4	N	1	3	a-TiO_2	1
58	Pd_1Ag_3/γ-Al_2O_3	92.0	93.6	750	5% H_2	4	N	1	3	γ-Al_2O_3	1
59	Pd_1Ag_3/r-TiO_2	90.0	93.4	700	100% H_2	4	Y	1	3	r-TiO_2	1
60	Pd_1Ag_3/ZSM-5	113.0	93.4	900	5% H_2	4	N	1	3	ZSM-5	1
61	Pd_1Ag_3/r-TiO_2	95.0	93.3	1000	5% H_2	4	N	0.2	0.6	r-TiO_2	1
62	Pd_1Ag_3/Ti-Mor	116.0	93.2	750	5% H_2	4	N	1	3	Ti-MOR	1
63	Pd_1Ag_3/a-Al_2O_3	93.0	93.1	750	5% H_2	4	N	1	3	a-Al_2O_3	1
64	Pd_1Ag_3/r-TiO_2	83.0	93.1	650	5% H_2	4	Y	1	3	r-TiO_2	1
65	Pd_1Ag_3/a-TiO_2	100.0	93.0	750	5% H_2	4	Y	1	3	a-TiO_2	1
66	Pd_1Ag_3/C	88.0	92.9	650	5% H_2	4	N	1	3	C	1
67	Pd_1Ag_3/GO	92.0	92.7	750	5% H_2	4	N	1	3	GO	1
68	Pd_1Ag_3/r-TiO_2	84.0	92.5	900	100% H_2	4	Y	1	3	r-TiO_2	1
69	Pd_1Ag_3/GO	87.0	92.5	750	5% H_2	4	Y	1	3	GO	1
70	Pd_1Ag_3/C	86.0	92.3	750	N_2	4	N	1	3	C	1
71	Pd_1Ag_3/a-TiO_2	100.0	92.2	700	5% H_2	4	Y	1	3	a-TiO_2	1
72	Pd_1Ag_3/r-TiO_2	91.0	91.9	750	5% H_2	4	N	0.01	0.03	r-TiO_2	1
73	Pd_1Ag_3/r-TiO_2	90.0	91.7	600	5% H_2	4	Y	1	3	r-TiO_2	1
74	Pd_1Ag_3/r-TiO_2	92.0	91.5	600	100% H_2	4	Y	1	3	r-TiO_2	1
75	Pd_1Ag_3/a-TiO_2	105.0	91.5	600	5% H_2	4	Y	1	3	a-TiO_2	1
76	Pd_1Ag_3/r-TiO_2	85.0	91.5	650	5% H_2	4	N	1	3	r-TiO_2	1
77	Pd_1Ag_3/r-TiO_x	81.0	91.2	700	5% H_2	4	N	1	3	r-TiO_x	1
78	Pd_1Ag_3/a-TiO_2	110.0	90.9	600	5% H_2	4	Y	1	3	a-TiO_2	1
79	Pd_1Ag_3/ZrO_2	89.0	90.6	750	5% H_2	4	N	1	3	ZrO_2	1
80	Pd_1Ag_3/SAPO-34	105.0	90.5	750	5% H_2	4	N	1	3	SAPO-34	1
81	Pd_1Ag_3/r-TiO_2	79.0	90.4	600	100% H_2	4	Y	1	3	r-TiO_2	1
82	Pd_1Ag_3/r-TiO_2	88.0	89.9	900	100% H_2	4	Y	1	3	r-TiO_2	1
83	Pd_1Ag_3/P25	100.0	89.8	750	5% H_2	4	N	1	3	P25	1
84	Pd_1Ag_3/r-TiO_2	77.0	89.8	600	100% H_2	4	Y	1	3	r-TiO_2	1
85	Pd_1Ag_3/r-TiO_2	96.0	89.6	900	100% H_2	4	Y	1	3	r-TiO_2	1
86	Pd_1Ag_3/GO	103.0	89.5	900	5% H_2	4	N	1	3	GO	1
87	Pd_1Ag_3/r-TiO_2	70.0	89.3	600	5% H_2	4	N	1	3	r-TiO_2	1
88	Pd_1Ag_3/r-TiO_2	75.0	88.9	1000	5% H_2	4	N	1	3	r-TiO_2	1

Supplementary Table 4. Continued from previous page.

89	Pd_1Ag_3/Y_2O_3	84.0	88.3	750	5% H_2	4	N	1	3	Y_2O_3	1
90	Pd_1Ag_3/HT	110.0	88.2	750	5% H_2	4	N	1	3	HT	1
91	Pd_1Ag_3/r-TiO_2	88.0	87.7	600	5% H_2	4	N	1	3	r-TiO_2	1
92	Pd_1Ag_3/r-TiO_2	74.0	87.5	600	100% H_2	4	Y	1	3	r-TiO_2	1
93	Pd_1Ag_3/r-TiO_2	89.0	87.2	1000	5% H_2	4	N	0.05	0.15	r-TiO_2	1
94	Pd_1Ag_3/r-TiO_2	107.0	87.1	900	100% H_2	4	Y	1	3	r-TiO_2	1
95	Pd_1Ag_3/P25	75.0	87.0	750	5% H_2	4	N	1	3	P25	1
96	Pd_1Ag_3/MCM-41	93.0	86.9	750	5% H_2	4	N	1	3	MCM-41	1
97	Pd_1Ag_3/r-TiO_2	90.0	86.7	1000	5% H_2	4	Y	0.01	0.03	r-TiO_2	1
98	Pd_1Ag_3/GO	77.0	85.1	600	5% H_2	4	N	1	3	GO	1
99	Pd_1Ag_3/r-TiO_2	104.0	83.4	750	vacuum	4	N	1	3	r-TiO_2	1
100	Pd_1Ag_3/Ti-MWW	116.0	83.3	750	5% H_2	4	N	1	3	Ti-MWW	1
101	Pd_1Ag_3/SiO_2	91.0	82.6	750	5% H_2	4	N	1	3	SiO_2	1
102	Pd_1Ag_3/C	75.0	82.2	750	5% H_2	4	N	10	30	C	2
103	Pd_1Ag_3/SiO_2	76.0	80.5	600	5% H_2	4	N	1	3	SiO_2	1
104	Pd_1Ag_3/r-TiO_x	45.0	78.1	600	5% H_2	4	N	1	3	r-TiO_x	1
105	$Pd_1Ag_3/CaCO_3$	90.0	77.6	750	5% H_2	4	N	1	3	$CaCO_3$	1
106	$Pd_1Ag_3/CaCO_3$	60.0	74.8	600	5% H_2	4	N	1	3	$CaCO_3$	1

Note: To reduce experimental errors, the reaction results of catalysts prepared under the same conditions in some different batches are listed in the table at the same time.

*: **Y** means that after the catalyst has been impregnated and dried, it needs to be calcined in air at 450°C for 4 hours and then reduced. **N** means direct reduction after the catalyst has been impregnated and dried.

**： 1 means co-impregnation. 2 means consecutive impregnation. Pd was successfully loaded first, followed by Ag.

#: The loading amount refers to the percentage of the input metal mass in the total mass at the beginning of synthesis.

15. Acetylene hydrogenation catalysts and the performance in literatures

Table S5. Top performance PdAg catalysts for the selective hydrogenation of acetylene reported in the literature

Entry	Catalyst	Conversion (%)	Selectivity (%)	Yield *(%)*	$C_2H_2 : H_2 : C_2H_4$	GHSV mL $g^{-1}h^{-1}$	*Reaction Temp.* ºC	Ref
1	Pd_1Ag_3/r-TiO_2 (T750)	100.0	97.2	97.2	1:10:100	96000	98	This work
2	Ag@PdAg	100.0	97.0	97.0	1:2:100	10050 h^{-1}	100	12
3	Ga-Ag@Pd/SiO_2	100.0	95.0	95.0	1:2:50	60000	120	13
4	$Pd_{0.005}Ag/SiO_2$	92.6	92.3	85.5	1:20:20	60000	240	14
5	Pd_7Ag_2/α-Al_2O_3	100.0	85.0	85.0	15:58:0.8	120000	280	15
6	PdAg/$Mg_{0.5}Ti_{0.5}O_y$	100.0	83.8	83.8	1:3:100	10050 h^{-1}	70	16
7	Pd_1Ag_3/HT	90.0	93.0	83.7	1:10:20	180000	-	17
8	Pd_1Ag_3/r-TiO_2 (T400)	96.0	85.9	82.5	1:10:100	96000	60	18
9	$Pd_{1.0}/Bi_2O_3/TiO_2$	90	91	81.9	1:20:20	1E+05	50	19
10	Pd-Ag/$MgCO_3$@α-Al_2O_3	89.0	92.0	81.9	1:18.6:58.2	8000 h^{-1}	70	20
11	Pd_1Ag_6/Al_2O_3	95.0	86.0	81.7	1:1.5:44	4000 h^{-1}	60	21
12	$PdAg_3/Al_2O_3$	93.6	84.9	79.5	1:5:90	1920000	132	22
13	Pd_1Ag_2/C	97.0	81.0	78.6	4:96:0	120000	95	23
14	Pd-Ag/SiO_2	99.3	78.0	77.5	1:35:70	28800	70	24
15	Pd_1Ag_1/α-Al_2O_3	95.0	80.0	76.0	1:1.1:52	2000 h^{-1}	30	25
16	PdAg/NiTi-LDH	90.0	82.0	73.8	1:2:100	10050 h^{-1}	80	26
17	PdAg MCs (1/1)/HT	90.0	82.0	73.8	1:2:93	8040 h^{-1}	77	27
18	$Pd_{0.03}Ag_{0.18}/Al_2O_3$(1100)	78.0	94.0	73.3	1:1.5:44	5760 h^{-1}	60	28
19	Pd_1Ag_2/Al_2O_3	90.0	80.0	72.0	1:17:100	10000 h^{-1}	90	29
20	$Pd_{0.03}Ag_{0.18}$/α-Al_2O_3	80.0	90.0	72.0	1:1.5:67.5	5760 h^{-1}	60	30
21	$Pd_{0.6}Ag_{0.4}$/Sib(400ºC)	93.0	77.0	71.6	4:96:0	1200000	95	31
22	Pd_1Ag_4/ glass fiber	80.0	80.0	64.0	0.5:0.8:52	3000000	115	32
23	50Pd50Ag/Al2O3	70.0	80.0	56.0	1:5:20	370000	50	33
24	Pd-Ag/Al_2O_3(1050)	80.0	70.0	56.0	1:1.5:60	5760 h^{-1}	60	34
25	$Pd_1Ag_{1.5}/Al_2O_3$	100.0	53.8	53.8	1:1.5:130	12000 h^{-1}	110	35
26	$Pd_{(0.97)}$@$Ag_{(1.50)}/TiO_2$	57.4	90.3	51.8	1:2:72	72000	60	36
27	$Pd_{20}Ag_{80}/Al_2O_3$	68.0	72.0	49.0	1:1:30	4000 h^{-1}	30	37
28	PdAg/K^+-γ-Al_2O_3	55.0	75.0	41.3	1:4:1	264000	50	38
29	Pd-Ag/C	43.0	80.0	34.4	4:96:0	300000	55	39
30	PdAg/TiO2	38.0	80.0	30.4	1:5:20	600000	65	40
31	PdAg/Na^+-β-zeolite	50.0	55.0	27.5	1:4:1	264000	60	41
32	Pd-Ag/SiO_2	17.5	80.0	14.0	1:5:20	600000	65	42
33	Pd-Ag/TiO_2-R	10.0	28.5	2.9	1:1:81	5400 h^{-1}	40	43

16. ICP results for PdAg/r-TiO_2 catalyst.

Table S6. Elemental analysis of Pd1Ag3 samples by ICP-OES.

Catalysts	ICP-OES		Ag : Pd
	Pd (%)	Ag(%)	
T150	1.000	3.013	3.013
T450	1.080	3.300	3.056
T600	1.040	3.090	2.971
T750	1.080	3.170	2.935
T900	0.096	0.273	2.844

17. EXAFS fitting results for PdAg/r-TiO_2 (T750) catalyst.

Table S7. EXAFS fitting results for T750 catalyst.

Sample	Shell	N[a]	R(Å)[b]	$\Delta\sigma^2$*10^3 ($Å^2$)[c]	ΔE_0 (eV)[d]	R factor
Ag foil	Ag-Ag	12.0	2.86	9.5	1.06	0.003
Ag_2O	Ag-O	1.9	2.06	0.7	4.40	0.016
Pd foil	Pd-Pd	11.9	2.74	5.3	-5.69	0.005
PdO	Pd-O	4.4	2.03	2.0	-0.55	0.017
T750 Ag	**Ag-Pd**	**3.9**	**2.85**	**5.9**	**3.69**	**0.006**
	Ag-Ag	**8.0**	**2.89**	**16.0**	**1.96**	

[a]N, coordination number; [b]R, the distance between absorber and backscatter atoms;

[c]σ^2, Debye-Waller factor to account for both thermal and structural disorders;

[d]ΔE_0, inner potential correction; R factor indicates the goodness of the fit.

R factor indicates the goodness of the fit. Fitting range: 3.0 ≤ *k* (/Å) ≤ 14.2 and 1.0 ≤ *R* (Å) ≤ 3.0 (Ag foil).; 3.0 ≤ *k* (/Å) ≤ 9.8 and 1.0 ≤ *R* (Å) ≤ 2.3 (Ag2O).; 3.0 ≤ *k* (/Å) ≤ 12.4 and 1.0 ≤ *R* (Å) ≤ 3.0 (Pd foil).; 3.2 ≤ *k* (/Å) ≤ 11.5 and 1.1 ≤ *R* (Å) ≤ 3.5 (PdO).;3.0≤ *k* (/Å) ≤ 13.0 and 1.1 ≤ *R* (Å) ≤ 3.0 (T750 Ag.

18. BET characterization.

Table S8. BET Surface Areas and Pore-Size Distribution of catalysts.

Entry	Catalysts	Surface area ($m^2 g^{-1}$)	Proe volume ($cm^3 g^{-1}$)	Average pore size (nm)
1	r-TiO_2	89.0	0.277	10.5
2	r-TiO_2 (750)	11.8	0.081	25.2
3	Pd_1Ag_3/r-TiO_2 (im)	76.2	0.278	11.6
4	Pd_1Ag_3/r-TiO_2 (750)	10.2	0.044	18.1
5	ZSM-5	293.2	0.116	5.3
6	ZSM-5 (750)	289.2	0.127	5.2
7	Pd_1Ag_3/ZSM-5 (im)	283.2	0.126	5.6
8	Pd_1Ag_3/ZSM-5 (750)	285.9	0.159	5.2

References

(1) Chen, X. B.; Liu, L.; Huang, F. Q. Black titanium dioxide (TiO_2) nanomaterials. *Chem. Soc. Rev.* **2015,** *44*, 1861.

(2) Funke, H.; Chukalina, M.; Scheinost, A. C. A new FEFF-based wavelet for EXAFS data analysis. *J. Synchrotron Radiat.* **2007,** *14*, 426.

(3) Ravel, B.; Newville, M. ATHENA, ARTEMIS, HEPHAESTUS: data analysis for X-ray absorption spectroscopy using IFEFFIT. *J. Synchrotron Radiat.* **2005,** *12*, 537.

(4) Funke, H.; Scheinost, A. C.; Chukalina, M. Wavelet analysis of extended x-ray absorption fine structure data. *Phys. Rev. B* **2005,** *71*, 094110.

(5) Shang, C.; Huang, S. D.; Liu, Z. P. Massively parallelization strategy for material simulation using high-dimensional neural network potential. *J. Comput. Chem.* **2019,** *40*, 1091.

(6) Huang, S. D.; Shang, C.; Kang, P. L.; Liu, Z. P. Atomic structure of boron resolved using machine learning and global sampling. *Chem. Sci.* **2018,** *9*, 8644.

(7) Huang, S. D.; Shang, C.; Zhang, X. J.; Liu, Z. P. Material discovery by combining stochastic surface walking global optimization with a neural network. *Chem. Sci.* **2017,** *8*, 6327.

(8) Shang, C.; Liu, Z. P. Stochastic Surface Walking Method for Structure Prediction and Pathway Searching. *J. Chem. Theory Comput.* **2013,** *9*, 1838.

(9) Zhang, X. J.; Shang, C.; Liu, Z. P. From Atoms to Fullerene: Stochastic Surface Walking Solution for Automated Structure Prediction of Complex Material. *J. Chem. Theory Comput.* **2013,** *9*, 3252.

(10) Shang, C.; Zhang, X. J.; Liu, Z. P. Stochastic surface walking method for crystal structure and phase transition pathway prediction. *Phys. Chem. Chem. Phys.* **2014,** *16*, 17845.

(11) Ma, S. C.; Shang, C.; Liu, Z. P. Heterogeneous catalysis from structure to activity via SSW-NN method. *Journal of Chemical Physics* **2019,** *151*, 050901.

(12) Ma, R.; He, Y.; Feng, J.; Hu, Z.-Y.; Van Tendeloo, G.; Li, D. A facile synthesis of Ag@PdAg core-shell architecture for efficient purification of ethene feedstock. *J. Catal.* **2019,** *369*, 440.

(13) Liu, F.; Xia, Y.; Xu, W.; Cao, L.; Guan, Q.; Gu, Q.; Yang, B.; Lu, J. Integration of Bimetallic Electronic Synergy with Oxide Site Isolation Improves the Selective Hydrogenation of Acetylene. *Angew. Chem. Int. Ed.* **2021,** *60*, 19324.

(14) Pei, G. X.; Liu, X. Y.; Wang, A.; Lee, A. F.; Isaacs, M. A.; Li, L.; Pan, X.; Yang, X.; Wang, X.; Tai, Z.; Wilson, K.; Zhang, T. Ag Alloyed Pd Single-Atom Catalysts for Efficient Selective Hydrogenation of Acetylene to Ethylene in Excess Ethylene. *ACS Catal.* **2015,** *5*, 3717.

(15) Li, Q.; Wang, Y.; Skoptsov, G.; Hu, J. Selective Hydrogenation of Acetylene to Ethylene over Bimetallic Catalysts. *Ind. Eng. Chem. Res.* **2019,** *58*, 20620.

(16) Liu, Y.; Zhao, J.; He, Y.; Feng, J.; Wu, T.; Li, D. Highly efficient PdAg catalyst using a reducible Mg-Ti mixed oxide for selective hydrogenation of acetylene: Role of acidic and basic sites. *J. Catal.* **2017,** *348*, 135.

(17) Studt, F.; Abild-Pedersen, F.; Bligaard, T.; Sorensen, R. Z.; Christensen, C. H.; Norskov, J. K. Identification of non-precious metal alloy catalysts for selective hydrogenation of acetylene. *Science* **2008,** *320*, 1320.

(18) Li, X.-T.; Chen, L.; Shang, C.; Liu, Z.-P. In Situ Surface Structures of PdAg Catalyst and Their Influence on Acetylene Semihydrogenation Revealed by Machine Learning and Experiment. *J. Am. Chem. Soc.* **2021,** *143*, 6281.

(19) Zou, S. H.; Lou, B. H.; Yang, K. R.; Yuan, W. T.; Zhu, C. Z.; Zhu, Y. H.; Du, Y. H.; Lu, L. F.; Liu, J. J.; Huang, W. X.; Yang, B.; Gong, Z. M.; Cui, Y.; Wang, Y.; Ma, L.; Ma, J. Y.; Jiang, Z.; Xiao, L. P.; Fan, J. Grafting nanometer metal/oxide interface towards enhanced low-temperature acetylene semi-hydrogenation. *Nat. Commun.* **2021,** *12*, 1.

(20) Che, C.; Wang, B.; Shan, C.; Chen, H.; Liu, W.; Tang, Y. An Effective Strategy to Prepare Pd-Ag/$MgCO_3$@alpha-Al2O_3 Catalyst for Selective Hydrogenation of Acetylene. *Catal. Lett.* **2017,** *147*, 483.

(21) Ravanchi, M. T.; Fard, M. R.; Sahebdelfar, S.; Bigdeli, P. Synthesis of Pd-Ag/Al_2O_3 catalyst by colloidal oxide method for acetylene selective hydrogenation: a study on the sintering of PdO nanoparticles. *Res. Chem. Intermed.* **2022,** *48*, 817.

(22) Smirnova, N. S.; Markov, P. V.; Baeva, G. N.; Rassolov, A. V.; Mashkovsky, I. S.; Bukhtiyarov, A. V.; Prosvirin, I. P.; Panafidin, M. A.; Zubavichus, Y. V.; Bukhtiyarov, V. I.; Stakheev, A. Y. CO-induced segregation as an efficient tool to control the surface composition and catalytic performance of $PdAg_3/Al_2O_3$ catalyst. *Mendeleev Commun.* **2019,** *29*, 547.

(23) Glyzdova, D. V.; Afonasenko, T. N.; Khramov, E. V.; Leont'eva, N. N.; Prosvirin, I. P.; Bukhtiyarov, A. V.; Shlyapin, D. A. Liquid-phase acetylene hydrogenation over Ag-modified Pd/Sibunit catalysts: Effect of Pd to Ag molar ratio. *App. Catal. a-Gen* **2020,** *600*, 117627.

(24) Jin, Y. M.; Datye, A. K.; Rightor, E.; Gulotty, R.; Waterman, W.; Smith, M.; Holbrook, M.; Maj, J.; Blackson, J. The influence of catalyst restructuring on the selective hydrogenation of acetylene to ethylene. *J. Catal.* **2001,** *203*, 292.

(25) Chen, W. S.; Wei, K. M. Single-stage treatment in selective hydrogenation of acetylene over CDS type of Pd-Ag/Al_2O_3 catalyst. *Can. J. Chem. Eng.* **2004,** *82*, 1217.

(26) Liu, Y. N.; Feng, J. T.; He, Y. F.; Sun, J. H.; Li, D. Q. Partial hydrogenation of acetylene over a NiTi-layered double hydroxide supported PdAg catalyst. *Catal. Sci. Technol.* **2015,** *5*, 1231.

(27) He, Y.; Liu, Y.; Yang, P.; Du, Y.; Peng, J.; Cao, X.; Yang, J.; Li, D. Fabrication of a PdAg mesocrystal catalyst for the partial hydrogenation of acetylene. *J. Catal.* **2015,** *330*, 61.

(28) Ravanchi, M. T.; Fadaeerayeni, S.; Fard, M. R. The effect of calcination temperature on physicochemical properties of alumina as a support for acetylene selective hydrogenation catalyst. *Res. Chem. Intermed.* **2016,** *42*, 4797.

(29) Zhang, Q. W.; Li, J.; Liu, X. X.; Zhu, Q. M. Synergetic effect of Pd and Ag dispersed on Al_2O_3 in the selective hydrogenation of acetylene. *App. Catal. a-Gen* **2000,** *197*, 221.

(30) Ravanchi, M. T.; Sahebdelfar, S.; Fard, M. R.; Fadaeerayeni, S.; Bigdeli, P. Pd-Ag/-Al_2O_3 Catalyst Deactivation in Acetylene Selective Hydrogenation Process. *Chem. Eng. Technol.* **2016,** *39*, 301.

(31) Glyzdova, D. V.; Afonasenko, T. N.; Khramov, E. V.; Leont'eva, N. N.; Trenikhin, M. V.; Kremneva, A. M.; Shlyapin, D. A. Effect of pretreatment with hydrogen on the structure and properties of carbon-supported Pd-Ag-nanoalloys for ethylene production by acetylene hydrogenation. *Molecular Catalysis* **2021,** *511*, 111717.

(32) Kotolevich, Y. S.; Mamontov, G. V.; Vodyankina, O. V.; Petrova, N. I.; Smirnova, N. S.; Tsyryul'nikov, P. G.; Trenikhin, M. V.; Nizovskii, A. I.; Kalinkin, A. V.; Smirnov, M. Y.; Goncharov, V. B. Catalytic Pd-Ag Nanoparticles Immobilized on Fiber Glass by Surface Self-Propagating Thermal Synthesis. *International Journal of Self-Propagating High-Temperature Synthesis* **2017,** *26*, 234.

(33) Delgado, J. A.; Benkirane, O.; Lachaux, S.; Claver, C.; Ferre, J.; Curulla-Ferre, D.; Godard, C. Controlled One-pot Synthesis of PdAg Nanoparticles and Their Application in the Semi-hydrogenation of Acetylene in Ethylene-rich Mixtures. *Chemnanomat* **2022,** *8*, e202200058.

(34) Komeili, S.; Ravanchi, M. T.; Taeb, A. The influence of alumina phases on the performance of the Pd-Ag/Al_2O_3 catalyst in tail-end selective hydrogenation of acetylene. *App. Catal. a-Gen* **2015,** *502*, 287.

(35) Wei, G.; Dai, W.; Li, Q.; Cao, W.; Zhang, J. Reverse Microemulsion Synthesis and Characterization of Pd-Ag Bimetallic Alloy Catalysts Supported on Al_2O_3 for Acetylene Hydrogenation. *China Petroleum Processing & Petrochemical Technology* **2012,** *14*, 59.

(36) Han, Y.; Peng, D.; Xu, Z.; Wan, H.; Zheng, S.; Zhu, D. TiO_2 supported Pd@Ag as highly selective catalysts for hydrogenation of acetylene in excess ethylene. *Chem. Commun.* **2013,** *49*, 8350.

(37) Kuhn, M.; Lucas, M.; Claus, P. Long-Time Stability vs Deactivation of Pd-Ag/Al_2O_3 Egg-Shell Catalysts in Selective Hydrogenation of Acetylene. *Ind. Eng. Chem. Res.* **2015,** *54*, 6683.

(38) Huang, W.; Li, A.; Lobo, R. F.; Chen, J. G. Effects of Zeolite Structures, Exchanged Cations, and Bimetallic Formulations on the Selective Hydrogenation of Acetylene Over Zeolite-Supported Catalysts. *Catal. Lett.* **2009,** *130*, 380.

(39) Glyzdova, D. V.; Vedyagin, A. A.; Tsapina, A. M.; Kaichev, V. V.; Trigub, A. L.; Trenikhin, M. V.; Shlyapin, D. A.; Tsyrulnikov, P. G.; Lavrenov, A. V. A study on structural features of bimetallic Pd-M/C (M: Zn, Ga, Ag) catalysts for liquid-phase selective hydrogenation of acetylene. *App. Catal. a-Gen* **2018,** *563*, 18.

(40) Riyapan, S.; Zhang, Y. Y.; Wongkaew, A.; Pongthawornsakun, B.; Monnier, J. R.; Panpranot, J. Preparation of improved Ag-Pd/TiO_2 catalysts using the combined strong electrostatic adsorption and electroless deposition methods for the selective hydrogenation of acetylene. *Catal. Sci. Technol.* **2016,** *6*, 5608.

(41) Huang, W.; Lobo, R. F.; Chen, J. G. Characterization of Na+-beta-zeolite supported Pd and PdAg bimetallic catalysts using EXAFS, TEM and flow reactor. *Journal of Molecular Catalysis a-Chemical* **2008,** *283*, 158.

(42) Zhang, Y.; Diao, W.; Monnier, J. R.; Williams, C. T. Pd-Ag/SiO_2 bimetallic catalysts prepared by galvanic displacement for selective hydrogenation of acetylene in excess ethylene. *Catal. Sci. Technol.* **2015,** *5*, 4123.

(43) Kontapakdee, K.; Panpranot, J.; Praserthdam, P. Effect of Ag addition on the properties of Pd-Ag/TiO_2 catalysts containing different TiO_2 crystalline phases. *Catal. Commun.* **2007,** *8*, 2166.